When things get too complicated, it sometimes makes sense to stop and wonder: Have I asked the right question?

- Enrico Bombieri
  Institute for Advanced Study
  Princeton, New Jersey

University of Alberta

Resource allocation, water relations and crown architecture examined at the tree and stand-level in northern conifers

by

Amanda Lynn Schoonmaker

A thesis submitted to the Faculty of Graduate Studies and Research
in partial fulfillment of the requirements for the degree of

Doctor of Philosophy

in

Forest Biology and Management

Renewable Resources

©Amanda Lynn Schoonmaker

Fall 2013
Edmonton, Alberta

Permission is hereby granted to the University of Alberta Libraries to reproduce single copies of this thesis and to lend or sell such copies for private, scholarly or scientific research purposes only. Where the thesis is converted to, or otherwise made available in digital form, the University of Alberta will advise potential users of the thesis of these terms.

The author reserves all other publication and other rights in association with the copyright in the thesis and, except as herein before provided, neither the thesis nor any substantial portion thereof may be printed or otherwise reproduced in any material form whatsoever without the author's prior written permission.

Dr. François Teste, Dr. Suzanne Simard and Dr. Robert Guy-

From my first day as a summer research assistant and the first directed study (the Drosera project) I conducted, I knew that I had found the type of work that could keep me excited for many more years to come.

Thank-you all for being excellent role models and providing me with the array of opportunities I received during my undergraduate years at UBC. I would not have pursued this path without these experiences and your guidance and encouragement.

Abstract

Variation in quantity of light has driven plants to employ many strategies in order to persist in high and low light. It is also a primary driver of lower branch mortality and crown recession. Fine roots and leaves are complimentary tissues representing belowground and aboveground resource acquisition. This balance is likely to the influence forest stands as they age.

The objective of my thesis is to understand how hydraulic architecture, crown form and resource allocation are affected by shading trees of opposing shade tolerance. Four tree species were examined: *Pinus banksiana, Pinus contorta, Picea glauca* and *Picea mariana*. The following are key findings of my thesis:

- A reduced light environment alters the xylem vulnerability of shoots. Shaded shoots are not as drought resistant as those in high light. The effect of shade on hydraulic conductivity is likely tied to both the position of the shoots being examined as well as the quantity of light reduced. Evaporative demand in an understory environment is low, however, a rapid change into full light could be detrimental for shaded conifers.
- Asymmetric shading (where part of the tree crown is fully illuminated while the other part is shaded) placed less-illuminated shoots at a greater disadvantage in terms of bud expansion and growth compared with uniform shading of the entire crown. Relative reductions in TNC appear to follow similar patterns to bud expansion and growth observations, suggesting that carbon dynamics or fluxes are playing a role in dictating physiological activity of branches. In all cases, responses to asymmetric shade were always more extreme in *Pinus contorta* compared with *Picea glauca*. This is likely due, in part, to different C storage patterns as *Pinus contorta* exhibited lower overall TNC concentrations and smaller (or non-existent) seasonal fluxes in TNC compared with *P.glauca*.

- In a *P.contorta* chronosequence, fine root surface area is the first stand parameter to level-off while wood production increases for another 30 years and leaf area to age 100. During the period of peak wood production, a number of pressures are also converging including: light asymmetry (driving crown recession), crown friction and reduced soil resources.

Acknowledgements

To my supervisors, Dr. Victor Lieffers and Dr. Simon Landhäusser: thank-you both for your guidance, support and encouragement throughout my program. I greatly appreciate the freedom I was given to explore the topics contained in this thesis. You both have made the difference between having a good graduate experience and the best experience a student could hope to expect.

If I did have a third co-supervisor, it would have had to been Dr. Uwe Hacke. Thank-you Uwe for always having an open door to your lab, whether it was for me to run vulnerability curves, light microscopy or just to stop by for an enlightening discussion on plant water transport.

To the graduate students in the Dr. Lieffers, Dr. Landhäusser and Dr. Hacke labs, thank-you for many thoughtful discussions and support throughout the years. I have enjoyed working with you all and hope to keep in touch with many of you in the coming years.

I would like to acknowledge all of the field technicians and summer assistants (J. Burko, T. Cullen, K. Dahl, D. Deshaies, C. Lecoutier, D. Goodsman, B. Irvine, J. Kleinitz, G. Kershaw, J. Langhorst, J. Snedden, E. Marenholtz, K. Mohr, R. Sheritt, C. Serben, J. Snedden, K. Solarik, K. Stang, K. Renkema) who worked tirelessly with me. Without these folks, none of this work would have made it further than my notebook.

Pak Chow, you are a patient teacher. I attribute a significant portion of my laboratory skills from you teachings and good lab practices. I hope to have a least two containers of marbles reserved for my test tubes in the future.

George Braybrook and De-Ann Rollings provided invaluable assistance with the SEM work. Your expertise on the operation of this instrument and uncanny ability to find nice, intact pits made all the difference.

Thank-you to West Fraser Mills Ltd. for their assistance in locating field sites. Debbie Mucha at the Alberta Foothills Research Institute kindly provided maps of fire origins in the western foothills.

Funding certainly does not grow on trees. An NSERC (National Science and Engineering Research Council) PGSM and CGSD, Alberta Ingenuity Scholarship and University of Alberta Dissertation Fellowship were all greatly appreciated as they provided direct support throughout my program. Research funding for these projects was provided by NSERC in association with Weyerhaeuser and West Fraser and Mixed wood Management Association grants to VJL and support from the Canada Research Chair program and the Canada Foundation for Innovation to UGH were all greatly appreciated.

Table of Contents

List of Tables

List of Figures

List of Symbols and Abbreviations

Symbol	Description
A_p	Inter-tracheid pit area per tracheid
D	Lumen diameter
DBH	Diameter at breast height
FFRF	Field fine root fraction
F_p	Fraction of tracheid surface area occupied by inter-tracheid pits
FRPF	Fine root particulate fraction
GPP	Gross primary productivity
k_h	Hydraulic conductivity
k_l	Leaf-area specific hydraulic conductivity
k_s	Sapwood-area specific hydraulic conductivity
$K_{s\text{-}p}$	Soil-to-plant hydraulic conductance
LA:SA	Leaf-area to sapwood-area ratio
LAI	Leaf-area index
LFRF	Lab fine root fraction
NPP	Net primary productivity
NSC	Non-structural carbon
P_{50}	Xylem pressure causing 50% loss in conductivity
R_c	Tracheid resistivity
R_L	Average lumen resistivity
r_p	Pit-area resistance
SDI	Stand density index
SI	Site index at a reference age
SLA	Specific leaf area
SRA	Specific root area
SRL	Specific root length
TBCF	Total belowground carbon flux
TNC	Total non-structural carbohydrates
TRCA	Total-root carbon allocation
ρ	Wood density

Chapter 1 Thesis introduction

1.1 PART 1: Water relations and shade tolerance

All trees require light, air, water and nutrients for survival, however trees show substantial variation in the quantity of light they require. Shade tolerant trees, such as spruce (*Picea glauca*), have the ability to survive long periods in partial to deep shade (Walters and Reich 1999). In contrast, pine (*Pinus contorta*) is shade intolerant because it dies in deep shade. Investigations exploring the mechanisms behind shade tolerance have generally focused on characteristics related to leaf development (Messier et al. 1999). However, shoot and root hydraulic architecture (the amount and quality of wood produced), water transport capability and carbohydrate reserve strategies are also likely related to shade tolerance. At the tree-level, these properties will influence crown form development. While at the stand-level, crown form will dictate standing LAI (leaf-area index) and stand productivity.

1.1.1 Factors influencing water movement in trees

How does water move in a tree? The cohesion-tension theory of sap states that water is transported through a plant in a meta-stable state under tension (negative pressure). The driving force for this water movement is by evaporation occurring at the cell walls of the stomates (Tyree and Zimmermann 2002). Though much of the discussion of water movement is focused on longitudinal movement (up or down), it is important to keep in mind that water also moves radially. This becomes particularly important when water is entering or exiting a plant. Tyree and Zimmermann have suggested that radial water flow into the roots and flow through leaf cells provide substantial resistance to rates of water flow. They speculate that at least 50 % of resistance to water flow is non-vascular in large trees.

Environmental conditions have a significant role to play in the hydraulic response of plants. Drought can significantly reduce flow of water in plants (Shumway et al 1993). Site conditions generally have a positive influence on hydraulic architecture. Increased earlywood relative to latewood (Reid et al 2003), tracheid length (Pothier et al 1989), and sapwood area (Shelburne and Hedden 1996) have all been known to increase on better sites relative to poor sites. However, in a water-limiting environment, fertilization may actually be detrimental as it can reduce root:leaf area ratios. This can have negative consequences for the water balance of these plants as roots are needed to take up water (Ewers et al 2000). Fertilization may also allow lower branches to be maintained for longer periods by increasing hydraulic conductivity and permeability to these branches (Amponsah et al 2004). Light is another environmental factor of importance that will be discussed in more detail in the next section.

1.1.4 Effects of shade and shade tolerance

Shade tolerance is an interesting term; it implies an ability of a species to survive in shade (Walters and Reich 1999) but specifies nothing directly about how this plant may tolerate shade. Canham (1988) hypothesized two extremes as possible mechanisms for shade tolerance: 1. Individuals would grow at a constant slow rate, even when increased light became available (perhaps as a result of development of a gap) or 2. Individuals would have very plastic growth rates, where the individual would grow very little under deep shade and be able to grow largely upon canopy opening.

Growth rates typically increase with increased light for most trees (Reich et al 1998, Fownes and Harrington 2004, Wright et al 1998). Allocation to root growth decreases under shaded conditions (Reich et al 1998, Fownes and Harrington 2004). Plants growing in shade will allocate more to leaf production than stem production relative to sun grown plants whereas sun grown plants will allocate more to stem growth (Schultz and Matthews 1993). Maximal growth

rates may be higher under high light for shade intolerant trees relative to shade tolerant trees (Walters et al 1993, Beaudet and Messier 1998, Wright et al 1998). Shade tolerant trees may allocate more RWR (g roots per g plant) under shade than an intolerant species (Walters et al 1993). In constrast, Messier et al (1999) suggested that shade-tolerant spruce and fir would generally have lower root:shoot ratios than shade-intolerant pines.

Leaf mass per unit area (g cm^{-2}) increases with increased light (Fownes and Harrington 2004, Walters et al 1993) and correspondingly, leaf area ratio (LAR, cm^2 g^{-1} plant) increased with decreased light (Walters et al 1993, Beaudet and Messier 1998, Schultz and Matthews 1993). Leaf weight ratio (g leaf g^{-1}plant) increases for plants grown in shade (Schultz and Matthews 1993). Messier et al (1999) suggested that shade tolerant spruces and firs could carry higher LAR than shade intolerant pines. This is supported by Pinol and Sala (2000) who found that sapwood:leaf area ratios increased in pines relative to Douglas-fir and sub-alpine fir. Photosynthetic rates are also generally higher for shade-intolerant species (Walters et al 1993).

Stomatal conductance is generally higher in sun branches relative to branches grown in shade (Sellin and Kupper 2004, Cochard et al 1999); similarly leaf specific hydraulic capacity was increased for sun grown plants relative to shade grown plants (Schultz and Matthews 1993, Shumway et al 1993) and shaded lodgepole pine branches had decreased hydraulic conductivity (Protz et al 2000). Resistance to water transport may increase (Sellin 1993) and earlywood:latewood ratios may decrease under shaded conditions (Protz et al 2000). Shade-intolerant species have higher rates of root and shoot conductance than shade tolerant species (Tyree et al 1998); similarly shade-tolerant maples were found to have leaf specific hydraulic capacities that were lower than their shade-intolerant counterparts (Woodrum et al 2003).

Overall, it appears that allocation to maximize light interception (increased leaf surface area) under shaded conditions is the primary strategy to growth and survival in shade. Allocation to stem growth and water transport capacity appears to diminish under shade. This effect of 'shade' may be more detrimental for

shade-intolerant species that inherently have greater hydraulic capacities than shade-tolerant species. There has certainly been a significant amount of focus on leaf specific attributes to explain differences in shade tolerance, however it might be emphasized that this parameter alone will not explain all the dynamics of shade tolerant and intolerant trees (Messier et al 1999, Givnish 1988). Survival in shade might be related to a tree switching its main goal from height growth to maximizing crown light interception, this is the concept of maximum sustainable height (Givnish 1988, Messier et al 1999). Gleeson and Tilman (1994) emphasize the least plastic traits of a plant will be the ones that determine or limit its distribution in a given environment. For many shade-intolerant plants, the ability to switch their inherent strategy from fast-growth to growth enhancing low light capture and resource conservation is likely to determine their survival in shade.

1.2 PART 2- Resource allocation and stand decline

Declining stand productivity of old stands is an almost universal occurrence in forests that span tree species and ecological biomes. There has been significant interest in understanding the causes of this decline and it has been a topic of intensive research. Net primary production (NPP), as depicted below, is a function of light energy available for photosynthesis (S_i), the proportion captured (P_i) and efficiency of conversion to carbohydrates (ε_i) and respiration (R) (Ryan et al. 1997):

$$NPP = \sum_{i=1}^{n} \varepsilon_i P_i S_i - R$$

It is readily apparent from this equation that respiration is a key metric. In fact, increasing respiration with stand development (as a consequence of increased woody biomass) was the long-standing explanation for stand decline (Whittaker and Woodwell 1967) but that hypothesis has been largely refuted (reviewed in Ryan et al. 1997, see also Litton et al. 2007). However, there are a variety of

alternative hypotheses in explanation of declining stand productivity. A seminal review by Ryan et al. (1997) overviewed the state of knowledge at the time and posed four questions as being critical to understanding changes in stand decline in older stands:

1. What causes leaf-area decline with age?
2. Does soil nutrition change and how does nutrition influence allocation to belowground, leaf area and photosynthesis?
3. What is the role and consistency of hydraulic limitations with tree height and it's influence on reducing photosynthesis.
4. Does allocation to fine roots and associated symbionts change with stand development and what causes these changes?

Since that time, additional questions and mechanisms have been proposed including:

5. The 'individual-tree, stand-structure hypothesis'. These authors contend the efficiency of growth is greatest in dominant trees and least in suppressed trees; thus the suppressed trees are not utilizing resources (nutrient and water) as efficiently as dominant trees, driving down the stands 'potential' for growth (Binkley et al. 2002).
6. A turgor limitation as gravitational effects of increasing height may lower inherent turgor pressure of cells high up in the canopy. Low turgor would slow down growth by reducing cell expansion and division (Ryan et al. 2006). This is a specific hypothesis that extends question 3 posed above.
7. A sink limitation hypothesis proposes that growth sinks in mature trees are not strong enough to stimulate the active transport of carbohydrates to new tissues (Ryan et al. 2006).

Almost all of these hypotheses have subsequent studies that appear to support and refute them. For example, for hypothesis 5, Binkley (2004) found

that for two mixed species stands in coastal Oregon that early in stand development there was generally a lack of dominance (all trees were contributing equally to production of a stand). As the stand developed there was a switch to dominance of large individuals and then it began to go back towards a lack of dominance at maturity. In contrast, growth efficiency of suppressed *Pinus contorta* was 28% higher than co-dominant and dominant trees in boreal forests of Alberta (Reid et al. 2004). Because of the widespread nature of forest decline with age, it has been suggested by at least one author that 'it is difficult to discard a simple, universal explanation' (Ryan et al. 2006). However, it may be entirely possible that though this pattern of decline is a consistent phenomenon that spans different ecosystem types and forest biomes; the mechanisms for decline may not converge. Therefore, it is crucial that these questions be addressed in a variety of forest biomes in order to better understand the generality of findings within specific studies.

In the paragraphs below, I will review current and relevant research findings relating to questions 1 and 4.

1.2.1 Question 1- declining leaf area

> 'The most important leaves of a tree are usually those at the top because it is with these that the tree can best compete with its neighbors for a place in the sun.' -Zimmerman (1978)

As stands develop, the light environment at both the stand and tree-level changes substantially. At the level of the individual tree, the lower crown positions go into ever-increasing darkness creating disparity between light levels in the upper versus lower crown positions. It is clear that crown recession is a consequence of these changes but it is up for debate if it is: (i) strictly the amount of light that is independently driving lower branch mortality (Mäkelä 1997) or (ii) if it is driven by intrinsic factors within the tree. At the stand-level, factors

contributing to leaf area decline may include: crown shyness/abrasions (Rudnicki et al. 2003, Fish et al. 2006, Meng et al. 2006b) and changes in growth efficiency and dominance relating to trees of different canopy positions (Binkley 2004, Reid et al. 2004, Sillett et al. 2010). However, the primary focus of the following paragraphs is directed towards tree-level considerations.

1.2.1.1 Light as a driver of lower branch mortality

Resources needed for plant survival include adequate light, water and nutrients. When a negative carbon balance is reached, where gross photosynthesis does not exceed respiration and growth demands, branch (Witowski 1997) or tree death is imminent. Clearly, the degree of shading does influence this basic principle, as photosynthetic light curves will dictate at what light level this negative C status should occur. However, branch or tree death that occurs above the light compensation point is indicative of other (possibly interacting) constraints related to water or nutrient availability.

The impact of shade on plant morphology and biomass allocation has been well-studied. Specific leaf mass increases with increasing shade (Walters et al. 1993, Fownes and Harrington 2004) and leaves become more horizontally distributed (Messier et al. 1999) to better capture light. In shade tolerant species, thinner and more horizontally dispersed leaf area is produced to more efficiently capture light (Givnish 1988, Chen et al. 1996, Messier et al. 1999, Williams et al. 1999) while shade intolerant species may forgo all other allocation demands in favor of leader extension to 'outgrow' the shade (eg. Naidu et al. 1998). Although empirical data is more limited, reduced root growth may be an additional consequence of shading (Reich et al. 1998, Messier et al. 1999, Fownes and Harrington 2004). Much less effort has focused on understanding how shade impacts root production and other components of the hydraulic architecture of woody species.

The ability to transport water does appear to diminish under shade (Schultz and Matthews 1993, Shumway et al. 1993, Protz et al. 2000, Sellin and

Kupper 2004, Cochard et al. 1999), yet it is unclear if this is a general phenomenon, if it is related to the inherent shade tolerance of a species or possibly linked to the branch position within the crown. Under closed canopy conditions, there have typically been clearer decreases in hydraulic conductivity from upper to lower branches (Zimmerman 1978, Protz et al. 2000, Burgess et al. 2006); suggesting that the light environment is likely a driving factor.

Shading will inherently reduce the photosynthetic potential of shaded branches. Reduced ability to transport water may further reduce photosynthesis and could drive early branch mortality, even prior to light levels leading to a negative carbon balance. Moreover, if these branches are also less capable of withstanding drought cycles, they may also succumb to drought-induced mortality at times of water deficits during the growing season.

1.2.1.2 Intrinsic factors within the tree

Indirect evidence suggests that light alone is not the sole driver of lower branch mortality. Two lab-based empirical studies have demonstrated a dichotomy in whole-tree versus partial-tree shading. Henriksson (2001) shaded whole mountain birch (*Betula pubscens*) as well as individual branches and found that individual branch shading eventually led to branch death while whole tree shading resulted in maintenance of all branches. Similarly, maintenance respiration was 50% of photosynthate allocated to individually shaded branches of 2-year old walnut (*Juglans regia*) and similar branches had only 30% of photosynthates allocated to respiration in unshaded branches (Lacointe et al. 2004).

Similarly, observations of amabilis fir (*Abies amabilis* (Dougl.) Forbes) also appear to corroborate the lab-based studies above. Sprugel (2002) showed that suppressed individauls would carry live branches in a light environment which would normally result in lower branch mortality of trees in a dominant canopy position.

At the tree level, source-sink dynamics are likely to influence allocation patterns and subsequent growth or survival of branches. Sink strength may be defined as potential for assimilate accumulation (Patrick 1993) and functionally operates via gradients in concentration in assimilates between sources and sinks (Sprugel et al. 1991). Similarly, a strong resource sink is likely capable of pulling resources from greater distances than a weaker sink (Sprugel et al. 1991). Growth activity and hormonal control are both potential mechanisms for sink strength (Sprugel et al. 1991). Disparity in the light environment within a tree crown could plausibly set-up a situation where the more illuminated part of the crown is physiologically more active (and therefore a stronger resource sink) than the shaded part of the crown.

Outside of light-disparity driven interactions, there may be additional factors that constrain the growth and development of lower branches. For example, lower branches may lose nitrogen to upper branches during periods of soil nutritional stress as was seen in an open *Eucalyptus globulus* plantation (Pate and Arthur 2000). Similarly, supplemental fertilization of *Pinus contorta* prolonged the life of lower branches (Amponsah et al. 2004).

Water stress may also limit lower branches more than upper branches. Even in illuminated conditions, lower branches may have lower conductance and sap flux than upper branches, as was seen in *Larix decidua* (Kupper et al. 2006); however, this is not universally documented and other studies have observed no difference in these types of parameters (Hubbard et al. 2002, Protz et al. 2000). The lack of difference may also be a consequence of adjustment of leaf area to sapwood area as observed in *Pinus ponderosa* (Hubbard et al. 2002).

1.2.2 Question 2- increased belowground allocation

> Changes in C flux and partitioning with forest development, particularly to roots, remain poorly understood. -Litton et al. (2007)

Plant roots are inherently difficult to study due to the fact that they are below ground. This difficulty continues to increase as plant size increases from a seedling to a mature tree. Consequently, it is not surprising that less effort has been focused on understanding belowground dynamics through stand development.

As soil resources become limiting, trees may place increased effort into root production in order to be more competitive. However, as tree size increases, there is ever increasing distance between leaves and roots which may actually result in reduced carbon to roots (Landhausser and Lieffers 2012) and lowered root production. Reduced root allocation would presumably lead to reduced water and nutrient uptake and, eventually, reduced photosynthetic capacity. Indirectly, this could be exhibited as increased water stress or reduced water transport to the upper crown (Mencuccini and Grace 1996, Menuccini 2003) or the commonly observed reduction in leaf area index with stand age (eg. Ryan et al. 1997, Smith and Resh 1999, Ryan et al. 2004). Tree carbon allocation relative to roots at both the tree and stand level are reviewed in the following paragraphs.

1.2.2.1 Tree-level considerations

The vast majority of carbon allocation work has been conducted under controlled greenhouse conditions on young seedlings therefore extrapolation to a 10-20 m tall tree should be taken with caution. With this in mind, however, for conifers carbohydrates are first allocated to shoot growth (Gordon and Larson 1968, Domisch et al. 2002) and then later to root growth (Schier 1970, Schneider and Schmitz 1989, Hansen and Beck 1994, Domisch et al. 2002, Kagawa et al. 2006). Occasionally, a bi-modal (Hansen et al. 1996) or continuous (Ursino et al. 1968) pattern of carbon allocation to roots has been observed.

In *Eucalyptus*, lower branches are the primary providers of carbohydrates for roots while mid- and upper branches primarily support shoot growth of upper crown (Pate and Arthur 2000). As described previously, lower branches appear to be at a disadvantage for C fixation for a suite of reasons. Therefore, as trees

increase in size, it is plausible that with the decline of lower shoots there is also a decline in carbohydrate resources in roots. This may be further exacerbated by the increasing physical distance between nutrient and water-gathering fine roots and carbon-producing leaves; which will inherently lower potential source-sink gradients (Landhausser and Lieffers 2012).

1.2.2.2 Stand-level considerations

Two types of data have been collected to represent belowground dynamics through stand development: fine root biomass and total belowground carbon flux (TBCF). Fine root biomass is analogous to leaf biomass or leaf area (Farrar and Jones 2003). TBCF is the total belowground flux in carbon, it encompasses belowground root production and respiration, root exudation and carbon used for mycorrhizas (Litton et al. 2007). In practice, it is often determined by calculating CO_2 efflux subtracted by aboveground litterfall (Litton et al. 2007). However, TBCF does not tell us the potential absorbing surface area of fine roots supplying the aboveground biomass in forests of different ages. Further, it does not separate allocation for those roots used in the acquisition of nutrients and water (analogous to aboveground leaf area) with the roots used for transport and structural support (analogous to the stem).

Few studies have examined simultaneously the standing mass of fine and coarse roots in relation to aboveground mass such as wood volume or leaf mass as stands age and move it shifts through stand development. When comparing the relationship between fine roots to leaf biomass, the two may increase together and then root mass may plateau and leaf mass may continue to increase later in stand development (Vogt et al. 1987) or both may continually increase with age (Litton et al. 2004).

Meta-analysis of carbon flux studies suggest that total respiration, foliage production, wood production and TBCF (includes root growth, respiration and turnover) all respond positively to increases in GPP across evergreen conifers, deciduous broadleaf and evergreen broadleaf forest types (Litton et al. 2007).

However, they found that the proportion of C dedicated to respiration and foliage remained constant, the fraction portioned out to wood increased with increasing GPP and the fraction portioned to TBCF appeared to decrease as stands aged (Litton et al. 2007). These results broadly suggest that wood production and belowground allocation are the most flexible sinks for C allocation while foliage and respiration are conservative. In addition, Litton et al. (2007) observed that during periods of greatest GPP, relative allocation to belowground was lowest. During later parts of the stand life-cyle, this may present the onset of a negative feedback loop where reduced root growth or allocation may trigger reduced GPP due to reduction in ability to aquire soil resources (water or nutrients).

When examined for an individual stand, the proportion of C allocated to TBCF (which includes root growth, respiration and turnover) appeared to increase with age in a short-rotation *Eucalyptus salgina* stand (Ryan et al. 2004). However, the actual quantity of C being allocated belowground was actually declining during stand development due to an overall decrease in NPP (Ryan et al. 2004), which is consistent with Litton et al. (2007). Litton et al. (2004) found the TBCA (total belowground carbon allocation which is a similar quantity to TBCF) was similar between young (12 years) and mature (100 years) lodgepole pine stands, in fact it did not even appear to vary with density in young stands. A similar stability in C allocation was obtained in a lodgepole pine chronosequence from age 15-100 years; however the decline in TRCA (total root carbon allocation) did occur at age 260 (Smith and Resh 1999). Smith and Resh (1999) also observed the characteristic peak and decline of both wood production and leaf area index with age.

1.3 PART 3: Study systems and tree species

1.3.1 Study systems

The study locations are located in two geographically distinct regions. The first region is north of Whitecourt, AB in the lower foothills natural sub-

region (Beckingham et al 1996). Average total precipitation in this region is 578 mm. Daily average temperature is 2.6 ºC with a mean monthly January being -12.1 ºC on average and July 15.7 ºC (Environment Canada 2011).

The second study region is located along a 33 km north-south band, south of Hinton, Alberta, Canada (53° 14.384' -117° 28.596' to 53° 3.43' -117° 4 .145'). Elevation ranged from 1420 – 1577m and all stands had south facing aspects. This elevation range is transitional between the upper foothills and the sub-alpine natural subregions (Beckingham et al 1996) of Alberta.

In both study regions, forest harvesting and oil and gas related activities are widespread. In the absence of man-made disturbances, forest fires will typically be stand-replacing.

1.3.2 Study species

The focus of the thesis will include the study of two shade intolerant pines (*Pinus banksiana* Lamb and *Pinus contorta* Dougl. Ex Loud.) and two shade tolerant spruces (*Picea mariana* (Mill) B.S.P. and *Picea glauca* (Moench)) (Klinka et al 1999). In the boreal forests of western Canada, both pine species occur as early-successional species the typically establish after stand-replacing disturbances. They often occur in monocultures or as overstory trees in mixed conifer and deciduous stands. *Picea glauca* is a common tree in upland areas of the boreal landscape. It can occur in monocultures as an overstory tree but will commonly regenerate underneath the overstory of aspen (*Populus tremuloides*) dominated stands. Eventually, the spruce will overtop the aspen and become a dominant tree. In contrast, *Picea mariana* is a common inhabitant of low-lying areas that are often poorly drained (Klinka et al 1999). In these areas, it forms the dominant tree species, sometimes co-occurring with *Larix laricina*. It is also often found regenerating in high densities underneath *Pinus contorta* and occasionally individuals may be found underneath aspen dominated stands.

1.4 Goals and structure of thesis

My overall objective is to understand how hydraulic architecture, crown form and resource allocation are affected by shading trees of opposing shade tolerance. The studies range from examinations at the scale of the individual wood cell to entire stands. Chapters 2-5 will utilize comparisons of shade tolerant (*Picea*) and intolerant (*Pinus*) genera. In chapter 6, I will explore the second hypothesis utilizing a single species (*Pinus contorta*) due to enormity of effort required to execute the project. I compare responses of species with different shade tolerance within the Pinaceae family. Light is a critical component that changes substantially through stand development and I expect that the mechanisms for responses will differ with tolerance. In order to address these goals, the following questions will be asked:

Q1: How do trees of opposing shade tolerance adjust hydraulically to the understory environment.

Chapter 2 provides a mechanistic context for branch-level adjustment to shade in the context of water transport.

Q2: Are seasonal carbohydrate changes in tissues of *Picea* and *Pinus* trees similar? **Q3:** Does cohort position (co-dominant versus suppressed) influence seasonal carbohydrate dynamics and fluxes in shade tolerant *Picea glauca*?

Chapters 3 and 4 were designed with the purpose of linking seasonal carbohydrate changes in important tissues of *Picea* and *Pinus* trees with seasonal growth changes and phenology. These studies provides a link between Chapter 2 and Chapter 5 in that it encompasses both the aspect of whole plant shading (as in Chapter 2) as well as the dynamics between upper and lower branches (the focus of Chapter 5).

Q4: What is the impact of asymmetrical vs. uniform crown shading on the mortality and growth of upper and lower branches within tree crowns? Are these impacts similar for species with opposing levels of shade tolerance?

Chapter 5 systematically explores the impact of asymmetrical vs. uniform crown shading on the mortality and growth of upper and lower branches within tree crowns. The results of this chapter apply to changes in crown structure and consequently tree leaf area dynamics.

Chapter 3 and 4 also describe seasonal C dynamics in relation to branch position, which will further support work in Chapter 5.

Q5: How does the interplay between the fundamental resource acquisition organs of forest trees change through stand development?

Chapter 6 examines stand-level changes in biomass allocation patterns in relation to functional root and leaf area development in a chronological sequence.

1.5 References

Amponsah, IG, Lieffers VJ, Comeau PG, Brockley RP (2004) Growth response and sapwood hydraulic properties of young lodgepole pine following repeated fertilization. Tree Physiol 24: 1099-1108

Beaudet M, Messier C (1998) Growth and morphological responses of yellow birch, sugar maple, and beech seedlings growing under a natural light gradient. Can J For Res 28: 1007-1015

Beckingham JD, Corns IGW, Archibald JH (1996) Field guide to ecosites of west-central Alberta. Northern Forestry Centre, Canadian Forest Service. 380 pp

Binkley D, Stape JL, Ryan MG, Barnard HR, Fownes J (2002) Age-related decline in forest ecosystem growth: an individual tree, stand-structure hypothesis. Ecosystems 5: 58-67

Binkley D (2004) A hypothesis about the interaction of tree dominance and stand production through stand development. For Ecol Manage 190: 265-271

Burgess SSO, Pittermann J, Dawson TE (2006) Hydraulic efficiency and safety of branch xylem increases with height in *Sequoia sempervirens* (D. Don) crowns. Plant Cell Environ 29: 229-239

Canham CD (1988) Growth and canopy architecture of shade-tolerant trees: response to canopy gaps. Ecology 69: 786-795

Chen HYH, Klinka K, Kayahara GJ (1996) Effects of light on growth, crown architecture, and specific leaf area for naturally established *Pinus contorta* var. *latifolia* and *Pseudotsuga menziesii* var. *glauca* saplings. Can J For Res 26: 1149-1157

Cochard H, Lemoine D, Dreyer E (1999) The effects of acclimation to sunlight on the xylem vulnerability to embolism in *Fagus sylvatica* L. Plant Cell Environ 22: 101-108

Domisch T, Finér L, Lehto T (2002) Growth, carbohydrate and nutrient allocation of Scots pine seedlings after exposure to simulated low soil temperature in spring. Plant Soil 246: 75-86

Ewers BE, Oren R, Sperry JS (2000) Influence of nutrient versus water supply on hydraulic architecture and water balance in *Pinus taeda*. Plant Cell Environ 23: 1055-1066

Farrar JF, Jones DL (2003) The control of carbon acquisition by and growth of roots *In* Root Ecology. *Eds* de Kroon H, Visser EJ. Springer-Verlag, Heidelberg, Germany. pp 91-119

Fish H, Lieffers VJ, Silins U, Hall RJ (2006) Crown shyness in lodgepole pine stands of varying stand height, density, and site index in the upper foothills of Alberta. Can J For Res 36: 2104-2111

Fownes JH, Harrington RA (2004) Seedling response to gaps: separating effects of light and nitrogen. For Ecol Manage 203: 297-310

Givnish TJ (1988) Adaptation to sun and shade: a whole-plant perspective. Aust J Plant Physiol 15: 63-92

Gleeson SK, Tilman D (1994) Plant allocation, growth rate and successional status. Func Ecol 8: 543-550

Gordon JC, Larson PR (1968) Seasonal course of photosynthesis, respiration and distribution of ^{14}C in young *Pinus resinosa* trees as related to wood formation. Plant Physiol 43: 1617-1624

Hansen J, Beck E (1994) Seasonal changes in the utilization and turnover of assimilation products in 8-year-old Scots pine (*Pinus sylvestris* L.) trees. Trees 8: 172-182

Hansen J, Vogg G, Beck E (1996) Assimilation, allocation and utilization of carbon by 3-year-old Scots pine (*Pinus sylvestris* L.) trees during winter and early spring. Trees 11: 83-90

Henriksson JH (2001) Differential shading of branches or whole trees: survival, growth, and reproduction. Oecol 126: 482-486

Hubbard RM, Bond BJ, Senock RS, Ryan MG (2002) Effects of branch height on leaf gas exchange, branch hydraulic conductance and branch sap flux in open-grown ponderosa pine. Tree Physiol 22: 575-581

Landhausser SM, Lieffers VJ (2012) Defoliation increases risk of carbon starvation in root systems of mature aspen. Trees 26: 653-661

Litton CM, Raich JW, Ryan MG (2007) Carbon allocation in forest ecosystems. Glob Change Biol 13: 2089-2109

Kagawa A, Sugimoto A, Maximov T (2006) Seasonal course of translocation, storage and remobilization of 13C pulse-labeled photoassimilate in naturally growing Larix gmelinii saplings. New Phytol 171: 793-804

Klinka K, Worrall J, Skoda L, Varga P, Krajina VJ (1999) The distribution and synopsis of ecological and silvical characteristics of tree species in British Columbia's forests 2nd ed. Canadian Cartographics Ltd Coquitlam, BC

Kupper P, Sellin A, Tenhunen J, Schmidt M, Rahi M (2006) Effects of branch position on water relations and gas exchange of European larch trees in an alpine community. Trees 20: 265-272

Lacointe A, Deleens E, Ameglio T, Saint-Joanis B, Lelarge C, Vandame M, Song GC, Daudet FA (2004) Testing the branch autonomy theory: a $^{13}C/^{14}C$ double-labelling experiment on differentially shaded branches. Plant Cell Environ 27: 1159-1168

Mäkelä A (1997) A carbon balance model of growth and self-pruning in trees based on structural relationships. For Sci 43: 7-24

Meng SX, Lieffers VJ, Reid DB, Rudnicki M, Silins U, Jin M (2006a) Reducing stem bending increases the height growth of tall pines. J Exp Bot 57: 3175-3182

Meng SX, Rudnicki M, Lieffers VJ, Reid DB, Silins U (2006b) Preventing crown collisions increases the crown cover and leaf area of maturing lodgepole pine. J Ecol 94: 681-686

Mencuccini M (2003) The ecological significance of long-distance water transport: short-term regulation, long-term acclimation and the hydraulic costs of stature across plant life forms. Plant Cell Environ 26: 163-182

Mencuccini M, Grace J (1996) Hydraulic conductance, light interception and needle nutrient concentration in Scots pine stands and their relations with net primary productivity. Tree Physiol 16: 459-468

Messier C, Doucet R, Ruel JC, Claveau Y, Kelly C, Lechowicz MJ (1999) Functional ecology of advance regeneration in relation to light in boreal forests. Can J For Res 29: 812-823

Naidu SL, DeLucia EH, Thomas RB (1998) Contrasting patterns of biomass allocation in dominant and suppressed loblolly pine. Can J For Res 28: 1116-1124

Pate JS, Arthur DJ (2000) Uptake, partitioning and utilization of carbon and nitrogen in the bark bleeding tree, Tasmanian blue gum (Eucalyptus globulus). Aust J Plant Physiol 27: 869-884

Patrick JW (1993) Sink strength: Whole plant considerations. Plant Cell Environ 16: 1019-1020

Pinol J, Sala A (2000) Ecological implications of xylem cavitation for several Pinaceae in the Pacific Northern USA. Func Ecol 14: 538-545

Potheir D, Margolis HA, Poliquin J, Waring RH (1989) Relation between the permeability and the anatomy of jack pine sapwood with stand development. Can J For Res 19: 1564-1570

Protz CG, Silins U, Lieffers VJ (2000) Reduction in branch sapwood hydraulic permeability as a factor limiting survival of lower branches of lodgepole pine. Can J For Res 30: 1088-1095

Reich PB, Tjoelker MG, Walters MB, Vanderklein DW, Buschena C (1998) Close association of RGR, leaf and root morphology, seed mass and shade tolerance in seedlings of nine boreal tree species grown in high and low light. Func Ecol 12: 327-338

Reid DEB, Lieffers VJ, Silins U (2004) Growth and crown efficiency of height repressed lodgepole pine; are suppressed trees more efficient? Trees 18: 390-398

Reid, DE, Silins U, Lieffers VJ (2003) Stem sapwood permeability in relation to crown dominance and site quality in self-thinning fire origin lodgepole pine stands. Tree Physiol 23: 833-840

Rudnicki M, Lieffers VJ, Silins U (2003) Stand structure governs the crown collisions of lodgepole pine. Can J For Res 33: 1238-1244

Ryan MG, Binkley D, Fownes JH (1997) Age-related decline in forest productivity: pattern and process *in* Advances in Ecological Research Vol 27. ISBN 0-12-013927-8

Ryan MG, Binkley D, Fownes JH, Giardina CP, Senock RS (2004) An experimental test of the causes of forest growth decline with stand age. Ecol Mon 74: 393-414

Ryan MG, Phillips N, Bond BJ (2006) The hydraulic limitation hypothesis revisited. Plant Cell Environ 29: 367-381

Schier GA (1970) Seasonal pathways of ^{14}C-photosynthate in red pine labeled in May, July, and October. For Sci 16: 1-13

Schneider A, Schmitz K (1989) Seasonal course of translocation and distribution of 14C-labelled photoassimilate in young trees of Larix decidua Mill. Trees 4: 185-191

Schoettle AW, Smith WK (1991) Interrelation between shoot characteristics and solar irradiance in the crown of Pinus contorta ssp. latifolia. Tree Physiol 9: 245-254

Schultz HR, Matthews MA (1993) Xylem development and hydraulic conductance in sun and shade shoots of grapevine (Vitis vinifera L.): evidence that low light uncouples water transport capacity from leaf area. Planta 190: 393-406

Sellin A (1993) Resistance to water flow in xylem of *Picea abies* (L.) Karst. trees grown under contrasting light conditions. Trees 7: 220-226

Sellin A, Kupper P (2004) Within-crown variation in leaf conductance of Norway spruce: effects of irradiance, vapour pressure deficit, leaf water status and plant hydraulic constraints. Ann For Sci 61: 419-429

Shelburne VB, Hedden RL (1996) Effect of stem height, dominance class, and site quality on sapwood permeability in loblolly pine, (*Pinus taeda* L.). For Ecol Manage 83: 163-169

Shumway D.L., Steiner K.C. & Kolb T.E. (1993) Variation in seedling hydraulic architecture as a function of species and environment. Tree Physiol 12: 41-54

Sillett SC, Van Pelt R, Koch GW, Ambrose AR, Carroll AL, Antoine ME, Mifsud BM (2010) Increasing wood production through old age in tall trees. Forest Ecol and Manage 259: 976-994

Sprugel DG (2002) When branch autonomy fails: Milton's Law of resource availability and allocation. Tree Physiol 22: 1119-1124

Sprugel DG, Hinckley TM, Schaap W (1991) The theory and practice of branch autonomy. Ann Rev Ecol Sys 22: 309-334

Tyree MT, Velez V, Dalling JW (1998) Growth dynamics of root and shoot hydraulic conductance in seedlings of five neotropical tree species: scaling to show possible adaptation to differing light regimes. Oecologia 114: 293-298

Tyree MT, Zimmermann MH (2002) Xylem Structure and the Ascent of Sap 2nd ed. Springer-Verlag, New York, NY

Ursino DJ, Nelson CD, Krotkov G (1968) Seasonal changes in the distribution of photo-assimilated 14C in young pine plants. Plant Physiol 43: 845-852

Vogt KA, Vogt DJ, Moore EE, Babatunde AF, Redlin MR, Edmonds RL (1987) Conifer and angiosperm fine-root biomass in relation to stand age and site productivity in Douglas-fir forests. J Ecol 75: 857-870

Walters MB, Kruger EL, Reich PB (1993) Relative growth rate in relation to physiological and morphological traits for northern hardwood tree seedlings: species, light environment and ontogenetic considerations. Oecol 96: 219-231

Walters MB, Reich PB (1999) Low-light carbon balance and shade tolerance in the seedlings of woody plants: do winter deciduous and broad-leaved evergreen species differ? New Phytol 143: 143-154

Williams H, Messier C, Kneeshaw DD (1999) Effects of light availability and sapling size on the growth and crown morphology of understory Douglas-fir and lodgepole pine. Can J For Res 29: 222-231

Witowski (1997) Gas exchange of the lowest branches of young Scots pine: a cost-benefit analysis of seasonal branch carbon budget. Tree Physiol 17: 757-765

Whittaker RH, Woodwell GM (1967) Surface area relations of woody plants and forest communities. Am J Bot 54: 931-939

Woodrum CL, Ewers FW, Telewski FW (2003) Hydraulic, biomechanical, and anatomical interactions of xylem from five species of *Acer* (Aceraceae). Am J Bot 90: 693-699

Wright EF, Coates KD, Canham CD, Bartemucci P (1998) Species variability in growth response to light across climatic regions in northwestern British Columbia. Can J For Res 28: 871-886

Zimmerman MH (1978) Hydraulic architecture of some diffuse-porous trees. Can J Bot 56: 2286-2295

Chapter 2 Hydraulic acclimation to shading in boreal conifers of varying shade tolerance

A version of this chapter has been published: Schoonmaker ALS, Hacke UG, Landhäusser SM, Lieffers VJ, Tyree MT (2010) Plant Cell Environ 33: 382-393

2.1 Introduction

Shade tolerant trees have adopted a suite of strategies to prolong their survival in shade (Walters and Reich 1999). These include changing the spatial arrangement and morphology of leaves, increasing the allocation of C towards leaf production in order to maximize light capture (Givnish 1988; Pearcy 2007), reducing allocation of C to the root system (Callaway 1992; Landhäusser and Lieffers 2001; Renninger et al. 2006; Pearcy 2007) and lowering respiration rates and photosynthetic compensation points of foliage (Callaway 1992). The sheltered environment of an understory also has reduced potential evaporative demands and wind speeds (Bladon et al. 2006). Given these changes, one also would expect the hydraulic architecture in these species to be altered by the sheltered understory environment. To date, however, little research has actually tested this idea in a field experiment.

Angiosperm seedlings grown under artificial shade or low light have demonstrated reduced leaf-specific conductivity (Schultz and Matthews 1993; Shumway et al. 1993; Brodribb et al. 2005) whereas suppressed (reduction in height growth due to shading and competition by surrounding overstory trees) conifers have previously showed no reduction (Renninger et al. 2007). Shading has been associated with reduced sapwood-area specific conductivity in lower branches relative to upper sun-exposed branches of *Pinus contorta* (Protz et al. 2000). Suppression reduced sapwood-area specific conductivity in *Pseudotsuga menziesii, Tsuga heterophylla* and *Picea abies* compared with released (previously-suppressed trees where the overstory had been removed) (Renninger et al. 2006) or sun-exposed (Sellin 1993) individuals.

The xylem pressure causing 50% loss in hydraulic conductivity (P_{50}), a proxy of cavitation resistance, was less negative in four artificially shaded European deciduous angiosperm seedlings (Barigah et al. 2006) as well as in shaded versus sun-lit branches of *Fagus sylvatica* (Cochard et al. 1999; Lemoine et al. 2002). The relative magnitude of the decline in cavitation resistance, however, did not appear to be related to the inherent shade tolerance of the individual angiosperms measured (Barigah et al. 2006). It is unclear whether these findings are more widely applicable to conifers and especially under field conditions.

The mechanism driving cavitation resistance in conifers is not completely understood. Most recently, Cochard et al. (2009) have suggested capillary failure as a possible candidate and further speculated that incomplete contact between the torus and pit chamber or pores within the torus could allow air entry. Across a variety of northern hemisphere conifer species, resistance to cavitation and pit resistance have been positively correlated (Pittermann et al. 2006a). Higher wood density and smaller diameter tracheids have also been correlated with increased cavitation resistance (Hacke et al. 2001; Pittermann et al. 2006b, Hacke and Jansen 2009). As tracheid diameter tends to be narrower in shaded branches or suppressed individuals (Protz et al. 2000; Renninger et al. 2006), it could be inferred that shading should increase resistance to cavitation; however, this relationship was not detected in shaded angiosperms (Cochard et al. 1999; Lemoine et al. 2002; Barigah et al. 2006). There appears to be a correlation between increased cavitation resistance and declining pit aperture diameter with height in both *Pseudotsuga menziesii* and *Sequoia sempervirens* (Burgess et al. 2006; Domec et al. 2006; Domec *et al.* 2008). Similarly, Mayr et al. (2002) found that the ratio pit aperture:pit diameter declined with increased elevation and cavitation resistance in *Picea abies*. There is little information, however, on how these characteristics change in understory conifers and how these are affected by the shade tolerance of the species. Given the uncertainties regarding cavitation resistance and how this relates to the tracheid anatomy of conifers, further investigation is warranted.

The objective of this study was to assess how understory shading influences the hydraulic architecture and tracheid anatomy of boreal conifers of varying shade tolerance, grown in either full light or under a deciduous-dominated canopy. I studied two shade intolerant pines (*Pinus banksiana* and *Pinus contorta*) and two shade tolerant spruces (*Picea mariana* and *Picea glauca*). In the boreal forests of western Canada, both pines are early-successional species that typically establish after stand-replacing disturbances. *Picea glauca* commonly regenerates underneath an overstory of aspen (*Populus tremuloides*) and will eventually overtop the aspen and become a dominant tree. In contrast, *Picea mariana* is a common inhabitant of low-lying areas that are often poorly drained. However, it is also often found regenerating in high densities underneath a canopy dominated by *Pinus contorta* and sparsely in the understory of aspen-dominated stands. *I* are hypothesizing that understory grown conifers will have: 1) increased vulnerability to embolism compared with open grown conifers, 2) lower sapwood-area specific conductivity driven by smaller tracheid diameters and 3) lower leaf-area specific conductivity and soil-to-plant hydraulic conductance compared to open grown conifers. Given that *Picea glauca* has shown greater morphological plasticity (relative to *Pinus contorta*) when grown in this type of shade (Landhäusser & Lieffers 2001) I are expecting that the differences between open and understory conifers will be larger in the shade-tolerant spruces than the shade-intolerant pines.

2.2 Methods

2.2.1 Study location and experimental design

One-year-old *Pinus banksiana* Lamb, *Pinus contorta* Dougl. Ex Loud., *Picea mariana* (Mill) B.S.P. and *Picea glauca* (Moench) Voss seedlings, nursery grown container stock grown from local seed sources, were planted in the spring of 2000 at the University of Alberta Farm (Ellerslie), Edmonton, Alberta (53°N 113° W). Forty seedlings of each species were planted in an open field at 1.0 m spacing. Another set of seedlings (50 of each species) were planted in a nearby aspen-dominated forest. Average leaf area index (LAI) in the stand was 1.82 ±

0.24 (mean ± SD) (LAI-2000, Licor, Lincoln NE) with an average light transmission of 21.5 ± 5.5%. Seedlings were arranged at 0.5m spacing in 10 separate plots (5 seedlings of each species) to account for the variability in light conditions in the understory environment. After the first establishment year, two seedlings of each species in each understory plot and 10 seedlings of each species in the open area were caged to prevent browsing over the following years. Seedlings were grown for a total of six years throughout which they were kept weed free. For the first 3 years, all seedlings were watered during periods of summer drought (June-August) and fertilized with a slow release fertilizer (Osmocote 14-14-14 N-P-K) in order to ensure establishment. After the third year, no additional watering or fertilization took place.

2.2.2 Growth measurements

Six trees of each species growing in the open field and deciduous understory were harvested in August 2007. Total height and diameter at the root base were measured to the nearest 0.5 mm. To determine whole tree leaf area (A_l), projected leaf area was determined on a sub-sample of fresh needles collected from each tree using Winfolia (Regent Instruments Inc. Quebec City, Quebec) image analysis software. Measured needles were oven-dried and weighed. The remaining needles on each tree were removed, oven-dried and weighed. The relationship between needle dry weight and projected leaf area from the sub-samples was used to calculate A_l for each tree.

2.2.3 Soil-to-plant hydraulic conductance

To determine soil-to-plant hydraulic conductance (K_{s-p}), 12 trees of each species growing in the open field and deciduous understory were selected. Measurements were conducted over four days (August 1, 2, 15 and 16, 2007) and six pine and spruce trees from the understory and open were measured each day (Saliendra et al. 1995; Andrade et al. 1998; Sellin 2001). A summary of ambient conditions during the four day period (Environment Canada 2009) is given in Table 1. The afternoon prior to the measurement day, a current year branch from

upper crown position was covered with foil and a plastic bag to reduce cuticular transpiration. Pre-dawn (3:00-6:00) and midday (11:30-15:00) water potential (Ψ_{plant}) measurements were made on current year shoots using a Scholander pressure chamber (PMS Instruments, Corvallis USA). Midday measurements of transpiration (E) were taken with a steady-state porometer (Li-cor 1600, Lincoln, NE) concurrently with the Ψ_{plant} measurements. Using these measurements, K_{s-p} was determined as:

$$K_{s-p} = \frac{E}{\Delta P} \text{ where } \Delta P = \Psi_{midday} - \Psi_{predawn} \quad (1)$$

Table 1: Average air temperature (Temp), photosynthetically active radiation (PAR) and vapor pressure deficit (VPD) during the period 11:00-15:00. PAR was measured in open conditions.

Date	Temp (° C)	PAR (μmol s^{-1} m^{-2})	VPD (kPa)
August 1 2007	21.3	1634.2	1.14
August 2 2007	25.3	1306.5	1.74
August 15 2007	18.6	745.7	0.96
August 16 2007	21.6	1264.2	1.35

2.2.4 Hydraulic conductivity and vulnerability curves

Hydraulic conductivity (k_h) was measured on two-year-old apical stem segments from late September to mid-October 2007. For the open-grown pines, however, two-year-old segments were too large for the apparatus so one-year-old stem segments were used. In order to ensure that one and two-year-old stems of open grown pines gave comparable results I measured conductivity and vulnerability curves on smaller *Pinus contorta* saplings that were growing adjacent to the open-grown individuals in this study. Vulnerability curves constructed from one and two-year-old stems of these smaller trees were not significantly different from one another (data not shown). I followed a similar

measurement procedure as in Pittermann et al. (2006a) and Hacke and Jansen (2009) where a 14.2 cm segment was sealed to hoses on both ends and a small pressure head of filtered (0.2 mm) 20 mM KCl + 1 mM $CaCl_2$ solution was applied with outflow being measured every 10 seconds on a balance (CP225D, Sartorius, Göttingen, Germany). When outflow stabilized (within 2-5 minutes), I used the average outflow over the previous 40 seconds in order to calculate hydraulic conductivity as expressed below:

$$k_h = \frac{\text{water flow} \times \text{segment length}}{\text{pressure head}} \quad (2)$$

Hydraulic conductivity was measured both before and after flushing the stems with the same solution for 20 minutes at a pressure of 10 kPa in order to remove any native embolism. Overall, there was little or no change between pre- and post-flushing measurements; thus the maximum conductivity was taken as the larger of the two values obtained. Cross-sectional sapwood area (A_{leader}) was measured with a stereomicroscope (MS5, Leica, Wetzlar, Germany) and image-analysis software (ImagePro Plus 6.1, Media Cybernetics, Silver Spring, MD, USA). All needles distal to the measured segment were collected and distal leaf area ($A_{distal\ leaf}$) was determined similarly as in whole-plant leaf area measurement. Thus, sapwood-area specific conductivity (k_s) and leaf-area specific conductivity (k_l) were expressed as:

$$k_s = \frac{k_h}{A_{leader}} \quad (3)$$

$$k_l = \frac{k_h}{A_{distal\ leaf}} \quad (4)$$

Vulnerability to cavitation was determined by centrifuging a 14.2 cm stem segment to a known negative pressure for 10 minutes and then measuring the resulting conductivity. Each segment was repeatedly measured through a series of pressures (5-9 pressures depending on the species x treatment) (for more details

see Pittermann et al. 2006a; Hacke and Jansen 2009). The relationship between loss of conductivity and xylem pressure was fitted to two functions commonly used for this type of data. The first was a sigmoidal-exponential function (Pammenter and Vander Willigen 1998):

$$PLC = \frac{100}{1 + e^{a(x-b)}} \quad (5)$$

where x is the xylem pressure (MPa) at a corresponding PLC and a and b are coefficients that describe the slope and xylem pressure at 50% loss of conductivity (P_{50}). The second was a Weibull function (Li et al. 2008):

$$PLC = 100[1 - e^{-\left(\frac{-x}{b}\right)^c}] \quad (6)$$

where b determines the xylem pressure at 63.2% loss of hydraulic conductivity and c the steepness of the slope at b. Of the two fitted functions, I chose the one resulting in the best fit for each curve. The vulnerability curves fitting the data for each species (Figure 1) were determined based on the best fit for all of the data for all stems measured. Additionally, individual curves for each measured stem were fitted in order to estimate individual P_{50} measures that were averaged between species and growing environment (Figure 2a).

2.2.5 Xylem anatomical measurements: light microscopy

The anatomical measurements and parameters derived from these measurements follow the methodology and modeling in Pittermann et al. (2006 a,b) and Sperry et al. (2007). The same apical stem segments used in k_s and vulnerability measurements were also used for the anatomical measurements. Tracheid diameters (D_m) were measured on 3 radial files (2-3 cells wide) on thin cross-sections of the entire stem with a Leica DM3000 microscope at 200× magnification and analyzed with image analysis software (Image Pro). This

generated between 500-1100 individual diameter measurements per stem that included early and latewood tracheids. Average lumen resistivity (R_L) and the average lumen diameter (D) corresponding to R_L for each stem were expressed as:

$$R_L = \frac{128\eta}{\pi \Sigma D_m^4} n \quad (7)$$

$$D = \sqrt[4]{\frac{128\eta}{\pi R_L}} \quad (8)$$

where η is the viscosity of water at 20°C, n is the number of measured tracheids and D_m is the measured diameters of individual tracheids. Additionally, all of the tracheids measured in a species x treatment combination were pooled and summarized in a frequency histogram (Appendix 2).

Using the same cross sections as above, tracheid density was also estimated by counting the number of tracheids in each radial profile (which contained no rays) and multiplying it by the fraction of tracheid-occupied sapwood. Tracheid length (L) and pit measurements were determined by digesting wood sections in a 1:1 mixture of glacial acetic acid (80%) and hydrogen peroxide (30%) for 48 hours at 60 °C (Chaffey 2002). Macerated tissues were mounted on slides and average tracheid length determined by measuring a minimum of 50 tracheids using a light microscope at 25× magnification with image analysis software. One-sided tracheid surface area and the total number and area of inter-tracheid pits were measured on 5 tracheids per stem. Given that inter-tracheid pits will occupy only the radial walls of a tracheids I divided the total area occupied by pits on one radial wall by two times the area of a single tracheid wall in order to obtain the fraction of tracheid surface area (F_p) occupied by inter-tracheid pits:

$$F_p = \frac{\text{total area occupied by pits}}{2 \text{ x one - sided tracheid area}} \quad (9)$$

If it is assumed that a tracheid may approximate a rectangle then the total inter-tracheid pit area per tracheid (A_p) can by given as:

$$A_p = 4DLF_p \quad (10)$$

Tracheid resistivity (R_c) is given as:

$$R_c = R_L + R_w = \text{tracheid density x } R_{xa} \quad (11)$$

where R_w is the end wall resistivity and R_{xa} is the inverse of k_s. Pit-area resistance (r_p) is given as:

$$r_p = \frac{R_w L' A_p}{2} \quad (12)$$

where L' is the distance between tracheid end walls, a parameter that is assumed to approximate half the tracheid length (L), because tracheids will overlap by half on average (Lancashire and Ennos, 2002; Pittermann et al. 2006a).

2.2.6 Xylem anatomical measurements: Scanning electron microscopy (SEM)

Due to the labor-intensive nature of SEM measurements, I focused on describing two species (*Pinus contorta* and *Picea mariana*). I measured pit anatomical parameters on the same plant material used in hydraulic and vulnerability curve measurements (n=6). Samples were prepared for SEM measurements following a modified procedure from Jansen, Pletsers & Sano (2008). Specifically, 1 cm long frozen wood sections were split in half and thawed in distilled water for five days. After soaking, they were subjected to an ethanol dehydration series (30, 50, 70 and 90% for 0.5 hour in each concentration), immersed for 12 hours in 100% ethanol and finally air-dried for at least 24 hours. I found this procedure was very effective in minimizing aspiration

of bordered pits. Dried samples were split again, mounted on aluminum stubs with silver paint (Ted Pella Inc, Redding CA) and a thin layer of chromium (1-2 nm) was applied with a sputter coater for 1 minute. Photographs were taken with a JEOL 6301F field-emission scanning electron microscope at an accelerating voltage of 2.5 kV. Only earlywood pits were used for measurements. Below I describe the measurement procedure for a single stem segment (24 stem segments in total were measured from each species x light treatment). For measurement of pit, aperture and torus area and diameter, photographs were taken at 1000x magnification, resulting in the use of 6-20 pits per image.

Approximately 25-60 pits were measured and averaged for each individual stem. For measurement of the margo parameters (strand length, width, pore size, pore fraction and extended torus) 17-21 individual pits were photographed at 5000-11000x magnification. For each pit, I randomly measured the length of 4-8 margo strands and 8-12 strand widths and obtained an average for each pit. I selected a representative section of intact margo (approximately ¼ - ½ of the entire margo area) and measured the area of each pore and determined the mean and maximum pore area for each pit. The pore fraction represents the area taken up by pores relative to the whole margo (strands and pores). The presence of an extended torus was defined as a bridge of amorphous material that continuously connects the central torus with the pit border (Sano et al. 1999). Individual pit-level measurements were averaged for each stem segment analysed. Image analysis software (ImagePro) was used in the measurement of all pit structures.

2.2.7 Wood density

Wood density (ρ) was measured by water displacement. Specifically, the bark and pith was removed with tweezers and a razor blade from a 2.5 cm long stem section that was subsequently inserted with a pin into a beaker of water on a balance to determine the fresh volume of wood. Stems were then oven-dried at 80 °C for 48 hours. Wood density was expressed as the dry mass divided by the fresh volume.

2.2.8 Statistical analysis

R (R Development Core Team 2006) statistical environment for statistical computing and graphics was used for all statistical analyses performed. The non-linear regression function nls was used to estimate parameters of the sigmoidal-exponential and Weibull functions used to fit the loss of conductivity versus xylem pressure data for each species x environment and individual stem segments. Plots of predicted-y versus residuals and calculated r^2 values were compared in order to determine which function best fit the data. T-tests (function t.test) were performed within species (not between) in order to separate means of open grown and understory saplings within each species. Means were considered significantly different at $\alpha \leq 0.05$. Assumptions of normality and homogeneity of variances was assessed with diagnostic plots, normality tests (function ad.test, cvm.test, lillie.test, pearson.test, sf.test) and an F-test (function var.test). Where variances were unequal, I used Welch's two sample t-test to account for unequal variances. Results of within species t-tests (p-values and degrees of freedom) are presented in supplemental materials (Appendix 3).

2.3 Results

Xylem pressure corresponding to a 50% loss in conductivity (P_{50}) was consistently less negative (more vulnerable) in all species grown in the understory (Figure 1, 2a). However, the greatest shift was observed in understory *Picea mariana* where the average P_{50} was 50% of open-grown saplings (Figure 2a). No statistical difference was detected in the average sapwood area specific conductivity (k_s) between open-grown and understory conifers (Figure 2b). Leaf area specific conductivity (k_l) was significantly lower in all understory conifers compared with their open-grown counterparts (Figure 3a). Soil-to-plant hydraulic conductance ($K_{s\text{-}p}$) increased in open grown *Pinus contorta* and *Picea glauca* compared with understory saplings while no change was observed between open and understory *Pinus banksiana* and *Picea mariana* (Figure 3b).

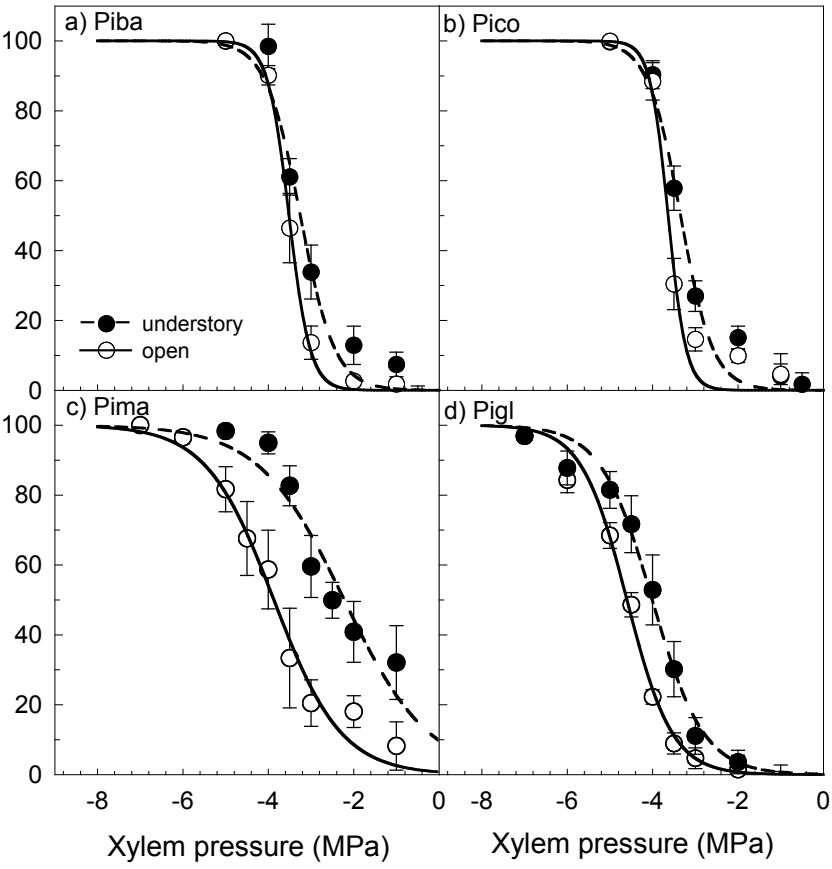

Figure 2.1: Vulnerability curves of a) Piba (*Pinus banksiana*) b) Pico (*Pinus contorta*) c) Pima (*Picea mariana*) and d) Pigl (*Picea glauca*) grown in an open field (open) or in an aspen dominated understory (understory). Error bars are 1 SEM. (n=6-9).

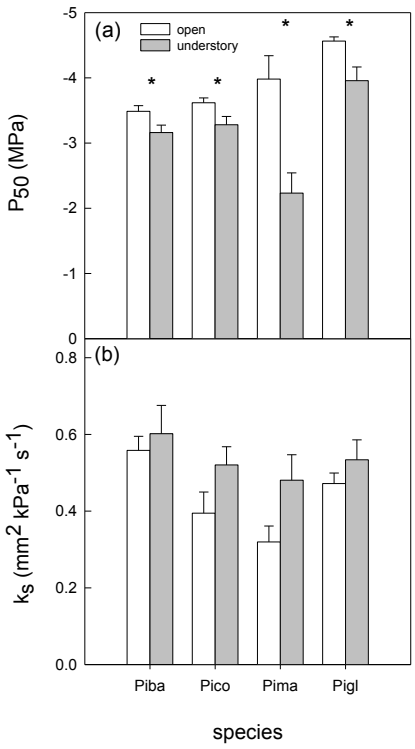

Figure 2.2: Average a) xylem pressure causing a 50% loss of conductivity (P_{50}) and b) sapwood area specific conductivity (k_s) for Piba (*Pinus banksiana*), Pico (*Pinus contorta*), Pima (*Picea mariana*) and Pigl (*Picea glauca*) grown in an open field (open) or under an aspen dominated understory (understory). Error bars are 1 SEM (n=6). * indicates the means of within species comparison are significant at $\alpha \leq 0.05$.

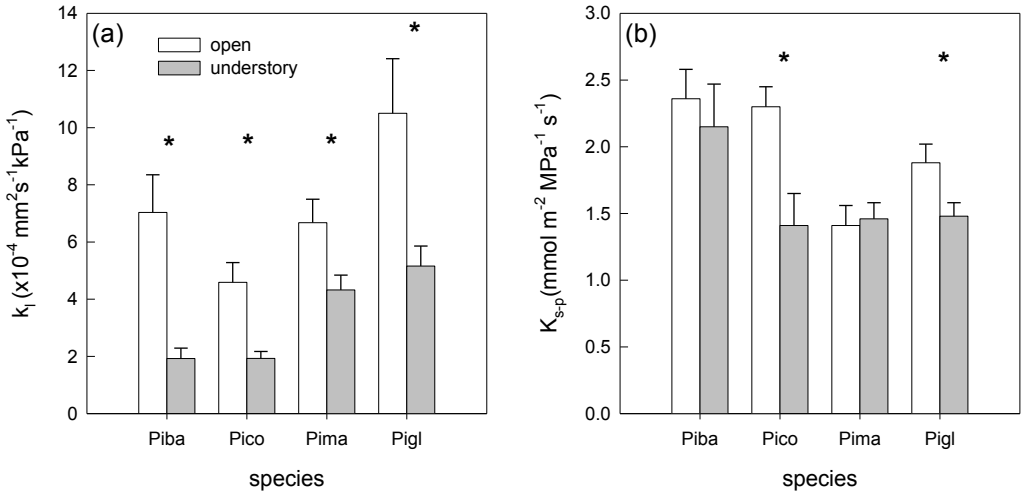

Figure 2.3: Average a) leaf area specific conductivity (k_l) and b) soil-to-plant hydraulic conductance (K_{s-p}) for Piba (*Pinus banksiana*), Pico (*Pinus contorta*), Pima (*Picea mariana*) and Pigl (*Picea. glauca*) grown in an open field (open) or under an aspen dominated understory (understory). Error bars are 1 SEM (n=6 or 12). * indicates the means of within species comparison are significant at $\alpha \leq 0.05$.

Wood density (ρ) was significantly higher in all understory saplings compared with open grown conifers (Figure 4a). There was no difference in tracheid length between open and understory conifers (Figure 4b). Average diameter (D) was significantly larger in open grown *Pinus contorta* and *Picea glauca* relative to their understory counterparts (Figure 4c). Corresponding with trends in ρ and D, tracheid density was also higher in understory *Pinus contorta*, *Picea mariana* and *Picea glauca* saplings relative to open grown saplings (Figure 4d).

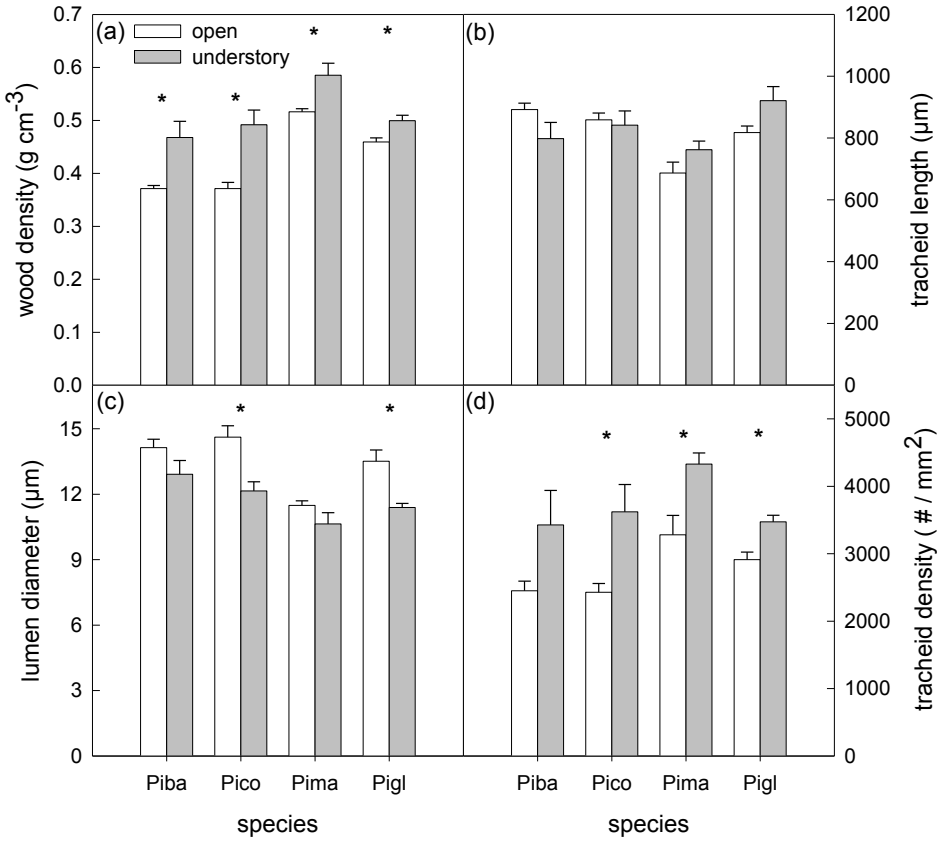

Figure 2.4: Average a) wood density, b) tracheid length, c) lumen diameter and d) tracheid density for Piba (*Pinus banksiana*), Pico (*Pinus contorta*), Pima (*Picea mariana*) and Pigl (*Picea glauca*) grown in an open field (open) or under an aspen dominated understory (understory). Error bars are 1 SEM (n=6). * indicates the means of within species comparison are significant at $\alpha \leq 0.05$.

On average, the width of margo strands was significantly reduced, while the maximum pore area was significantly larger in understory *Pinus contorta* and *Picea mariana* compared with open grown individuals (Figure 5 and Figure 6a, c). There was no difference in margo strand length between open and understory conifers (Table 2). Mean pore area, fraction of area occupied by pores (pore fraction), extended torus area and the occurrence of torus extensions were significantly higher in *Picea mariana* grown in the understory compared with the open (Figure 6b, d, e, f). No difference was detected in these parameters between understory and open-grown *Pinus contorta* (Figure 6b, d, e, f). Open-grown *Pinus contorta* had significantly larger tori and pit aperture diameters compared with understory saplings (Table 2). Tori and overall pit diameters were also

significantly larger in open-grown *Picea mariana* (Table 2). The ratio of torus:pit area was also larger in open-grown individuals of *Pinus contorta*, while the torus:aperture area ratio was significantly larger in open-grown *Picea mariana* compared with understory saplings (Table 2).

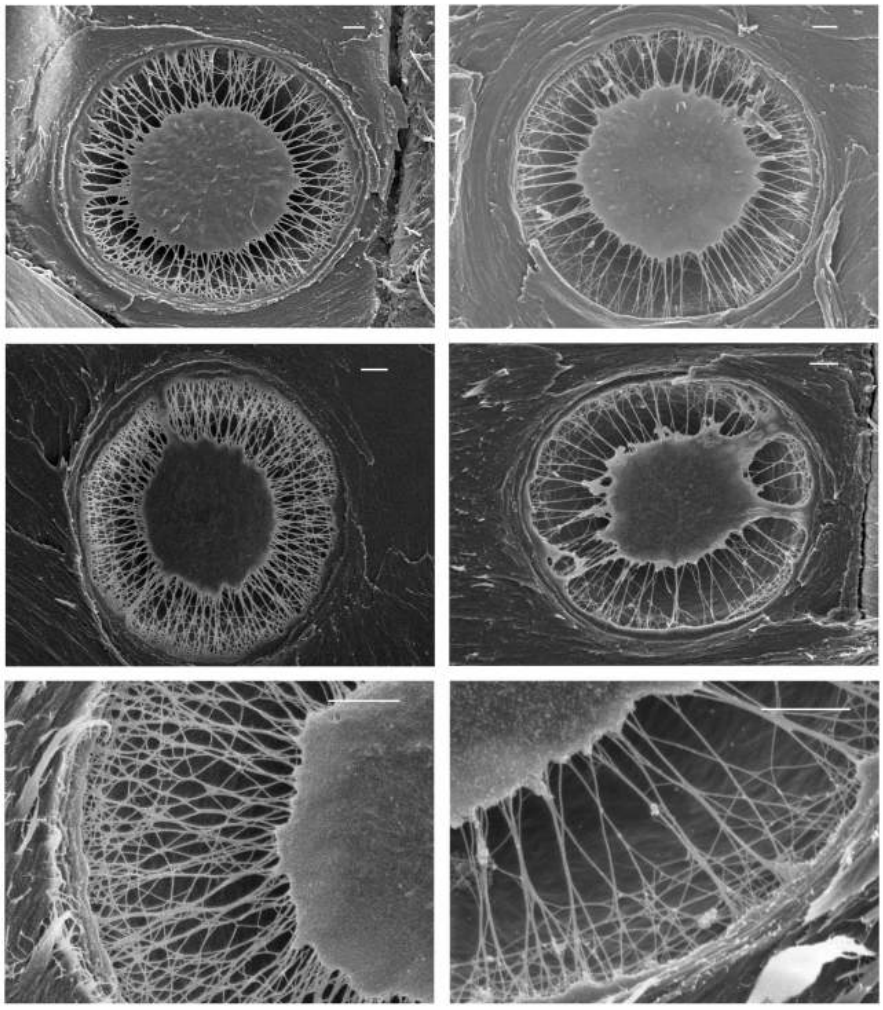

Figure 2.5: SEM images showing typical bordered pit structures of a) open grown *Pinus contorta*, b) understory *Pinus contorta*, c) open grown *Picea mariana* and d) understory *Picea mariana*. Close-up view of margo in e) open grown *Picea mariana* and f) understory *Picea mariana*. Scale (white bar) represents 1 µm.

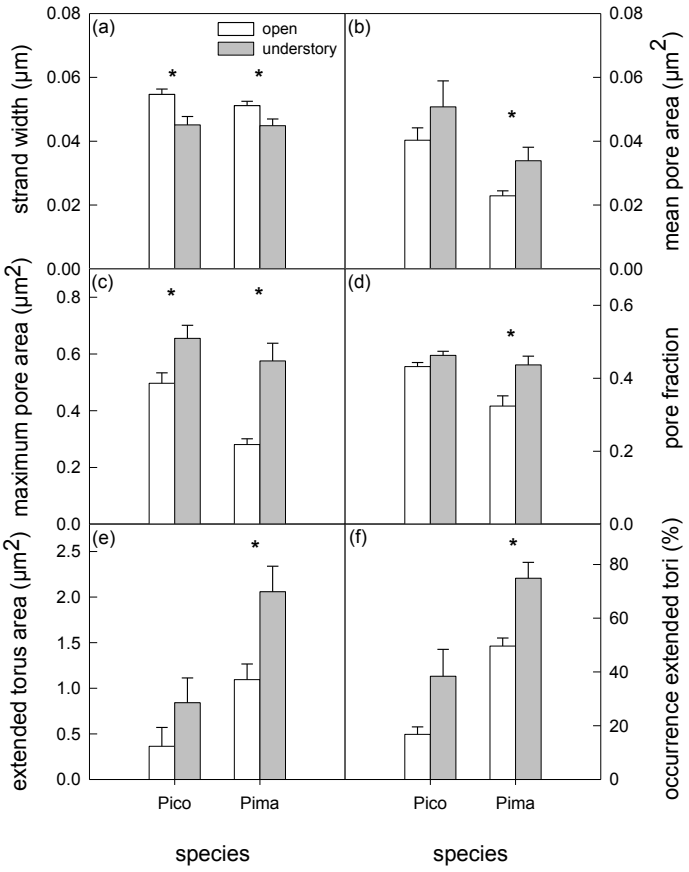

Figure 2.6: Average a) margo strand width, b) mean pore area, c) maximum pore area, d) pore fraction, e) extended torus area and d) occurrence of extended torus for *Pinus contorta* and *Picea mariana* grown in an open field (open) or under an aspen dominated understory (understory). Error bars are 1 SEM (n=6). * indicates the means of within species comparison are significant at $\alpha \leq 0.05$.

Tracheid resistivity (R_c) showed no consistent trend between open and understory saplings (Table 3). Corresponding with larger values of D, open-grown *Pinus contorta* and *Picea glauca* had lower lumen resistivities (R_L) (Table 3). The importance of R_w is clearly seen in the wall fraction, as the end wall component comprised upwards of 75% of total resistivity across all open-grown conifers but was 72% in shaded conditions for both pines and 61-62% in the spruces (Table 3). Pit resistance (r_p) was higher in open-grown individuals of *Pinus contorta* compared with those in the understory (Table 3). The number of pits per tracheid was higher in open-grown *Picea mariana* compared with understory but remained unchanged in all other conifers (Table 3).

Table 2.2: Results from SEM measurements: Mean strand length, torus/pit area, aperture/pit area, torus/aperture area, torus diameter, pit diameter and aperture diameter for *Picea contorta* and *Picea mariana* grown in an open field (open) or in an aspen dominated understory (understory). Values in brackets are 1 SEM (n=6). Bold values indicate the means of within species comparison are significant at $\alpha \leq 0.05$.

Species	strand length (μm)	torus/pit area	aperture/pit area	torus/aperture area	torus diameter (μm)	pit diameter (μm)	aperture diameter (μm)
Pinus contorta							
open	2.61 (0.10)	**0.29 (0.01)**	0.12 (0.01)	2.37 (0.16)	**6.37 (0.21)**	11.77 (0.34)	**4.15 (0.11)**
understory	2.59 (0.04)	**0.27 (0.00)**	0.11 (0.01)	2.42 (0.22)	**5.63 (0.22)**	10.93 (0.30)	**3.66 (0.15)**
Picea mariana							
open	2.51 (0.07)	0.23 (0.01)	0.09 (0.00)	**2.55 (0.10)**	**5.21 (0.09)**	**10.88 (0.15)**	3.27 (0.08)
understory	2.40 (0.07)	0.23 (0.00)	0.10 (0.00)	**2.14 (0.10)**	**4.65 (0.11)**	**9.88 (0.17)**	3.19 (0.10)

Table 2.3: Results from light microscope measurements: Mean tracheid resistivity (R_c), lumen resistivity (R_L), end-wall resistivity (R_w), wall fraction, pit area resistance (r_p), number of pits per tracheids and pit fraction (Fp) for *Pinus banksiana*, *P.contorta*, *Picea mariana* and *P. glauca* grown in an open field (open) or in an aspen dominated understory (understory). Values in brackets are 1 SEM (n=6). Bold values indicate the means of within species comparison are significant at $\alpha \leq 0.05$.

Species	R_c (MPa s mm^{-4})	R_L (MPa s mm^{-4})	R_w (MPa s mm^{-4})	Wall fraction ($R_w R_c^{-1}$)	r_p (MPa s m^{-1})	# pits / tracheid	F_p
Pinus banksiana							
open	4.47 (0.34)	1.06 (0.11)	3.41 (0.32)	0.76 (0.02)	2.43 (0.31)	18.78 (1.03)	0.06 (0.01)
understory	6.53 (1.51)	1.63 (0.29)	4.89 (1.30)	0.72 (0.03)	2.39 (0.45)	20.18 (1.68)	0.07 (0.01)
Pinus contorta							
open	7.09 (1.45)	**0.96 (0.15)**	6.14 (1.31)	**0.86 (0.01)**	**4.53 (0.85)**	17.58 (1.57)	0.07 (0.00)
understory	7.19 (0.87)	**2.02 (0.19)**	5.18 (0.65)	**0.72 (0.02)**	**2.84 (0.43)**	16.03 (0.93)	0.07 (0.01)
Picea mariana							
open	11.28 (1.96)	2.39 (0.19)	8.89 (1.83)	0.76 (0.03)	2.86 (0.54)	**21.03 (1.14)**	0.06 (0.00)
understory	9.94 (1.38)	3.58 (0.68)	6.36 (1.49)	0.61 (0.07)	2.31 (0.49)	**15.20 (1.72)**	0.06 (0.01)
Picea glauca							
open	6.30 (0.49)	**1.32 (0.20)**	4.98 (0.52)	**0.79 (0.03)**	3.15 (0.18)	25.65 (2.11)	0.07 (0.00)
understory	6.96 (1.00)	**2.46 (0.17)**	4.51 (1.06)	**0.62 (0.05)**	2.48 (0.41)	22.51 (1.73)	0.06 (0.00)

Average height, root collar diameter, and total leaf area on leading shoots were significantly larger in all open-grown conifers compared with understory conifers (Table 4). Leader leaf area to xylem area (LA:SA) was consistently higher in shaded conditions. When LA:SA was expressed on a whole plant basis,

however, the same trend observed in leading shoots was only expressed in *Picea mariana.* *Pinus contorta* showed the opposite pattern (significantly higher LA:SA in open compared with understory) and no difference was observed between open and understory grown *Pinus banksiana* or *Picea glauca* (Table 4).

Table 2.4: Mean height, root collar diameter, total leaf area (A_l), and leader LA:SA for Piba (*Pinus banksiana*), Pico (*P.contorta*), Pima (*Picea mariana*) and Pigl (*P. glauca*) grown in an open field (open) or under an aspen dominated understory (understory) in August 2007. Values in brackets are 1 SEM (n=6 except $K_{s\text{-}p}$ where n=12). Bold values indicate the means of within species comparison are significant at $\alpha \leq 0.05$.

Treatment	Height (m)	Root collar diameter (mm)	A_l (m^2)	*Leader LA:SA (cm^2mm^{-2})	Whole-plant LA:SA
Pinus banksiana					
open	**2.68 (0.15)**	**41.9 (3.6)**	**3.1 (0.4)**	**9.2 (1.4)**	2212 (186)
understory	**0.78 (0.10)**	**10.0 (0.5)**	**0.2 (0.02)**	**34 (3.4)**	1714 (183)
Pinus contorta					
open	**2.49 (0.17)**	**48.4 (4.6)**	**5.3 (0.9)**	**8.8 (0.7)**	**2829 (245)**
understory	**0.72 (0.07)**	**10.0 (0.6)**	**0.1 (0.03)**	**28 (3.0)**	**1644 (220)**
Picea mariana					
open	**1.83 (0.16)**	**33.8 (2.9)**	**1.7 (0.3)**	**5.3 (0.7)**	**1854 (128)**
understory	**0.78 (0.06)**	**9.3 (0.5)**	**0.2 (0.02)**	**11 (1.1)**	**2950 (230)**
Picea glauca					
open	**1.82 (0.20)**	**35.7 (2.9)**	**2.6 (0.5)**	**4.6 (1.2)**	2432 (226)
understory	**0.68 (0.07)**	**10.0 (0.5)**	**0.2 (0.04)**	**11 (0.6)**	2713 (236)

*Leader LA:SA was measured from the 1 (open grown pines) or 2 (all other treatments) year old shoots used in hydraulic measurements.

2.4 Discussion

All four conifer species demonstrated significantly less negative average P_{50} values when grown in the shade, indicating that they were all more susceptible to drought-induced cavitation compared with their open grown counterparts. This result supports my first hypothesis that understory trees will show increased vulnerability to embolism and is in line with earlier studies on angiosperms (Cochard et al. 1999; Barigah et al. 2006). Interestingly, the magnitude of this response, both in terms of the average P_{50} (Figure 2a) and shifting of the entire vulnerability curve (Figure 1) was greater in the shade-tolerant spruces, *Picea*

mariana in particular, compared to the shade-intolerant pines. This indicates that the spruces appear to have greater plasticity in cavitation resistance than the pines. In contrast, Barigah et al. (2006) did not observe a change in the magnitude of cavitation resistance in angiosperms of differing shade tolerance.

Although understory trees had significantly greater wood densities and reduced tracheid diameters (D), they also had more vulnerable xylem, which contrasts with previous work where increased cavitation resistance was positively correlated with increasing wood density and decreasing D (Hacke et al. 2001; Hacke and Jansen 2009). Based on my SEM measurements I suggest three possible mechanisms (that may also operate simultaneously) by which understory conifers could become more susceptible to cavitation. Mechanism 1: The width of margo strands was significantly smaller in both understory conifers (*Pinus contorta* and *Picea mariana*) measured (Figure 6a). From this and the fact that there were fewer margo strands in understory conifers, I could infer that that these strands would be more likely to tear and prevent the torus from sealing properly. Similarly, Domec et al. (2006) found that margo strand thickness was related to vulnerability in roots, trunkwood and branches of *Pseudotsuga menziesii*. Mechanism 2: Increased vulnerability could be driven by increased occurrence and size of torus extensions (Figure 6 e, f). It is possible that these extensions are less flexible than the 'regular' margo strands and may prevent complete sealing of the torus. my SEM measurements support this idea as both the occurrence and the area of extensions were significantly larger in shaded *Picea mariana* trees (Figure 5d). Although I did not observe a statistical difference in torus extensions for *Pinus contorta*, the average occurrence and size of torus extensions were in the same direction. Also, the difference in vulnerability was much larger between open and understory *Picea mariana* than it was in *Pinus contorta*, thus it would make sense that the magnitude of the response would be less in *Pinus contorta*. In support of this mechanism, Cochard et al. (2009) have suggested that capillary failure is a strong candidate driving cavitation resistance in conifers. They further speculated that air could seed in through lack of contact between the torus and pit wall. Mechanism 3: The ratio of torus:aperture area was significantly larger in

open grown *Picea mariana* compared with understory individuals (Table 2). Given that both open and understory saplings had similar sized apertures, the smaller tori observed in understory *Picea mariana* would be more easily dislodged or not completely cover the pit aperture, allowing air entry to adjacent tracheids. Domec et al. (2008) also found increased ratio of torus to aperture diameter in *Pseudotsuga menziesii* corresponding with increased height and cavitation resistance. However, in their case, this ratio appeared to be mainly driven by the pit aperture size. Interestingly, both the average torus diameter and pit aperture diameters were significantly larger in open-grown *Pinus contorta* relative to understory individuals suggesting that Mechanism 3 cannot explain the differences in P_{50} found in this particular species.

We observed no decline in k_s as a result of understory shading (Figure 2b). This was an unexpected result as increased transport capacity typically corresponds with larger diameter tracheids (Pittermann et al. 2006a, b; Hacke and Jansen 2009). Given these results, how can understory conifers with significantly smaller diameter tracheids (*Pinus contorta* and *Picea glauca*) still have comparably efficient xylem to open-grown conifers? It is possible that longer tracheids could offset smaller diameter tracheids to some extent. Hacke and Jansen (2009) actually observed a positive relationship between tracheid length and k_s. However, I did not observe a significant difference in tracheid length between open and understory conifers (Figure 4b). A more probable explanation relates to the reduced proportion of total resistivity attributed to the end wall of the tracheid; the end-wall fraction tended to be reduced in all understory conifers (significantly so for *Pinus contorta* and *Picea glauca*; Table 3). However, it was not the area or number of pits driving a decrease in end-wall resistivity as there was no statistical difference in these parameters between open and understory conifers (Table 3). I did observe within the margo that the mean pore area in *Picea mariana* and maximum pore area in *Pinus contorta* and *Picea mariana* were significantly greater in the understory compared with the open (Fig 5 and 6c); larger pores would allow water to pass more easily through the bordered pit and would decrease end-wall resistivity (Hacke et al. 2004; Wilson et al. 2008).

This agrees with a tendency for higher pit resistances in open-grown conifers (Table 3). Similarly, Domec et al. (2006) observed a tradeoff between pit conductivity and P_{50} in *Pseudotsuga menziesii*.

Our results contrast a series of earlier studies where shading actually resulted in decreased sapwood-area conductivity in conifers (Sellin 1993, 2001; Protz et al. 2000; Reid et al. 2003; Renninger et al. 2007). I are suggesting three possibilities that could account for the discrepancy between my study and the previous investigations. Firstly, the absolute amount of shade could have influenced previous results. All studies had coniferous overstories that probably cast deeper and more continuous shade relative to my deciduous stand. Secondly, I examined apical shoots, whereas these studies measured either lateral branches or stem sections from lower sections in the crown; it is possible that competition for resources between upper and lower branches or even along the primary stem could have had an impact on k_s. Thirdly, genetic differences between suppressed and dominant trees could have influenced k_s in previous studies (Sellin 1993, 2001; Reid et al. 2003) as suppressed trees may simply be genetically inferior and slower growing compared with dominant trees in the same stand.

The significant decline of leaf area specific conductivity (k_l) in all four shade grown conifers and the decline of soil-to-plant hydraulic conductance (K_{s-p}) in shade grown *Pinus contorta* and *Picea glauca* (Figure 3) support my final (third) hypothesis. The lack of response in K_{s-p} in *Picea mariana* could be the result of a relatively greater sensitivity to drought (in the open-grown environment) inducing reduced transpiration and subsequently lower K_{s-p} (Zwiazek and Blake 1989). In the case of *Pinus banksiana*, I do not have any direct evidence but this species may be similarly sensitive to drought as in *Picea mariana*. The magnitude of decrease in k_l in the shade ranged from 35-72% for the four conifers measured. This is consistent with Shumway et al. (1993), Shultz and Matthews (1993) and Sellin (2001) who reported reductions in k_l in shaded plants. However, Renninger et al. (2007) reported no difference in k_l between suppressed and released *Pseudotsuga menziesii* and *Tsuga heterophylla*. The suppressed trees in that particular study also had reduced LA:SA relative to released trees. In my study,

the shoots I used to measure k_l all had higher LA:SA in the shade relative to the open.

Our original hypotheses had suggested that shade tolerant species (as opposed to shade intolerant species) would show greater differences in hydraulic parameters between open and understory environments. I found this was true in terms of cavitation resistance and in various characteristics of bordered pit anatomy. However, I saw little difference between shade tolerant and intolerant species in terms of water transport efficiency and most other structural anatomical observations (wood density, tracheid length and diameter etc.). In fact, it seems more likely that differences in their ecological distributions appeared to dictate their plasticity in wood development. *Pinus banksiana*, for example, typically showed the least hydraulic and anatomical responses to understory shading; it is typically a dominant tree on dry habitats. On the other hand, *Picea mariana*, was probably the most variable in its responses and as such appeared to have the greatest plasticity. This species inhabits a wide range of habitat types which are likely to vary enormously in water availability. Thus, a strategy which could presumably reduce the investment of carbon into wood production (i.e. producing wood that is less cavitation resistant when grown in conditions not prone to high potential evapotranspiration) could be adaptive.

2.4.1 Conclusions

Overall, for plants growing in an understory, both evaporative demand and light availability decline. Lower evaporative demand results in reduced need for water while low light levels limit the amount of carbon fixation. The decline in k_l and $K_{s\text{-}p}$ in the understory environment supports the notion of reduced need for water under these circumstances. Increased LA:SA in the leading shoots are indicative of a shift in allocation from stem and root growth (hydraulics) to leaf area (light capture) development in the understory. In terms of the type of xylem produced, my data show that understory trees tended to produce narrower tracheids. Surprisingly, these tracheids were still capable of comparable flow to that of open grown trees with larger diameter tracheids. This was probably driven

by changes in pit structure, which is supported from my observations of larger maximum pore sizes in the margo of shaded *Pinus contorta* and *Picea mariana*. Having relatively efficient sapwood water transport means that understory conifers could invest less carbon into wood production by producing bordered pits with a more porous but fragile structure, corresponding with increased xylem vulnerability. A potential drawback of this strategy is that a rapid change in evaporative demand caused by the formation of a canopy gap could be detrimental for some shaded conifers. For an open grown conifer, the risk of losing the capacity to transport water in order to 'save' carbon is too large, thus they have employed the strategy of a more conservative bordered pit design and compensated for increased pit resistance by larger lumen diameters.

2.5 References

Andrade JL, Meinzer FC, Goldstein G, Holbrook NM, Cavelier J, Jackson P, Silvera K (1998) Regulation of water flux through trunks, branches, and leaves in trees of a lowland tropical forest. Oecol 115: 463-471

Barigah TS, Ibrahim T, Bogard A, Faivre-Vuillin B, Lagneau LA, Montpied P, Dreyer E (2006) Irradiance-induced plasticity in the hydraulic properties of saplings of different temperate broad-leaved forest tree species. Tree Physiol 26: 1516

Bladon KD, Silins U, Landhausser SM, Lieffers VJ (2006) Differential transpiration by three boreal tree species in response to increased evaporative demand after variable retention harvesting. Agri For Meteor 138: 104-119

Brodribb TJ, Holbrook NM, Hill RS (2005) Seedling growth in conifers and angiosperms: impacts of contrasting xylem structure. Austral J Bot 53: 749-755

Burgess SO, Pittermann J, Dawson TE (2006) Hydraulic efficiency and safety of branch xylem increases with height in *Sequoia sempervirens* (D. Don) crowns. Plant Cell Environ 29: 229-239

Callaway RM (1992) Morphological and physiological responses of three California oak species to shade. Inter J Plant Sci 153: 434-441

Chaffey NJ (2002) Wood microscopical techniques. In: Chaffey NJ, ed. Wood formation in trees. New York, USA: Taylor & Francis, 17-40

Cochard H, Hölttä T, Herbette S, Delzon S, Mencuccini M (2009) New insights into the mechanisms of water-stress induced cavitation in conifers. Plant Physiology 10.1104/pp.109.138305

Cochard H, Lemoine D, Dreyer E (1999) The effects of acclimation to sunlight on the xylem vulnerability to embolism in *Fagus sylvatica* L. Plant Cell Environ 22: 101-108

Domec JC, Lachenbruch B, Meinzer FC (2006) Bordered pit structure and function determine spatial patterns of air-seeding thresholds in xylem of Douglas-fir (Pseudotsuga menziesii; Pinaceae) trees. Am J Bot 93: 1588-1600

Domec JC, Lachenbruch B, Meinzer FC, Woodruff DR, Warren JM, McCulloh KA (2008) Maximum height in a conifer is associated with conflicting requirements for xylem design. Proceed Nat Acad Sci 105: 12069-12074

Environment Canada. (2009) National climate data and information archive. URL http://www.climate.weatheroffice.ec.gc.ca/Welcome_e.html

Givnish TJ (1988) Adaptation to sun and shade: a whole-plant perspective. Aust J Plant Physiol 15: 63-92

Hacke UG, Jansen S (2009) Wood anatomical features associated with hydraulic traits in three boreal conifer species. New Phytol 182: 675-686

Hacke UG, Sperry JS, Pockman WT, Davis SD, McCulloh KA (2001) Trends in wood density and structure are linked to prevention of xylem implosion by negative pressure. Oecol 126: 457-461

Hacke UG, Sperry JS, Pittermann J (2004) Anaylsis of circular bordered pit function II. Gymnosperm tracheids with torus-margo pit membranes. Am J Bot 91: 386-400

Jansen S, Pletsers A, Sano Y (2008) The effect of preparation techniques on sem-imaging of pit membranes. IAWA J 29: 161-178

Landhäusser SM, Lieffers VJ (2001) Photosynthesis and carbon allocation of six boreal tree species grown in understory and open conditions. Tree Physiol 21: 243-250

Lancashire JR, Ennos AR (2002) Modelling the hydrodynamic resistance of bordered pits. J Exp Bot 53: 1485-1493

Lemoine D, Cochard H, Granier A (2002) Within crown variation in hydraulic architecture in beech (*Fagus sylvatica* L): evidence for a stomatal control of xylem embolism. Ann For Sci 59: 19-27

Li Y, Sperry JS, Taneda H, Bush SE, Hacke UG (2008) Evaluation of centrifugal methods for measuring xylem cavitation in conifers, diffuse- and ring-porous angiosperms. New Phytol 177: 558-568

Mayr S, Wolfschwenger M, Bauer H (2002) Winter-drought induced embolism in Norway spruce (*Picea abies*) at the Alpine timberline. Physiol Plant 115: 74-80

Messier C, Doucet R, Ruel JC, Claveau Y, Kelly C, Lechowicz MJ (1999) Functional ecology of advance regeneration in relation to light in boreal forests. Can J For Res 29: 812-823

Pammenter NW, Vander Willigen C (1998) A mathematical and statistical analysis of the curves illustrating vulnerability of xylem to cavitation. Tree Physiol 18: 589-593

Pearcy RW (2007) Responses of plants to heterogeneous light environments. In: Pugnaire FI, Valladares F, eds. Functional plant ecology. Boca Raton, FL: CRC Press, 213-246

Pittermann J, Sperry JS, Hacke UG, Wheeler JK, Sikkema EH (2006a) Inter-tracheid pitting and the hydraulic efficiency of conifer wood: the role of tracheid allometry and cavitation protection. Am J Bot 93: 1265-1273

Pittermann J, Sperry JS, Wheeler JK, Hacke UG, Sikkema EH (2006b) Mechanical reinforcement of tracheids compromises the hydraulic efficiency of conifer xylem. Plant Cell Environ 29: 1618-1628

Protz CG, Silins U, Lieffers VJ (2000) Reduction in branch sapwood hydraulic permeability as a factor limiting survival of lower branches of lodgepole pine. Can J For Res 30: 1088-1095

R Development Core Team (2006) R: A language and environment for statistical computing. R Foundation for Statistical Computing, Vienna, Austria. ISBN 3-900051-07-0, URL http://www.R-project.org

Reid DB, Silins U, Lieffers VJ (2003) Stem sapwood permeability in relation to crown dominance and site quality in self-thinning fire-origin lodgepole pine stands. Tree Physiol 23: 833-840

Renninger HJ, Gartner BL, Meinzer FC (2006) Effects of release from suppression on wood functional characteristics in young Douglas-fir and western hemlock. Can J For Res 36: 2038-2046

Renninger HJ, Meinzer FC, Gartner BL (2007) Hydraulic architecture and photosynthetic capacity as constraints on release from suppression in Douglas-fir and western hemlock. Tree Physiol 27: 33-42

Saliendra NZ, Sperry JS, Comstock JP (1995) Influence of leaf water status on stomatal response to humidity, hydraulic conductance, and soil drought in *Betula occidentalis*. Planta 196: 357-366

Sano Y, Kawakami Y, Ohtani J (1999) Variation in the structure of intertracheary pit membranes in *Abies sachalinensis*, as observed by field-emission scanning electron microscopy. IAWA J 20: 375-388

Schultz HR, Matthews MA (1993) Xylem development and hydraulic conductance in sun and shade shoots of grapevine (*Vitis vinifera* L.): evidence that low light uncouples water transport capacity from leaf area. Planta 190: 393-406

Sellin A (1993) Resistance to water flow in xylem of *Picea abies* (L.) Karst. trees grown under contrasting light conditions. Trees 7: 220-226

Sellin A (1997) Variation in shoot water status of *Picea abies* (L.) Karst. trees with different life histories. For Ecol Manage 97: 53-62

Sellin A (2001) Hydraulic and stomatal adjustment of Norway spruce trees to environmental stress. Tree Physiol 21: 879-888

Shumway DL, Steiner KC, Kolb TE (1993) Variation in seedling hydraulic architecture as a function of species and environment. Tree Physiol 12: 41-54

Sperry JS, Hacke UG, Field T, Sano Y, Sikkema EH (2007) Hydraulic consequences of vessel evolution in angiosperms. Inter J Plant Sci 168: 1127-1139

Sperry JS, Hacke UG, Pittermann J (2006) Size and function in conifer tracheids and angiosperm vessels. Am J Bot 93: 1490-1500

Walters MB, Reich PB (1999) Low-light carbon balance and shade tolerance in the seedlings of woody plants: do winter deciduous and broad-leaved evergreen species differ? New Phytol 143: 143-154

Wilson JP, Knoll AH, Holbrook, NM, Marshall, CR (2008) Modeling fluid flow in *Medullosa*, an anatomically unusual Carboniferous seed plant. Paleobiol 34: 472-493

Zwiazek JJ & Blake TJ (1989) Effects of preconditioning on subsequent water relations, stomatal sensitivity, and photosynthesis in osmostically stressed black spruce. Can J Bot 67: 2240-2244

Chapter 3: Non-structural carbon in *Pinus contorta* and *Picea glauca*: variation related to tissues, phenology and season

3.1 Introduction

Water soluble sugars, starch, sugar alcohols, and lipids, represent most of the pool of non-structural carbon (NSC) compounds that are readily available for respiration, growth, reproduction, defense or storage for future use. In conifers, most research on carbon compounds and their dynamics has been focused on temperate species (e.g. Ludovici et al. 2002; Hoch et al. 2003 and others). Unlike in temperate and milder climatic regions, boreal climates have an extended period with frozen soils and very cold air temperatures during which most functions in trees are arrested. Information on NSC in these boreal and montane climatic regions is sparse; Ericsson (1979) and Bansal and Germino (2009) have described the seasonal reserves in needles of boreal *Pinus sylvestris* L. and montane *Abies lasciocarpa* (Hook.) Nutt. and *Pseudotsuga menziesii* Mirb., while Hoch et al. (2002) examined stem, branch and root wood in high-elevation *Pinus cembra* L. The aim of my study is to quantify seasonal changes in storage reserves of roots, stem, branches and foliage of two coniferous species with different growth strategies (*Pinus contorta* Loudon and *Picea glauca* (Moench) Voss) growing in a boreal climate with cold winters resulting in a distinct dormant season.

Single tissues studies comprise the large majority of seasonal NSC work (Ericsson 1979; Höll 1985; Fischer and Höll 1991, 1992; Bansal and Germino 2009). Of the few studies that have measured multiple tissues concurrently (Webb and Kilpatrick 1993; Hoch et al. 2002, 2003) only two studies (Gholz and Cropper 1991; Ludovici et al. 2002) spanned both the growing and dormant season and included roots; both of these studies were conducted on *Pinus* species growing in the southern United States. Clearly, there is a need to study different species, in other climatic regimes in order to better generalize dynamics of NSC and the inter-tissue responses within coniferous trees.

An understanding of the relationship between growth, phenology and storage compounds over a full season is needed in order to properly relate NSC to performance; however, studies of this type are largely lacking (Ryan 2011). While it is well known that there is a build-up of foliar starch in the spring period, corresponding with shoot expansion in conifers (Krueger and Trappe 1967; Ericsson 1979; Pomeroy et al. 1970; Fisher and Höll 1991; Webb and Kilpatrick 1993; Ludovici et al. 2002; Bansal and Germino 2009), there is little information that relates root growth to seasonal carbohydrates. Deans and Ford (1986) described root diameter growth and starch reserves in root bark of *Picea sitchensis* and found root diameter growth occurred before shoot growth when roots were in close proximity to the tree bole, however, when the roots were further away from the bole diameter growth did not initiate until after shoot flush. This was an interesting finding; however, this study did not report data from aboveground tissues (either in carbohydrates or growth). The other study which related shoot and root growth to NSC was conducted on *Pseudotsuga menziesii* seedlings. In this study, peak starch concentrations in roots coincided with fine root growth, which preceded budbreak (Krueger and Trappe 1967). Seedlings in this study, however, were young and the climate on this site did support photosynthesis nearly year-round. To my knowledge, no studies have compared the seasonal NSC dynamics of tree species with different growth strategies and linked them to their phenological stages and root and shoot growth patterns. In addition, I believe that species from colder climates, with extended periods of frozen conditions, will have different strategies for NSC storage than those from temperate regions.

Our objectives were to understand (1) how NSC varies with times of growth and from summer to winter, (2) how NSC may co-vary within different parts of the tree, and (3) how they vary between trees with different growth strategies. In this study, I compare the patterns of change in NSC concentrations in various tissue-organs, in an annual cycle of phenological stages in two boreal conifers: early successional, fast growing and shade intolerant lodgepole pine

(*Pinus contorta*) and later-successional, slower growing and shade tolerant white spruce (*Picea glauca*).

3.2 Methods

3.2.1 Study site and tree selection

Eight study sites were selected near Whitecourt, Alberta, Canada (54.14N -115.68W) in the lower foothills natural sub-region of Alberta (Beckingham and Archibald 1996). Site elevation ranged from 1000 to 1100 m. The average total precipitation in this region is 578 mm and total precipitation in 2007 was 560 mm. Daily average temperature is 2.6 ºC with a mean monthly temperature of -12.1 ºC in January and 15.7 ºC in July (Environment Canada 2010). Sites were located in stands consisting primarily of a mixture of white spruce (hereafter spruce) and lodgepole pine (hereafter pine) regenerated from either natural regeneration or planting after harvests between 1979 and 1981; trees at these stands ranged in height from 5-10 m and had been pre-commerically thinned at about year 10 and trees had not reached crown closure. A more detailed summary of tree and stand characteristics can be found in Table 1. Soil temperature data loggers (Hobo, Onset Computer Corp, Pocasset MA, USA) were installed at each site at a depth of 10 cm. At each of the eight stands, 10 dominant/co-dominant and healthy white spruce trees and 10 lodgepole pine were selected and tagged for future sampling.

Table 3.1 Average stand and tree attributes of sampled trees. Values in brackets are ranges of mean values across eight sites.

Stand type	basal area (m^2 ha^{-1})	density (stems ha^{-1})	diameter (cm)	height (m)	live crown ratio
Pinus contorta	22 (16-30)	2899 (1433-6132)	9.1 (8.0-10.7)	8.5 (7.7-9.9)	0.77 (0.71-0.81)
Picea glauca	same as above	same as above	8.5 (7.5-9.4)	7.3 (6.6-8.0)	0.87 (0.78-0.91)

3.2.2 Collection procedure

Collection dates were as follows: 31-May-2007 (prior to shoot expansion), 11-June-2007 (at the very beginning of shoot expansion), 28-June-2007 (shoot expansion well under way), 19/20-July-2007, 2-Sept-2007, 21/22-Nov-2007 (beginning of true dormant season). In 2008, three additional collections were made on 7/8-April-2008 (end of dormant season), 7/8-May-2008 (period where trees are likely to have recently come out of dormancy) and 3-June-2008 (at the beginning of shoot expansion again). At each collection, samples were obtained between 9 AM and 6 PM. I expected diurnal variation in total nonstructural carbohydrates to be negligible (Bansal and Germino 2009). In order to avoid auto-correlation in time and effects of wounding, a different tree was sampled at each site for each collection date. At each tree, the following was collected: (1) two upper branches located at the base of the upper ¼ of the whole tree; branches were taken from a south and north direction and pooled into a single sample. One-year old twig and needles (flushed in 2006) and current year twig and needles (flushed in 2007) were collected separately, (2) two lower branches (south and north) located at the lowest branch whorl that still had evidence of flushing buds, (3) a sample of the bole (2.5 ×7.5 × 2.5 cm deep) at 1.3m height was extracted with a chisel; this was then separated into xylem and bark (which comprised all tissues exterior to xylem) tissues, (4) a lateral root was collected by following a lateral root from the base of the tree until the diameter was 1.0 cm and a 10 cm length of root section was obtained. All samples were placed in plastic bags and stored on dry ice (with the exception of sampling periods where air temperatures were below -5ºC and then ice or snow was used) until returning from the field. Samples were then stored at -20ºC until further processing.

3.2.3 Tree growth measurements

I measured root and stem diameter increment of the year of sampling (2007) as well as the previous year (2006) of all of the sampled trees. For root measurements, I used a light microscope and image analysis software for all diameter measurements and I scanned sanded stem sections and used

SigmaScanPro software to measure ring width. I also measured annual extension of twigs during the first 4 collections (May 31-July 19, 2007).

3.2.4 Carbohydrate analysis

Samples were oven-dried for 1 hour at 100 ºC and then the temperature was lowered to 70 ºC until constant weight. Tissues were ground in a Wiley-mill (Thomas Scientific, Swedesboro New Jersey, USA) to pass 40 mesh. Analysis of total sugars and starch (total nonstructural carbohydrates, TNC) followed the procedure developed by Chow and Landhäusser (2004). Briefly, 50 mg of dried, ground tissue was put through an ethanol extraction (3 times) to extract the soluble sugars. The extract was treated with phenolsulfuric acid to breakdown the sugars into monosaccharides and analyzed for total sugar colorimetrically. The sample residue was analyzed for starch using a mixture of digestive enzymes including α-amylase and amyloglucosidase to breakdown the starch into glucose and analyzed colorimetrically.

3.2.5 Sugar alcohol analysis

It has been previously demonstrated that the vast majority of sugar alcohols in other *Pinus* and *Picea* species occur as cyclitols (pinitol in particular) (Hoch et al. 2003), and thus I focused on this group of sugar alcohols. I used an approach that was originally adapted for a simple extraction of pinitol from soybean leaves (Streeter 2001). Ground material (100 mg) was extracted twice with ethanol at room temperature, the first time with 5 ml 89% ethanol for 1 hour, the second time with 5 ml 80% ethanol for another hour. The extracts were pooled together and dried in a 70 °C oven for 24 hours. The residue was then dissolved in 1.0 mL distilled water and 0.375 mL chloroform, and stored at 4ºC overnight. After centrifuging, the top aqueous layer was separated and then heated in a 65 ºC water bath for 30 min to remove trace chloroform. Once cooled down, the solution was poured through a tandem of two resin columns, the first one acidic with 1 ml Dowex 50WX8 resin and the second one basic with 1 ml Dowex 1X8 resin. The final eluant containing the cyclitols was collected in clean,

pre-weighed vials. I dried the purified sample at 70 ºC for 24 hours and weighed the final product.

3.2.6 Lipid analysis

We used the modified Bligh and Dyer method (Bligh and Dyer 1959) with a Folch wash to extract lipids (Nelson and Dickson 1981). Dried tissues (100 mg) were extracted twice with 3 mL of a 2:1 (v/v) chloroform and methanol solution followed by a third extraction with 3 ml of a 1:2 (v/v) chloroform and methanol solution. All supernatants were pooled together and the Folch wash was performed by adding 4.5 mL of a 3.6 mM $CaCl_2$ solution. Samples were shaken and after centrifugation, the upper aqueous phase was discarded and the lower chloroform phase was transferred to a glass vial. The chloroform was evaporated under a stream of N_2. Lipids were re-constituted in 150 uL of chloroform and applied onto a thin layer chromatography plate (Whatman 60Å silica gel 250 μm thick on polyester backing). Plates were developed twice in a mixture of petroleum ether / diethyl ether / acetic acid (90:20:1 v/v/v) to separate lipids into triglycerides, diglycerides and free fatty acids (Höll 1985). Lipid standards of glyceryl trioleate, 1,3-diolein, γ-linolenic acid and oleic acid were developed at the margin of the plate as references. Plates were stained with 0.2% (w/v) naphthol blue black in 1 M NaCl for 10 min to visualize lipids. The amount of lipid by re-elution of triglycerides, diglycerides and free fatty acids in the chromatogram with 2:1 chloroform/methanol solution was quantified after drying and weighing.

3.2.7 Statistical analysis

We used a model-selection approach to build a linear model to summarize my findings. Fixed effects in my models included species, tissue-type and sampling date and the random effect was the site or tree. As advocated by Zuur et al. (2009), I first compared models with the most general fixed structure and allowed the random structure to vary. Once the best random model was chosen I used this random structure to build the fixed structure. For each of TNC, sugars

and starch, sugar alcohols and lipids, the best model was a three factor model with species, tissue-type and sampling date. Addition of a random component did not improve the fit of the linear model. From this model I then used the 95% coverage region of the posterior probability distribution (using the *sim* function in the library *arm* (Gelman et al. 2010; R Development Core Team 2010) to generate confidence intervals around my point estimates; these intervals were used as my basis of comparison (Gelman and Hill 2007). Equality of variance and normality of the data in the linear model were assessed graphically. In addition, I examined potential auto-correlation among tissues within trees (which can be assessed with diagnostic plots and by fitting a random effect for an individual tree). As I did not find evidence of auto-correlation, I assumed that the sampled trees behaved similarly, i.e., did not have consistently higher or lower sugars and starches relative to other trees.

3.3 Results

3.3.1 Seasonality in soluble sugar and starch concentrations

Concentrations of total non-structural carbohydrates (TNC; sum of soluble sugars and starch) in the needles and bark of spruce were typically two-fold higher compared with pine (Figure 1a, b, e). In contrast, the twigs, xylem and roots of both species were often, though not always, similar in concentration (Figure 1c,d,e,f). Concentrations of TNC increased in May and peaked in late spring (June) in all tissues measured for both species (Figure 1). In winter, a secondary peak in TNC was observed in the needle, twig, and root tissues of both species (Figure 1a-d, f). However, this peak was not observed in the bark tissues of either species (Figure 1e) while the xylem showed a decline in TNC from April to May in both species and a slight reduction in early fall in spruce (Figure 1e). In spruce, there was a pronounced reduction in TNC concentrations in the needles, bark and roots during the second sampling period in mid-June (2007) (Figure 1c-d). This depression corresponded with the extension of shoots (insets Figure 1c-d). In terms of stem xylem, TNC levels were highest from June until at least mid-

July; corresponding with peak diameter growth of the stem (inset graph figure 1e). In spruce roots, TNC also showed a decline with time of leaf flush, followed by a recovery in late June and then declined to a low level by mid-July where it remained stable until the following June (Figure 1f). Root diameter growth, however, continued to increase after late July (Figure 1f). Root TNC in pine showed a continual drop after mid June and reached its lowest level in September. This was coupled with root growth between late June and September (inset Figure 1f).

Spruce showed a greater degree of TNC flux between spring and winter periods compared with pine (Figure 2). This was particularly evident in needle and bark and xylem bark tissues (Figure 2b). There was a minor degree of TNC flux between spring and winter in root and needle tissues of pine (Figure 2a).

For both species the accumulation of starch in most above ground tissues began in early May and corresponded with above-zero soil and air temperatures (Figure 3). However, starch concentrations in roots at this time were much lower than in the aboveground components (Figure 3). In spruce, there was a distinct mid-June decline in starch across all measured tissues and a subtler decrease in the starch levels in needles of pine (Figure 3). Starch concentrations in spruce and pine were similar in twigs, xylem, and roots. However, starch concentrations in needle and bark tissues were typically 1.5-3.0 times higher in spruce than in pine. After June, starch concentrations continued to decline in both species and by November, starch concentrations were negligible in all measured tissues (Figure 3).

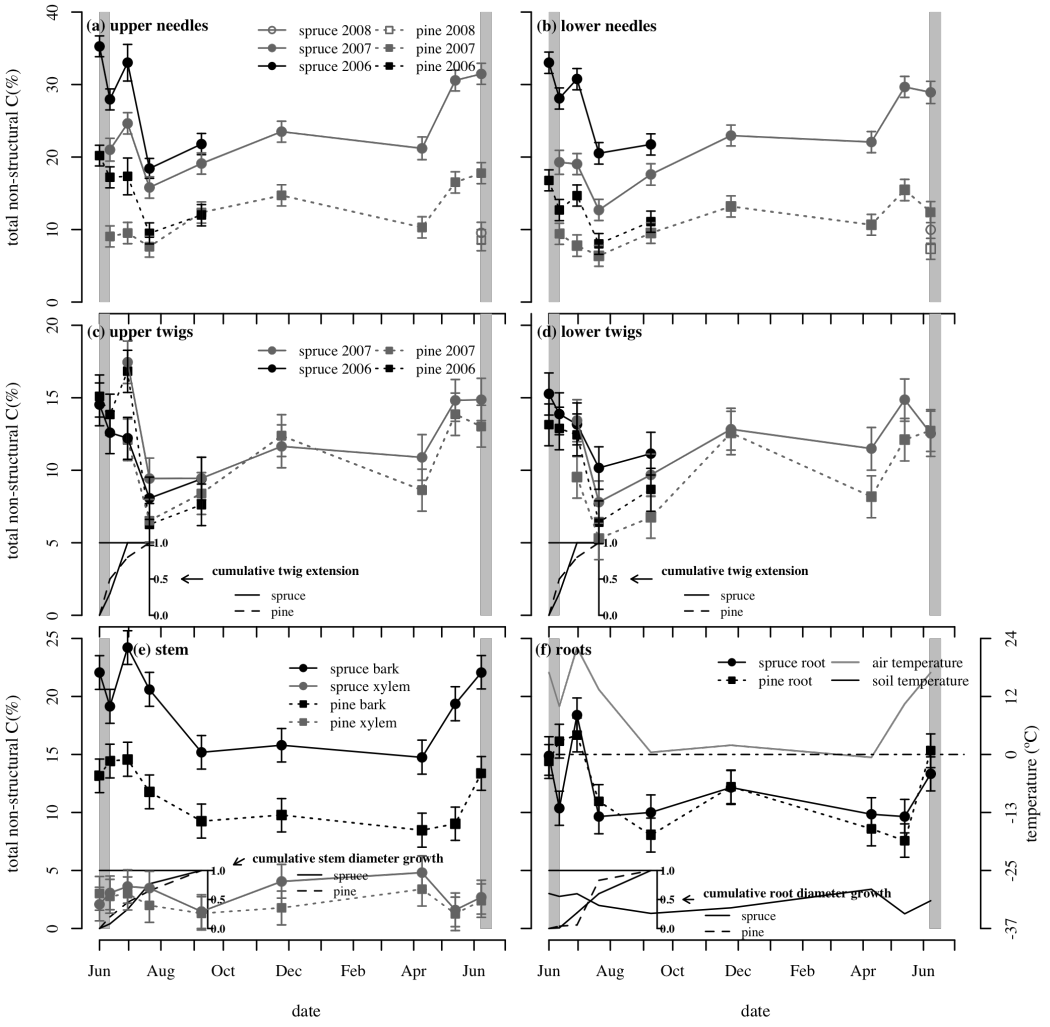

Figure 3.1: Seasonal course of total non-structural carbohydrates in (a-b) upper and lower needles, (c-d) twigs tissues, (e) bark and xylem and (f) roots of pine (*Pinus contorta*) and spruce (*Picea glauca)*. In addition, (f) also includes air temperature and soil temperature at 10 cm depth. The shaded region in (a-d) represents the period of shoot expansion and the year associated with tissues in legends indicates the year in which shoots expanded. Figure insets represent cumulative (c-d) twig extension, (e) stem diameter growth and (f) root diameter growth in *Pinus contorta* and *Picea glauca*. Error bars represent 95% confidence intervals (n=8).

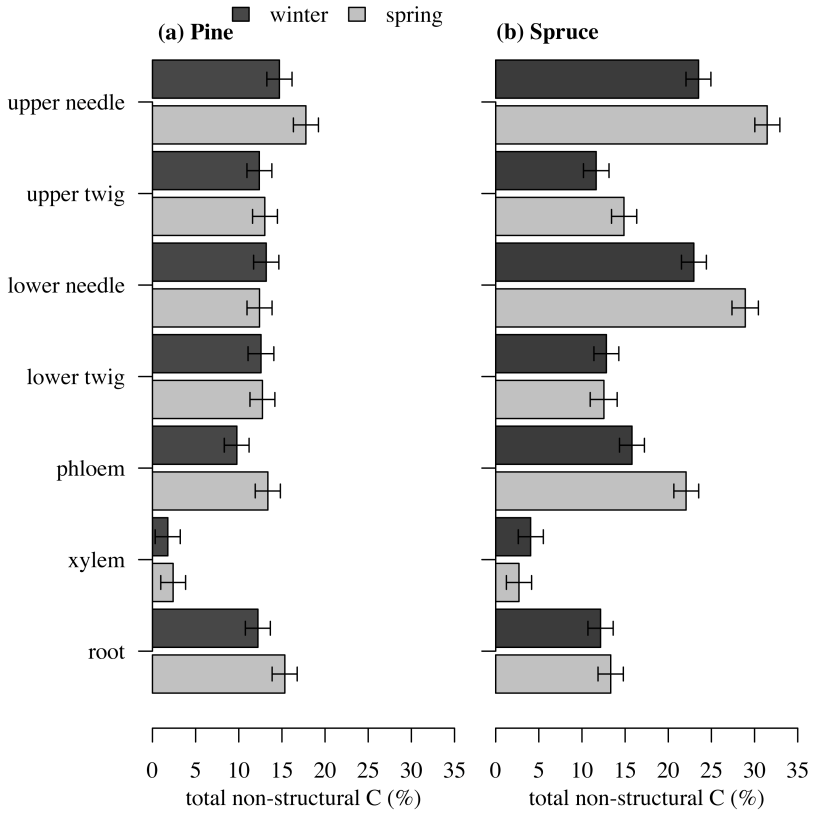

Figure 3.2: Comparison of total non-structural carbohydrates in needles, twigs, bark, xylem and roots at two sampling periods, winter (23-Nov-2007) and spring (3-June-2008) in (a) pine (*Pinus contorta)* and (b) spruce (*Picea glauca)*. Error bars represent 95% confidence intervals (n=8).

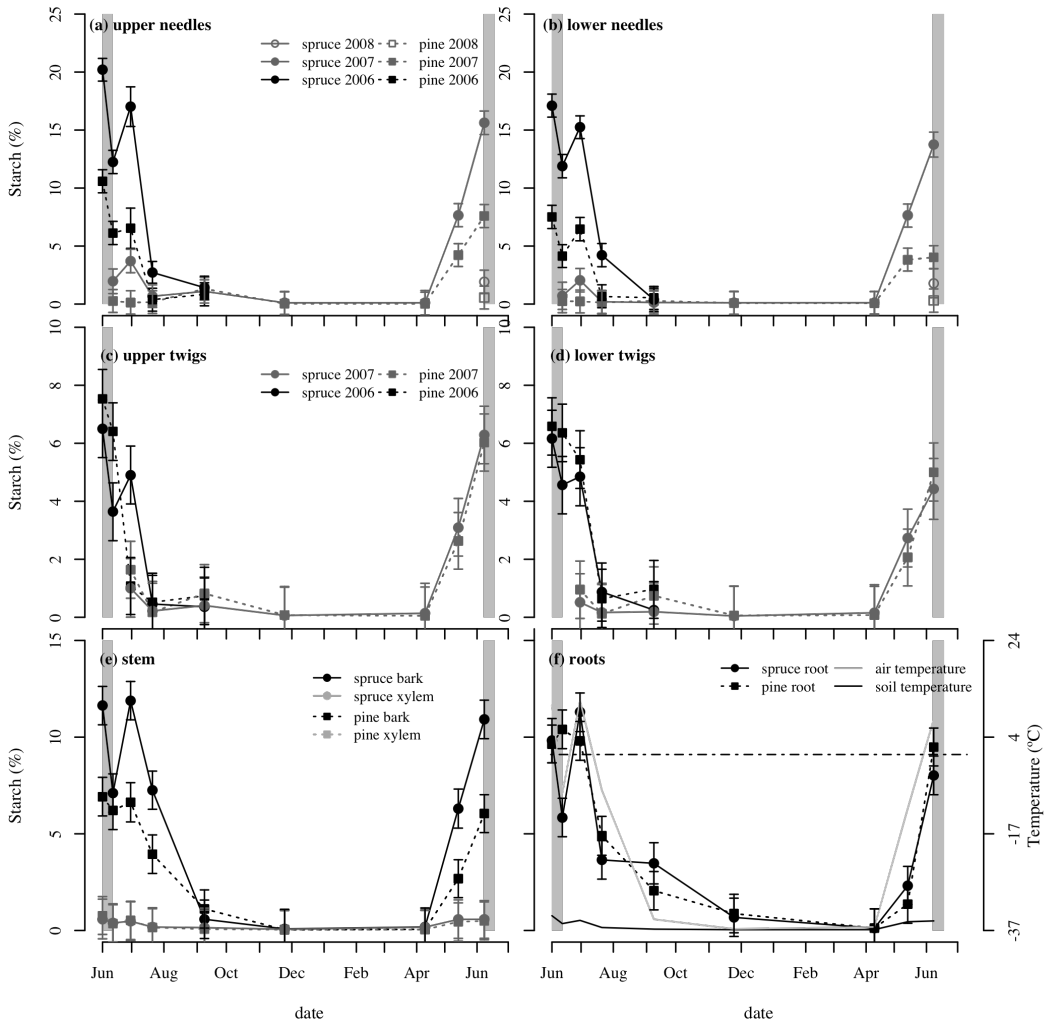

Figure 3.3: Seasonal course of starch in (a-b) upper and lower needles, (c-d) twigs tissues, (e) bark and xylem and (f) roots of pine (*Pinus contorta*) and spruce (*Picea glauca)*. In addition, (f) also includes air temperature and soil temperature at 10 cm depth. The shaded region in (a-d) represents the period of shoot expansion and the year associated with tissues in legends indicates the year in which shoots expanded. Error bars represent 95% confidence intervals (n=8).

Seasonal concentrations of soluble sugars in the needles of pine and spruce tended to be highest during winter but there was also a lesser peak in June (Figure 4a,b). In twig, bark, xylem and root tissues, sugar concentrations were highest during the winter (Figure 4c-f). In both species, there was a steep decline in sugars in the xylem from late winter (April) to spring (May) (Figure 4e), corresponding with time of TNC increase in other tissues. In spruce sugar

concentrations were 50% higher in the bark and needles compared to pine. In the twigs, soluble sugar concentrations were higher in spruce relative to pine during the growing season but had converged to similar levels by the late fall (Figure 4c,d). In the root tissues, however, there were no differences between the two species (Figure 4f).

3.3.2 Seasonality in sugar alcohols and lipids

Sugar alcohols tended to be higher in pine needles on most sampling dates (Figure 5); however, sugar alcohols in the twigs of pine were clearly higher than in spruce (Figure 5). In the bark, spruce maintained much higher levels of sugar alcohols than the pine. Sugar alcohols in spruce peaked at nearly 5% of dry weight by late winter (April) and then declined sharply into May and June. In the bark of pine, however, sugar alcohols had little seasonal variation except for a slight increase in mid-June that corresponded with a second peak in spruce as well (Figure 5).

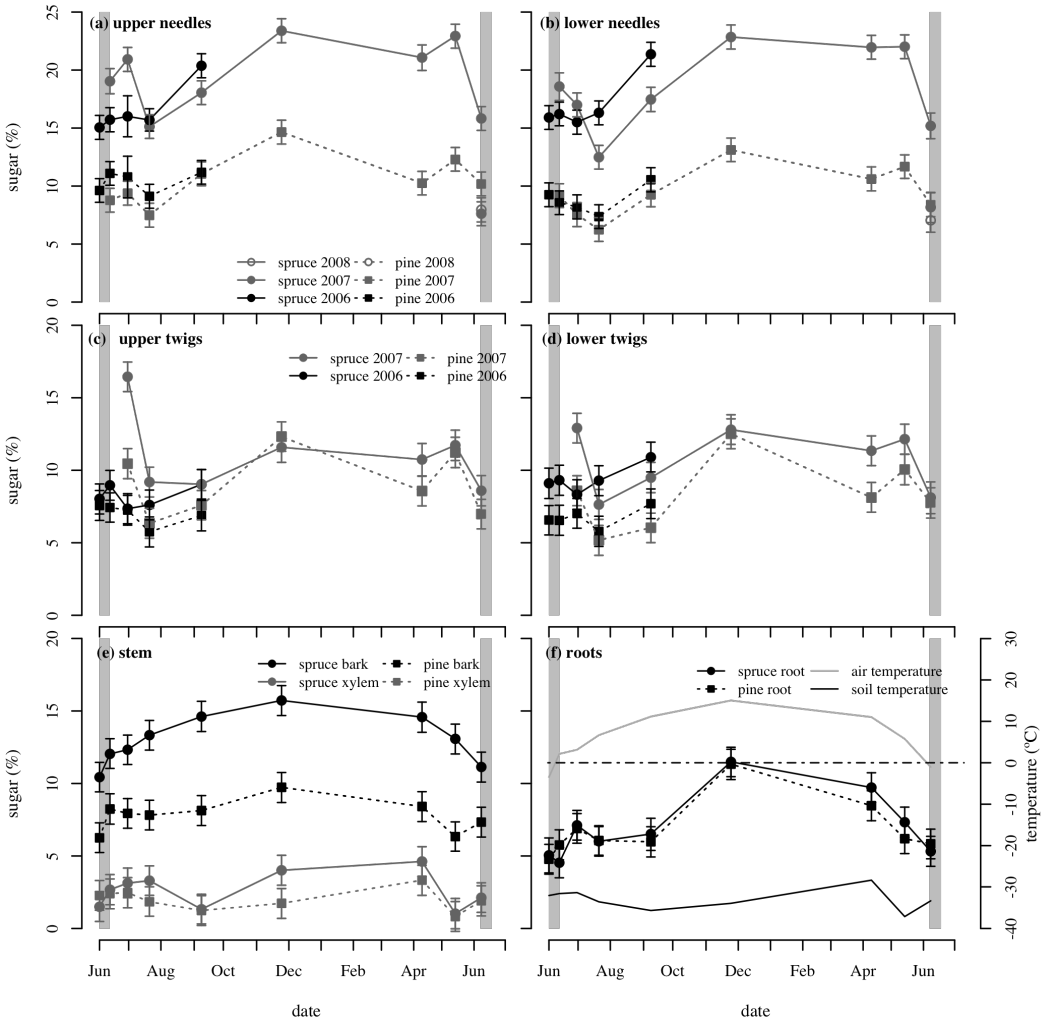

Figure 3.4: Seasonal course of soluble sugars in (a-b) upper and lower needles, (c-d) twigs tissues, (e) bark and xylem and (f) roots of pine (*Pinus contorta*) and spruce (*Picea glauca)*. In addition, (f) also includes air temperature and soil temperature at 10 cm depth. The shaded region in (a-d) represents the period of shoot expansion and the year associated with tissues in legends indicates the year in which shoots expanded. Error bars represent 95% confidence intervals (n=8).

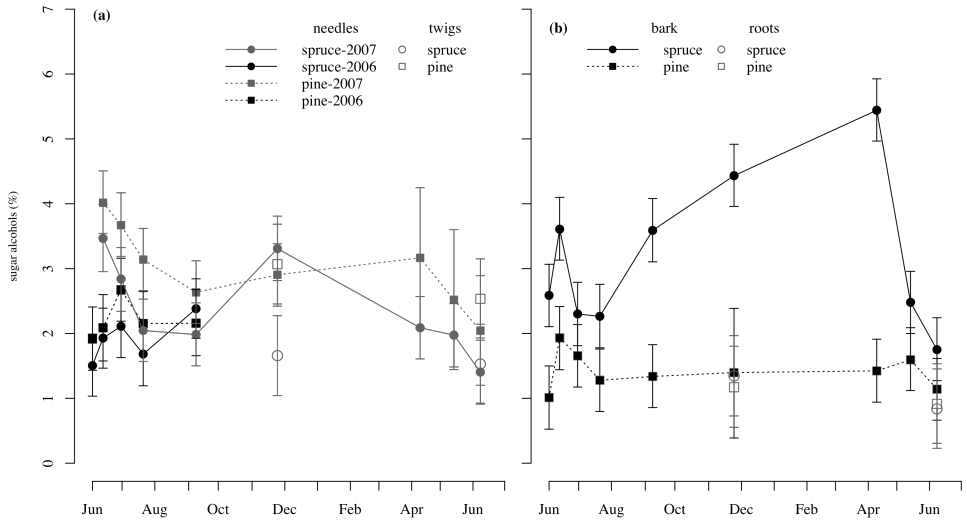

Figure 3.5: Seasonal course of sugar alcohols in (a) currently expanded (flushed in 2007) and one-year old (flushed in 2006) needles and twigs and (b) bark and roots of pine (*Pinus contorta*) and spruce (*Picea glauca)*.Error bars represent 95% confidence intervals (n=8).

Lipids were only assessed at two sampling dates (November 23, 2007 and June 3, 2008) in upper needle and twig, bark, and root tissues (Figure 6). Lipid concentrations in the tissues ranged from ~ 1-4% dry weight with the exception of pine bark had ~ 9% lipid by dry weight (Figure 6); there was little evidence of seasonality in any of the tissues assessed. Again, with the exception of much higher concentrations of lipids in the bark of pine, lipids were similar in concentration between the species (Figure 6).

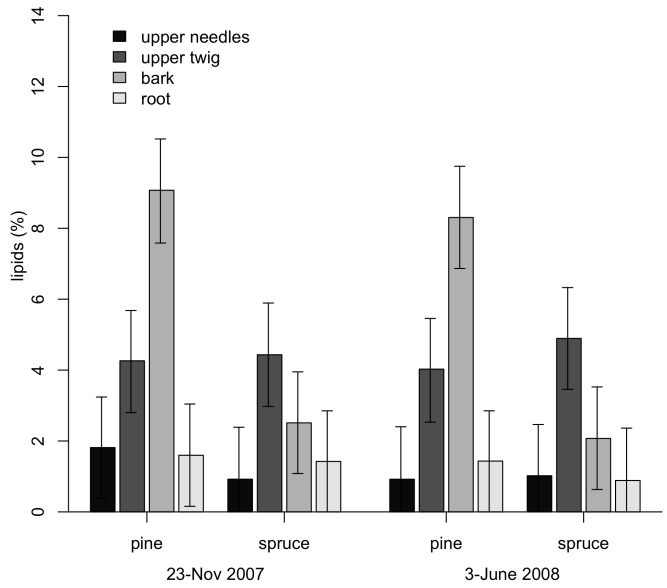

Figure 3.6: Lipid concentration in the winter (23-Nov-2007) and late-spring (3-June-2008) in needles, twigs, bark and roots of pine (*Pinus contorta*) and spruce (*Picea glauca)*.Error bars represent 95 % confidence intervals (n=5).

3.3.3 Contribution of starch, sugars, lipids and sugar alcohols to total NSC pool

Overall, TNC made up the largest pool of NSC in these trees with values ranging from 70-90% in spruce and 50-85% in pine (Figure 7). However there was virtually no starch in winter, which appears to have been primarily shifted to the soluble sugar pool. Lipids made up 20% of the NSC pool in the twigs of pine and up to 40% in the bark. In spruce twigs, lipids contributed up to 25% of the total NSC. In the rest of the tissues sampled, lipids contributed less than 10% to the NSC pool in both pine and spruce (Figure 7). In both species and across tissues, sugar alcohols contributed 5-20% of the NSC pool (Figure 7).

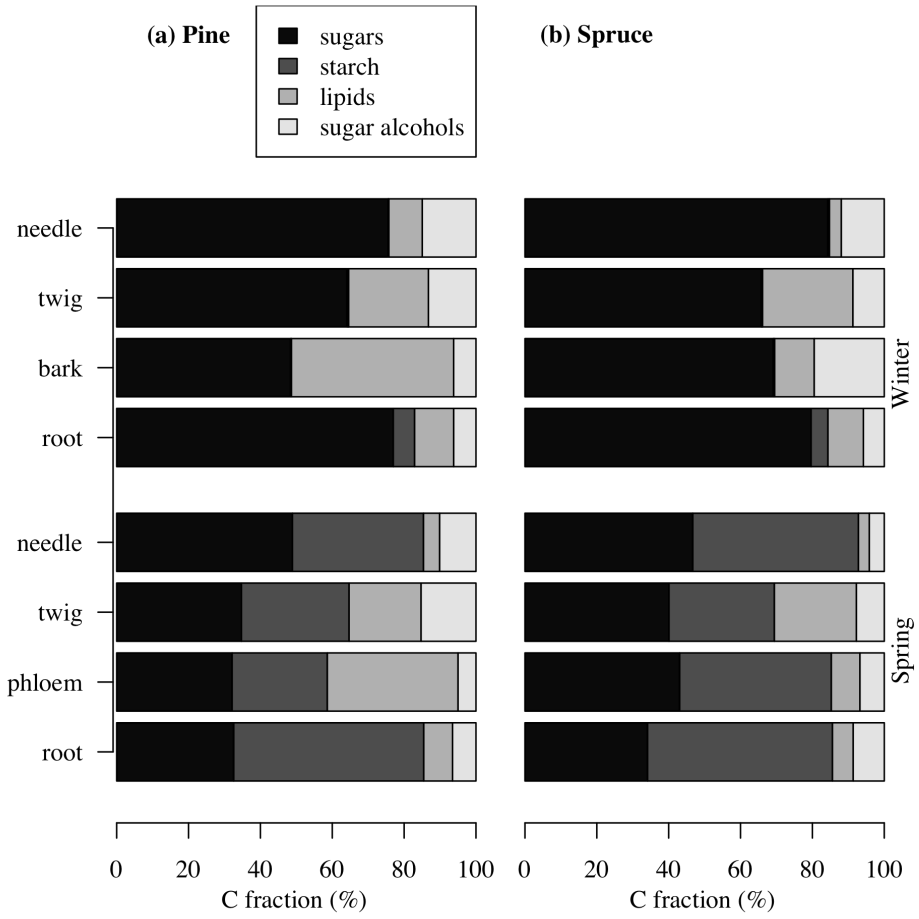

Figure 3.7: Proportions of NSC compounds (sugar alcohols, starch, soluble sugars, and lipids) for needles, twigs, bark and roots of (a) pine (*Pinus contorta)* and (b) spruce (*Picea glauca)* in winter (23-Nov-2007) and spring (3-June-2008)

3.4 Discussion

An unexpected result of this study was the fact that although there were large differences in TNC concentrations between the two species, these differences were dependent on the tissue being examined and the date on which they were collected. In needles and bark tissues, TNC concentrations were often twice as high in spruce relative to pine. Differences in TNC concentrations in twig, xylem and root tissues, however, were smaller or only different between the two species at specific times of the year. White spruce is shade tolerant and longer lived than lodgepole pine and maintaining higher intrinsic TNC levels is

consistent with its conservative growth strategy compared with the shade intolerant and faster growing lodgepole pine. Similarly, low levels of TNC concentrations were also found in the shoots of other fast growing southern pines (i.e. *Pinus taeda* (Ludovici et al. 2002) and *Pinus elliotii* (Gholz and Cropper 1991)). Presumably, fast growing species achieve superior growth rates by allocating more carbon to growth than to storage. However, this strategy places these trees at greater risk of carbon limitation in the event of conditions that limit photosynthesis. In contrast, *Pinus sylvestris* and *Picea abies* both maintained higher TNC concentrations in tissues (Hoch et al. 2003); *P. sylvestris*, however is a much longer-lived species compared to *P. contorta*.

In mid-June, almost all tissues (except for twigs) in spruce, showed a consistent reduction in starch concentration, followed by a strong recovery two weeks later. The reduction in spruce was likely a consequence of the accelerated shoot expansion after bud flush. Except for a minor decline in needle starch (lower needles only) in mid-June, pine did not show the same tree-wide reduction in starch during shoot expansion. This dissimilarity is likely related to the more gradual expansion of the shoots in pine, which may draw less on the existing reserves during the shoot expansion period and accounts for the small decline in starch observed in needles in pine but not in the other tissues. Webb and Kilpatrick (1993) also observed a similar reduction in starch in the needles (but not in twig bark) during the rapid shoot flush in *Pseudotsuga menziesii* seedlings; while Ericsson (1979) found a more subtle effect in the needles of *Pinus sylvestris* where he similarly attributed the lowered accumulation rates of starch (and declines in some cases) to the expansion of shoots.

Although most of the measured tissues in both species experienced their maximum starch concentrations prior to the onset of shoot growth in the spring; the timing of decline in starch content was delayed in the stem bark and roots compared to the crown tissues (needles and twigs). For needle tissues in evergreen conifers, this appears to be a common pattern corresponding with shoot expansion, regardless of climate and species (Fischer and Höll 1991; Gholz and Cropper 1991; Hoch et al. 2002, 2003; Bansal and Germino 2009). The slower

decline of TNC in bark and roots in early summer also corresponded with the continued growth of the stem and roots during the summer (see insets Figure 1). Stem diameter growth in pine and spruce was observed from the first sampling date (31-May) and both species followed similar cumulative growth patterns. Diameter growth was ~80% complete by mid-July and was effectively terminated by early September, corresponding with the nearly zero starch concentrations and lowest overall TNC concentrations in the bark. Additionally, there were clear differences in TNC between upper and lower twigs during the shoot expansion phase (see also Gholz and Cropper 1991; Webb and Kilpatrick 1993); these differences largely disappeared by the fall.

Root diameter growth was initiated later than stem growth; in both pine and spruce only one out of eight trees sampled in mid-June showed any evidence of visible root diameter growth. By late June, half of the spruce trees exhibited root diameter growth, compared with only one out of eight pine trees. This corresponded with the large decline in TNC concentrations in spruce roots in mid-June as shoot growth was maximized which likely meant that little newly assimilated carbohydrates were allocated below ground; consequently, spruce roots could not replenish TNC at the same rate that they were being utilized for growth. Deans and Ford (1986) found that the onset of root diameter growth was closely tied to the proximity to the bole; increased distance from the crown meant a later start in diameter growth. In fact, root diameter growth was not observed in roots > 1.0 m from the tree base until after shoot expansion had occurred. However, in *Pseudotsuga menziesii* seedlings, fine root activity (measured as numbers of white root tips) showed bimodal activity both preceeding and after shoot expansion (Krueger and Trappe 1967). In my study, my roots were collected between 0.5-2.0 m away from the tree base.

In the boreal forest, the extended period of soil temperatures below 0°C, is likely to be the most influential factor in the growth and C allocation of roots. This is largely what differentiates roots of trees growing in a temperate climate from those trees growing in a boreal or high elevation climate. Overwinter root growth is not possible and roots have a shorter period to build up carbohydrate

reserves as photosynthesis is also limited by a shortened growing season. Although all tissues began accumulating starch in early May, starch build-up in roots was lagging, which could be due to the cooler soil temperatures lagging behind the air temperature or due to active sinks which are more proximate to the needles. In contrast, non-structural carbohydrate concentrations (starch in particular) in roots of trees growing in temperate climates appear to increase before (Krueger and Trappe 1967; Ludovici et al. 2002) or concurrently (Gholz and Cropper 1991) with the spring peak in needle TNC levels, with rebuilding of roots starch reserves at the beginning of the fall (Ludovici et al. 2002) and late winter (Krueger and Trappe 1967; Gholz and Cropper 1991). As a result, maximum root starch concentrations in the spring were much higher in trees growing in temperate climates; ~19% in *Pinus taeda* (Ludovici et al. 2002) versus ~10% in *Pinus contorta* and *Picea glauca* in my study. It appears that starch reserves in the boreal trees never really have the opportunity to build-up the way they could in a more favorable climate. This may also explain why I observed large differences in TNC between pine and spruce in aboveground tissues but only minor differences in belowground tissues.

In the winter months I also observed a pronounced increase in soluble sugars, which is consistent with findings from other studies in temperate (Krueger and Trappe 1967; Pomeroy et al. 1970; Fischer and Höll 1991) and northern climates (Ericsson 1979). However, the patterns of sugar accumulation were not the same between tissues; sugar concentrations in the bark had a single peak in the winter months, whereas the shoots (needles and twigs) produced a bimodal response with a spring and winter peak. The spring peak is likely related to shoot growth and the large mobilization and production of sugars in the crown of the trees in the spring. This bimodal pattern was also found in the roots although the magnitude of the spring/summer peak was less than the winter peak. Although I did not differentiate between different groups of sugars; the overall increase in sugars during winter was likely driven by reducing sugars (i.e. fructose and glucose) and spring peaks driven by sucrose (Pomeroy et al. 1970; Fischer and Höll 1991).

Overall, TNC and sugar concentrations in the xylem of both species were low (5% or less) compared to the other tissues, which agrees with findings for *Picea abies* and *Pinus sylvestris* and *Pinus elliottii* (Höll 1985; Gholz and Cropper 1991; Fischer and Höll 1992; Hoch et al. 2002, 2003). However, it is worth noting that the sugar concentrations in the ray cells of the xylem would have been substantially higher given that these living cells make up only a small fraction of the xylem (Schoonmaker et al. 2010). Interestingly the xylem contained little starch, even during the spring and early summer when other tissues had high levels of starch. The xylem of both species showed a sharp drop in sugar concentration in early May prior to shoot expansion followed by a recovery in June. In this study, this drop corresponded to a build-up of TNC reserves in other tissues and the onset of cambial activity as I noted observable stem growth as early as late May. The repair of xylem (Brodersen et al. 2010) and increased respiration of tissues in spring could also account for this decline.

We observed some large differences in concentrations of sugar alcohols between pine and spruce and at different sample times. First, in needles and twigs, pine tended to have higher values than spruce, while in stem bark, spruce had higher concentrations. Second, in the stem bark of spruce there was large buildup of sugar alcohols over the winter followed by a sharp decline in May and June; this also suggests a winter storage role for bark sugar alcohols. The reasons for these variations across seasons and different species may relate to differences in frost tolerance; however, sugar alcohols also need to be considered in relation to the strategies for the use of NSC storage pools. Concentrations of sugar alcohols in my study ranged from 1-5% of dry weight; in root wood and branch wood, *Pinus cembra, Picea abies* and *Pinus sylvestris* contained 1-1.5% (Hoch et al. 2002, 2003). It is not surprising that my values tend to be higher, as the previous studies were measuring xylem tissues which would have much more diluted carbohydrate pools. Ericcsson (1979) observed the seasonal variation in sugar alcohols in needles of *Pinus sylvestris* to flux by 2.5% which is comparable to my results.

Overall, lipid concentrations were low; the single exception was in the bark of pine, where lipid concentrations were up to 10%, contributing between 20-40% of the NSC pool (depending on the time of year) in pine. In the roots and stem and branch sapwood of *Pinus cembra,* lipids can represent between 50% and 70% of the NSC pool (Hoch et al. 2002). However in my species, the remaining tissues (needles, twigs and roots) had quantities that were much lower (< 25% of the NSC pool or < 4% of dry weight) and more similar to lipid concentrations found in needles of *Pinus sylvestris* (Fisher and Höll 1991).

In general the slower growing and long-lived spruce had higher TNC concentrations than the fast-growing pine and the differences between these species were most striking in the needles and bark. Spruce also had wider absolute seasonal changes in TNC (and in sugar alcohols in some tissues) than the pine, which suggests that storage plays a more important role in spruce than in pine. In these boreal species, there was a build-up of sugars in the xylem and sugar alcohols in bark tissues during winter; presumably the sugars offered protection from extremely low temperatures. The sugar alcohols may also contribute to the start-up of physiological processes in spring. Most tissues accumulated starch in the spring and early summer and then starch declined sharply in late summer. In these boreal species, however, roots seem to have lower accumulation of non-structural carbon (NSC) than in conifers from temperate sites, likely because of the short growing season. Overall, this study shows that NSC dynamics in trees are complex. Knowledge of the NSC dynamics of a species is essential to develop sampling schemes that avoid developing erroneous conclusions about physiological processes.

3.5 References

Bansal S, Germino MJ (2009) Temporal variation of nonstructural carbohydrates in montane conifers: similarities and differences among developmental stages, species and environmental conditions. Tree Physiol 29: 559-568

Beckingham JD, Archibald JH (1996) Field Guide to Ecosites of Northern Alberta. University of British Columbia Press, Vancouver, British Columbia

Bligh EB, Dyer WJ (1959) A rapid method of total lipid extraction and purification. Can J Bio Physiol 37: 911-917

Brodersen CR, McElrone AJ, Choat B, Matthews MA, Shackel KA (2010) The dynamics of embolism repair in xylem: In vivo visualizations using high-resolution computed tomography. Plant Physiol 154: 1088–1095

Chow PS, Landhäusser SM (2004) A method for routine measurements of total sugar and starch content in woody plant tissues. Tree Physiol 24: 1129-1136

Deans JD, Ford ED (1986) Seasonal patterns of radial root growth and starch dynamics in plantation-grown Sitka spruce trees of different ages. Tree Physiol 1: 241-251

Environment Canada (2010) National climate data and information archive. [WWW document]. URL http://www.climate.weatheroffice.ec.gc.ca/Welcome_e.html [accessed on 1 July 2010]

Ericsson A (1979) Effects of fertilization on the seasonal changes of carbohydrate reserves in different age-classes of needle on 20-year-old Scots pine trees (*Pinus sylvestris*). Physiol Plant. 45: 270-280

Fischer C, Höll W (1991) Food reserves of scots pine (*Pinus sylvestris* L.) I. Seasonal changes in the carbohydrate and fat reserves of pine needles. Trees 5:187-195

Fischer C, Höll W (1992) Food reserves of scots pine (*Pinus sylvestris* L.) II. Seasonal changes and radial distribution of carbohydrate and fat reserves of pine wood. Trees 6:147-155

Gelman A, Hill J (2007) Data analysis using regression and multilevel/hierarchical models. Cambridge University Press, New York, NY

Gelman A, Su Y, Yajima M, Hill J, Grazia Pittau M, Kerman J, Zheng T (2010) arm: Data Analysis Using Regression and Multilevel/Hierarchical Models. R package version 1.3-08. http://CRAN.R-project.org/package=arm

Gholz HL, Cropper WP (1991) Carbohydrate dynamics in mature *Pinus elliottii* var. *elliottii* trees. C J For Res 21: 1742-1747

Hoch G, Popp M, Körner C (2002) Altitudinal increase of mobile carbon pools in *Pinus cembra* suggests sink limitation of growth at the Swiss treeline. OIKOS 98: 361-374

Hoch G, Richter A, Körner C (2003) Non-structural carbon compounds in temperate forest trees. Plant Cell Environ 26: 1067-1081

Höll W (1985) Seasonal fluctuation of reserve materials in the trunkwood of spruce [*Picea abies* (L.) Karst.]. J Plant Physiol 117: 355-362

Krueger KW, Trappe JM (1967) Food Reserves and Seasonal Growth of Douglas-fir seedlings. For Sci 13: 192-202

Ludovici KH, Allen HL, Albaugh TJ, Dougherty PM (2002) The influence of nutrient and water availability on carbohyrate storage in loblolly pine. For Ecol Manage 159: 261-270

Nelson EA, Dickson RE (1981) Accumulation of food reserves in cottonwood stems during dormancy induction. Can J For Res 11: 145-154

Pomeroy MK, Siminovitch D, Wightman F (1970) Seasonal biochemical changes in the living bark and needles of red pine (*Pinus resinosa*) in relation to adaptation to freezing. Can J Bot 48: 953-967

R Development Core Team (2010) R: A language and environment for statistical computing. R Foundation for Statistical Computing, Vienna, Austria. ISBN 3-900051-07-0, URL http://www.R-project.org/

Ryan MG (2011) Tree responses to drought. Tree Physiol 31: 237–239

Schoonmaker AL, Hacke UG, Landhäusser SM, Lieffers VJ, Tyree MT (2010) Hydraulic acclimation to shading in boreal conifers of varying shade tolerance. Plant Cell Environ 33: 382-393

Streeter JG (2001) Simple partial purification of d-pinitol from soybean leaves. Crop Sci 41: 1985-1987

Webb WL, Kilpatrick KJ (1993) Starch content in Douglas-fir: Diurnal and seasonal dynamics. For Sci 39: 359-367

Zuur AF, Ieno EN, Walker NJ, Saveliev AA, Smith GM (2009) Mixed effects models and extensions in ecology with R. Springer, New York. pp 1-574

Chapter 4: Impact of light availability on the seasonal dynamics of non-structural carbon in *Picea glauca*

Introduction

The impact of light on plant form and function has been extensively studied (e.g. Messier et al. 1999 and many others). Survival in a low-light environment involves changing morphological and physiological characteristics in order to more efficiently capture light and/or reduce carbon costs. Even with the higher efficiency of light capture, however, photosynthetic rates are reduced in shaded understory conditions (Man and Lieffers 1997). The reduction in photosynthesis is translated into reduced growth and increased allocation to aboveground tissues, particularly leaves (Landhäusser and Lieffers 2001). Reduced assimilation rates might also affect the non-structural carbon (NSC; soluble sugars, starch, sugar alcohols and lipids) available for future growth and consequently the ability to respond to environmental disturbances. Few studies, however have examined how NSC is impacted by shaded environments.

Of the studies that have compared NSC in trees growing in reduced light environments, the responses to shade have been mixed. In angiosperms, shaded plants were found to have either lower (Naidu and DeLucia 1997; Gleason and Ares 2004; Machado and Reich 2006; Imagi and Seiwa 2010) or no difference (Imagi and Seiwa 2010) in total non-structural carbohydrates (TNC) (soluble sugars and starch) compared with fully exposed individuals. The discrepancy between these reports could be due to several factors (1) species selection (e.g. plasticity in shade tolerance), (2) when and how long the shade treatment has been applied, (3) timing of reserve measurement, (4) the age of the trees being examined and/or (5) the tissue being examined (e.g. roots or shoots).

In conifers, it has been observed that within the tree crown, where light availability generally declines from the top to the bottom of and with depth into the crown, it appears that lower branches contain lower concentrations of TNC compared with upper branches (Gholz and Cropper 1991; Webb and Kilpatrick

1993); however, this response may be seasonally dependent. Therefore it is important to study the seasonal dynamics within different tissues of the entire tree as differences in TNC may be seasonally dependent or restricted to certain components of the trees. It is still unclear if the differences in TNC reserves observed between crown positions is a direct response to lower light or to factors related to the competition for resources among branches within a tree.

My objective was to measure and compare seasonal dynamics of NSC in white spruce (*Picea glauca* (Moench) Voss) trees growing under field conditions in either: full light or in a forest understory. White spruce is considered a moderately shade tolerant long-lived tree species common to the boreal forest region of North America. Given that light levels are reduced in an understory, I hypothesized that TNC reserves should be overall much lower in spruce growing in a light-limited environment.

4.2 Methods

4.2.1 Study site and tree selection

Sixteen study sites were selected near Whitecourt, Alberta, Canada in the lower foothills natural sub-region (Beckingham et al. 1996). Average total precipitation in this region is 578 mm and total precipitation in 2007 was 560 mm. Daily average temperature is 2.6 ºC with a mean monthly temperature in January of -12.1 ºC and 15.7 ºC in July (Environment Canada 2010). Eight sites were located in mixedwood stands (elevation range 910-938 m) with an understory of white spruce and sub-alpine fir (*Abies lasciocarpa* (Hook)Nutt.) and overstory of aspen (*Populus tremuloides* (Michx.) Á. Löve & D. Löve). The average light level at 1.3 m height, at mid-day in July was measured at 7% of full sunlight. However, based upon the light absorption of aspen canopies in this area, it can be expected that light levels were about 30% at the top of the understory spruce crowns (Constabel and Lieffers 1996). The other eight stands (elevation range 1004-1102 m) were mixed stands of white spruce and lodgepole pine that had originated after commercial harvesting between 1979-1981. These stands were

pre-commercially thinned at year 10 and had not reached crown closure at the time of my measurements. Temperature sensors and data loggers (Hobo, Onset Computer Corp, Pocasset MA, USA) were installed at each site, at a depth of 10 cm, to record soil temperatures. At each of the 16 sites, 9 relatively similar-sized white spruce trees were selected and tagged for future sampling. Within a site, trees were dominant or co-dominant, similar in height and free of visible disease. Across all sites, however, the trees ranged from 5-10 m in height. In the open-grown stands, the selected trees received direct sunlight, while in the mixed-wood stands, the largest spruce in these stands were still below the canopy of the aspen. A summary of tree and stand characteristics are found in Table 1.

Table 4.1: Stand and tree attributes of open and understory-grown *Picea glauca*. Values in brackets are ranges of mean values across the eight site locations for each of the open and understory-grown white spruce.

Stand type	tree age (years)	basal area (m^2 ha^{-1})	density (stems ha^{-1})	diameter (cm)	height (m)	live crown ratio
Open-grown						
Picea glauca	25-27	22 (16-30)	2899 (1433-6132)	8.5 (7.5-9.4)	7.3 (6.6-8.0)	0.87 (0.78-0.91)
Understory-grown						
Picea glauca	24-53	41 (22-58)	3865 (1899-7331)	7.7 (6.4-10.4)	8.1 (6.6-10.1)	0.78 (0.69-0.82)

In each stand, two additional sample trees were selected and cored near the tree base to determine tree age.

4.2.2 Collection procedure

Collection dates were as follows: 31-May-2007, 11-June-2007, 28-June-2007, 19/20-July-2007, 2-Sept-2007, 21/22-Nov-2007, 7/8-April-2008, 7/8-May-2008 and 3-June-2008. For each tree, the following tissues were collected: (1) two upper branches located at the base of the upper ¼ of the whole tree; branches were taken from a south and north direction and pooled into a single sample. One-year old twig and needles (flushed in 2006) and current year twig and needles (flushed in 2007) were collected separately, (2) two lower branches

(south and north) located at the lowest branch whorl that still had evidence of flushing buds, (3) a sample of the bole (2.5 × 7.5 × 2.5 cm deep) at 1.3m height was extracted with a chisel; this was then separated into xylem and bark (all tissues exterior to the xylem) tissues, (4) a lateral root segment was collected by exposing a lateral root from the base of the tree until the root diameter was 1.0 cm and then a 10 cm long segment of the root was obtained. All samples were placed in plastic bags and stored on dry ice (with the exception of sampling periods where air temperatures were below -5ºC and then ice or snow was used) until returning from the field. Samples were stored at -20ºC until further processing.

4.2.3 Tree growth measurements

We measured root and stem diameter increment of the year of sampling (2007) as well as the previous year (2006) of all of the sampled trees. For root measurements, I used a light microscope and image analysis software for all diameter measurements. I scanned sanded stem sections and used SigmaScanPro software to measure ring width. I also measured annual extension of twigs during the first 4 collections (31-May-2007 to 19-July-2007).

4.2.4 Carbohydrate analysis

Samples were heated in an oven for 1 hour at 100ºC and then the temperature was dropped to 70ºC and dried until constant weight. Tissue was ground in a Wiley-mill (Thomas Scientific, Swedesboro New Jersey, USA) to pass 40 mesh. Analysis of total sugars and starch followed the procedure developed by Chow and Landhäusser (2004). Briefly, 50 mg of dried, ground tissue was put through an ethanol extraction (3 times) to extract the soluble sugars. The extract was treated with phenolsulfuric acid to breakdown the sugars into monosaccharides and analyzed for total sugar colorimetrically. The starch in the sample residue was converted to glucose using a mixture of digestive enzymes including α-amylase and amyloglucosidase and the glucose was assessed colorimetrically.

4.2.5 Sugar alcohol (cyclitol) analysis

It has been previously demonstrated that the vast majority of sugar alcohols in other *Pinus* and *Picea* species occur as cyclitols (pinitol in particular) (Hoch et al. 2003). I extracted cyclitols following Streeter (2001), where ground material (100 mg) was extracted twice with ethanol at room temperature, and then the extracts were pooled together and dried at 70°C for 24 hours. The residue was then dissolved in 1.0 mL distilled water and 0.375 mL chloroform, and stored at 4ºC overnight. After centrifuging, the top aqueous layer was separated and then heated in a 65ºC water bath for 30 min to remove trace chloroform. This layer was then poured through two resin columns for purification. The final eluant containing the cyclitols was collected in clean, pre-weighed vial and dried at 70ºC for 24 hours before weighing the final product.

4.2.6 Statistical analysis

We used a model-selection approach (Zuur et al. 2009) to build a linear model to summarize my findings instead of standard multiple comparisons tests. From this model I then used the 95% coverage region of the posterior probability distribution (using the *sim* function in the library *arm* (R Development Core Team 2010; Gelman et al. 2010.) to generate 95% confidence intervals around my point estimates; these intervals were used as my basis of comparison (Gelman and Hill 2007). Fixed effects in my models included species, tissue-type and sampling date and the random effect was the site or tree. Equality of variance and normality of the data in the linear model were assessed graphically. In addition, I checked for auto-correlation among tissues within trees (which can be assessed with diagnostic plots and by fitting a random effect for an individual tree).

4.3 Results

In the spring prior to and during bud flush, open grown trees generally had slightly higher TNC (soluble sugars and starch) concentrations in mature needles (in both the upper and lower positions); however, by mid-July these differences were no longer apparent (Figure 1a-b). In the twigs, TNC concentrations largely

overlapped in both groups although there was a slight separation between open and understory trees in the upper twigs during the spring (Figure 1c-d). In the bark tissues there was a tendency for higher TNC in open grown trees during the winter period; however, it was only during the September and April sampling dates that clear differences were detected (Figure 1e). Overall TNC concentrations in the xylem of both open and understory trees were largely similar; it was only in July that TNC was higher in open grown trees (Figure 1e). In roots, between late June and September there were large fluctuation in TNC in both environments where understory trees had higher TNC in July , while the reverse was true in September (Figure 1f). Roots from open grown trees tended to initiate diameter growth earlier than roots in understory trees (inset Figure 1f). In both, open and understory trees, the needles, bark and roots showed a decline in TNC in mid-June (Figure 1), which corresponded with the period of shoot expansion (insets Figure 1).

Starch concentrations in the needles and twigs were similar between open and understory trees although there was some evidence of higher starch in needles and upper twigs in open grown trees in June (Figure 2a-c). For needles of both open and understory trees there was a mid-June decline in starch followed by a rebound in late-June (Figure 2a-b). With the exception of a larger mid-June drop in starch in open grown trees, starch concentrations in bark and xylem were virtually identical between open and understory trees (Figure 2e).

Soluble sugar concentrations in the needle and twig tissues of open and understory trees were very similar (Figure 3a-d). There was a slight tendency for higher sugar concentrations in the bark of open grown trees during fall and winter (Figure 3e). Sugar concentrations in the xylem tended to be bimodal with an early summer and winter peak observed in both open and understory trees (Figure 3e) and in summer sugars tended to be higher in open trees. Sugar alcohols were similar between open and understory trees except for late fall and late winter where open grown trees were higher (Figure 4).

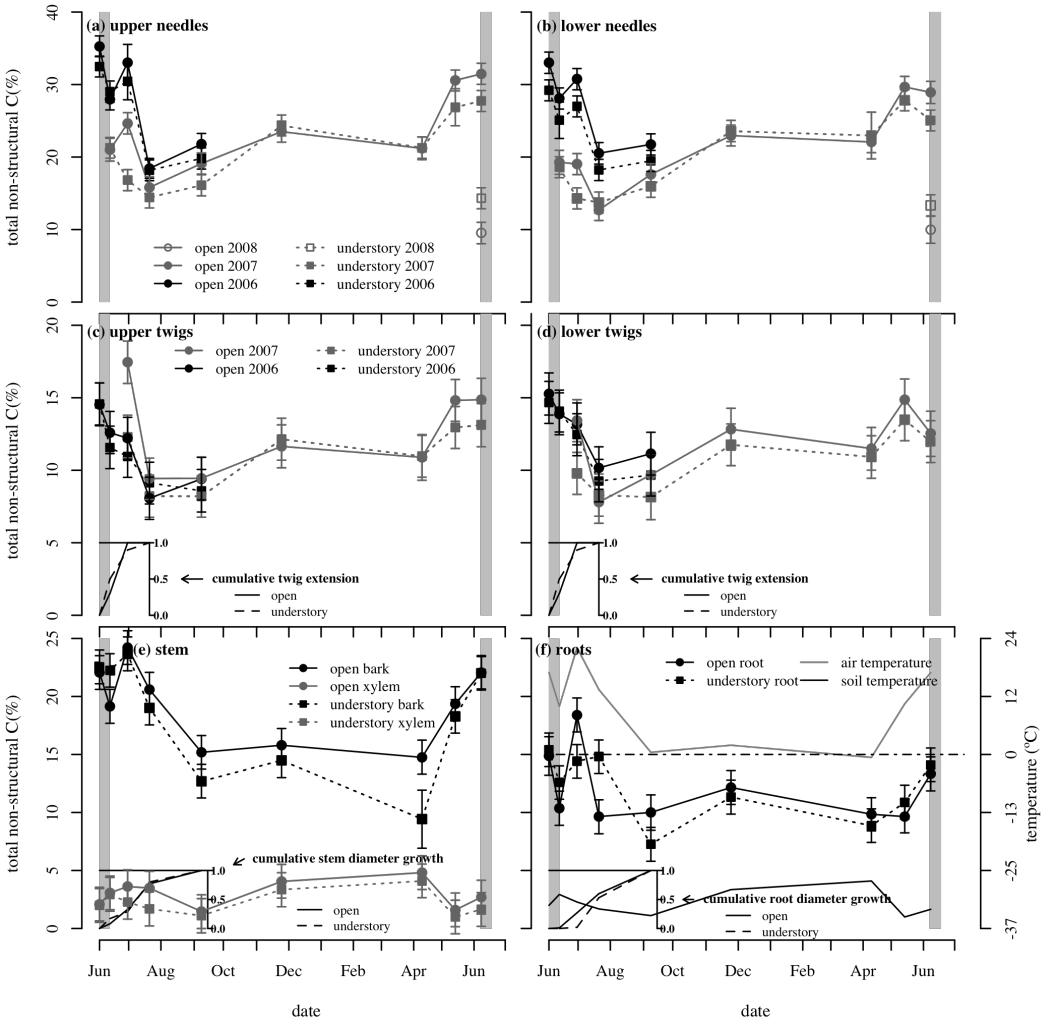

Figure 4.1: Seasonal course of total non-structural carbohydrates in (a,b) upper and lower needles, (c,d) twigs tissues, (e) bark and xylem and (f) roots of open-grown and understory *Picea glauca*. In addition, (f) also includes air temperature and soil temperature at 10 cm depth. The shaded region in (a-d) represents the period of shoot expansion and the year associated with tissues in legends indicates the year in which shoots expanded. Figure insets represent cumulative (c-d) twig extension, (e) stem diameter growth and (f) root diameter growth in open-grown and understory *Picea glauca*. Error bars represent 95% confidence intervals (n=8).

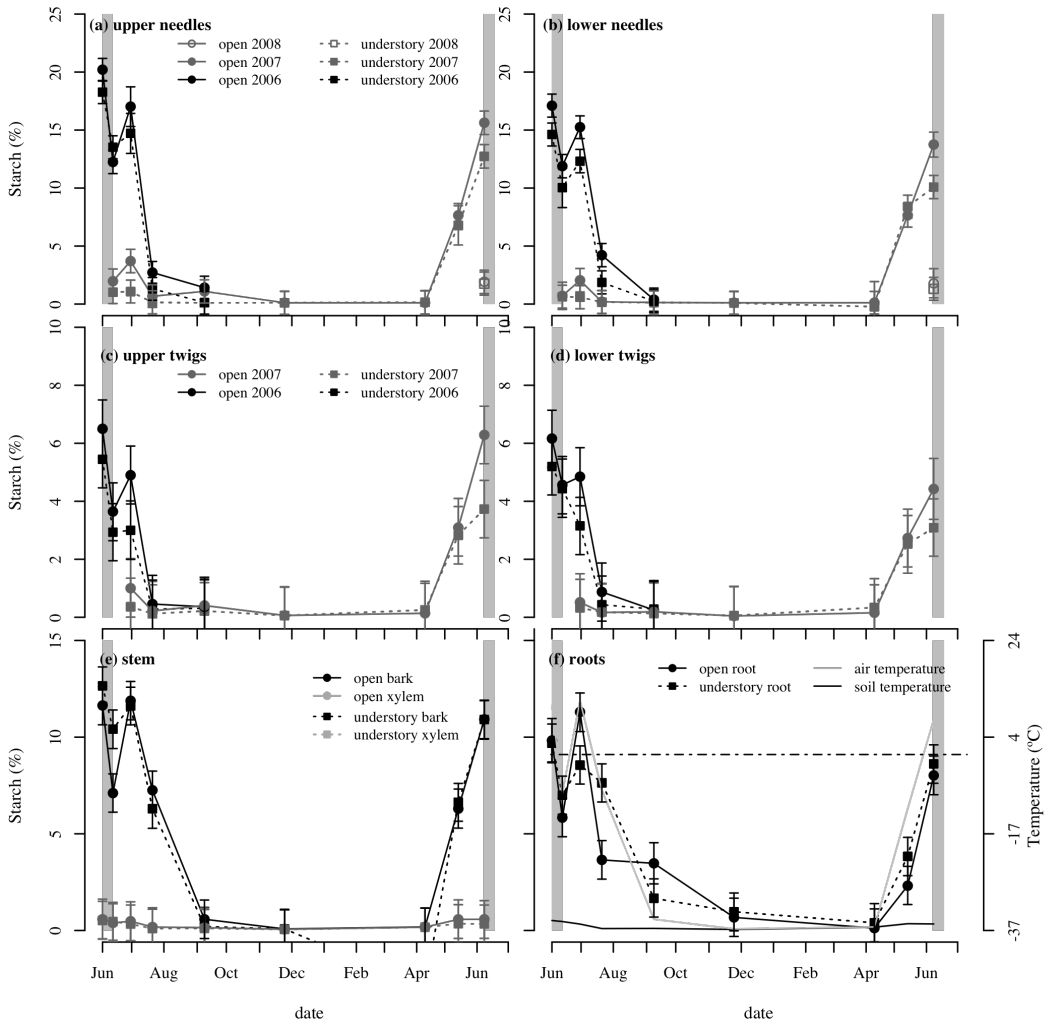

Figure 4.2: Seasonal course of starch in (a-b) upper and lower needles, (c-d) twigs tissues, (e) bark and xylem and (f) roots of open-grown and understory *Picea glauca*. In addition, (f) also includes air temperature and soil temperature at 10 cm depth. The shaded region in (a-d) represents the period of shoot expansion and the year associated with tissues in legends indicates the year in which shoots expanded. Error bars represent 95% confidence intervals (n=8).

Understory and open grown trees were similar in both height and diameter (Table 1). However, open-grown trees had larger growth in stem diameter and branch length (Table 2). Root diameter growth in open grown trees was on average higher, although much more overlap existed (Table 2). Interestingly, by the end of June, 50% of open grown trees and only 10% of understory trees

showed diameter growth (see also inset Figure 1e); it was not until mid-July that all trees were showing observable root diameter increment.

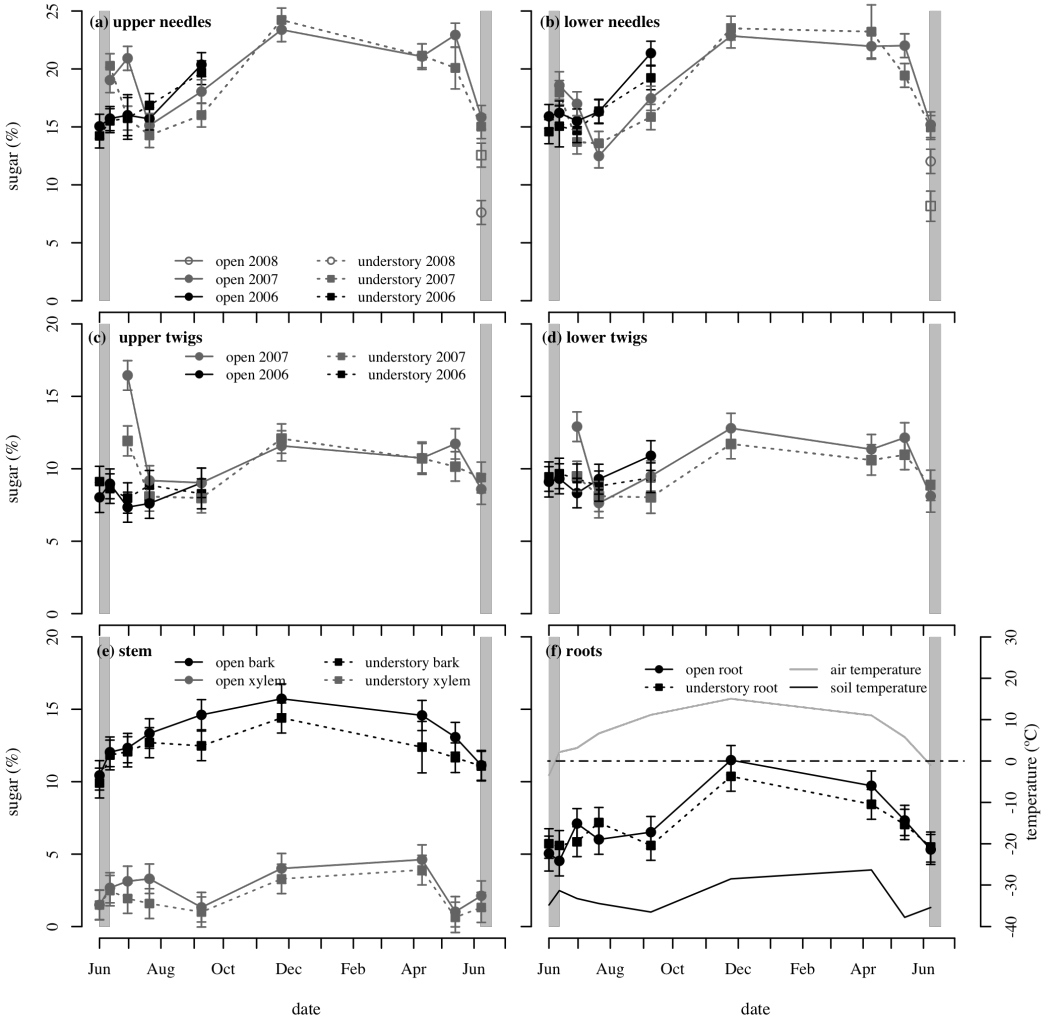

Figure 4.3: Seasonal course of soluble sugars in (a-b) upper and lower needles, (c-d) twigs tissues, (e) bark and xylem and (f) roots of open-grown and understory *Picea glauca*. In addition, (f) also includes air temperature and soil temperature at 10 cm depth. The shaded region in (a-d) represents the period of shoot expansion and the year associated with tissues in legends indicates the year in which shoots expanded. Error bars represent 95% confidence intervals (n=8).

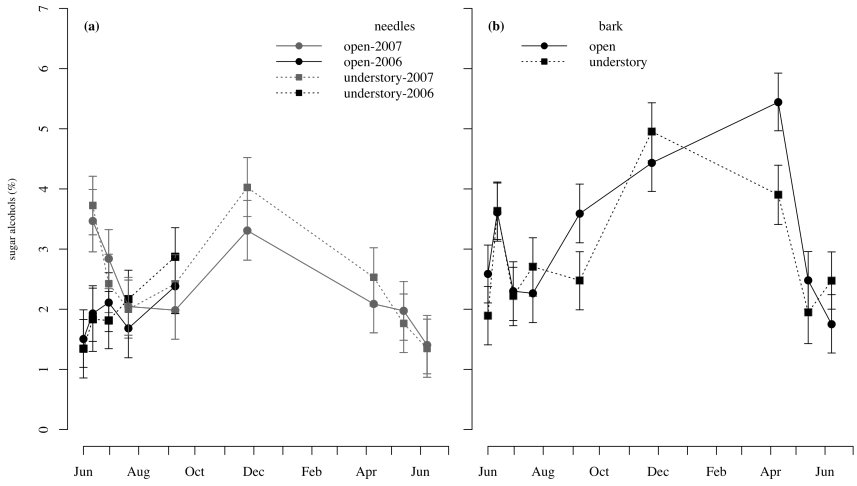

Figure 4.4: Seasonal concentrations of sugar alcohols in open-grown and understory *Picea glauca*. (a) needle tissues that flushed in 2007 and 2006 and (b) bark tissues. Error bars represent 95% confidence intervals (n=8).

Table 4.2: Year-end growth measurements of stem and root diameter and shoot extension of open-grown and understory *Picea glauca*. Root and stem measurements are means of trees sampled from four collections between Sept-2007 and May-2008 (n=32). Branch measurements are means of the 19-July-2007 collection (n=8).

Tissue	year	Open		Understory	
		mean	confidence interval	mean	confidence interval
root (mm)	2007	**0.58**	0.45-0.69	**0.45**	0.32-0.57
	2006	**0.52**	0.39-0.63	**0.39**	0.27-0.51
stem (mm)	2007	**3.50**	3.17-3.84	**1.68**	1.33-2.02
	2006	**3.64**	3.34-3.95	**1.82**	1.51-2.12
	2005	**3.80**	3.48-4.12	**1.97**	1.66-2.29
upper branch (cm)	2007	**15.3**	12.9-17.8	**9.62**	7.17-12.1
	2006	**16.6**	14.2-19.0	**10.9**	8.42-13.3
lower branch (cm)	2007	**8.29**	5.76-10.8	**6.54**	4.13-9.03
	2006	**9.54**	7.06-12.0	**7.81**	5.42-10.2

4.4 Discussion

Overall, across all the tissues and dates measured, TNC concentrations in open-grown spruce were only about 10% higher relative to spruce trees growing in an understory. Given that light in the understory was reduced by 70-90%, this difference was smaller than what I had expected. Of the few studies that have quantified carbohydrate responses in a reduced light environment (none of which were conducted on conifers), Naidu and DeLucia (1997) and Gleason and Ares (2004) found overall concentrations of TNC were reduced by up to 50% in shaded *Querucs rubra, Fraxinus uhdei* and *Acacia koa* seedlings compared to fully illuminated plants. However, the response of shade-tolerant *Quercus mongolica* to low-light was tissue-specific (Imagi and Seiwa 2010) as they observed no change in root TNC in shade, yet found a significant reduction in the stem TNC. Surprisingly, in the same study, shading had no effect on TNC reserves in the shade-intolerant *Castanea crenata.* Considering my study and the others described, the results seem to suggest that TNC responses to shade appear not to be generalizable across species or that there are other factors confounding the responses.

One important consideration with white spruce growing under a deciduous aspen canopy is the fact that during the spring and fall, these trees have about a month of high light conditions while the aspen canopy does not carry leaves (Constabel and Lieffers 1986). At these times, the spruce trees are photosynthetically active (Man and Lieffers 1997) and these periods of high light may provide a significant opportunity for understory spruce to build up TNC in their tissues. Secondly, it is possible that the slower growth of understory trees may actually result in decreased sink strength within the tree which could lead to proportionally higher TNC build-up in foliage and other tissues. This has been observed in trees with poor growth related to low temperatures (Hoch et al. 2002; Bansal and Germino 2009; Hoch and Körner 2009) or drought (Galvez et al. 2011). Conversely, under conditions that favor accelerated growth, such as fertilization, trees have responded with declines in TNC (Gholz and Cropper 1991; Ludovici et al. 2001; Goodsman et al. 2010).

In April and May, prior to shoot expansion, TNC in needles and twigs increased, mostly as a result of an increase in starch concentrations. This build-up was more pronounced in open-grown trees. Once the spruce had flushed, however, there was a steep decline in starch (and consequently TNC), coinciding with the expansion of leaf and shoot tissues. The fact that open-grown trees grew considerably more than understory trees is likely related to a larger build-up of TNC early in the spring and summer due to the greater exposure to light. Surprisingly, both open and understory trees maintained high starch concentration in needles and twigs late into June after shoot expansion had occurred. At that time I had expected carbohydrates to move to lower organs such as the stems and roots, as these organs were still actively growing. It is possible that the high starch levels in the needles and twigs at this time might be related to a period of high photosynthesis associated with favorable moisture conditions (which is typical in this region in June) and coupled with long days (~17 hours).

TNC in the bark was very similar in open and understory trees during the growing season, yet diverged in fall and winter; this appeared to be driven by higher sugar concentrations in open-grown spruce. Interestingly, sugar alcohols were also higher at times in open grown trees during the fall and winter. It is not clear why the bark of open-grown trees would require higher sugar or sugar alcohol concentrations in the winter but it might relate to a need for greater osmotic adjustments and frost protection in open-grown trees or it could simply be a consequence of less C availability to the understory spruce. In both open and understory trees, however, there was a steep decline in sugar alcohols between early April and mid May that corresponded with an increase in TNC in other tissues. This might suggest that sugar alcohols in the bark tissues are needed for frost protection during the winter months.

Soluble sugar concentrations in the stem xylem were higher in the open-grown trees in midsummer, but for the rest of the year the TNC and sugar levels of open and understory trees closely tracked each other. This build-up of xylem sugar in midsummer in open grown trees may simply have been a result of more C availability. During the winter, soluble sugars in the xylem were nearly 5% of

dry weight in both understory and open-grown trees; this is striking considering the ray cells only account for ~10% of the xylem tissue (Schoonmaker et al. 2010). Surprisingly, there was little starch in the stem xylem even during early June when the other tissues accumulated considerable concentrations of starch while soluble sugars in the stem xylem show seasonal fluctuations and decreased significantly between early April and May and may have contributed to metabolic activity in early spring.

In the roots, I observed some differences in TNC between open and understory trees from late-June until early September. These differences in early and mid summer may either relate to a true difference in strategy in carbon movement between open and understory trees or it may also simply be a consequence of differences related to the phenological stage of the trees in the open and understory because the understory trees were growing at slightly lower elevation and flushed earlier than the open grown trees. Presumably the build-up in TNC reserves in roots in spring and early summer could be used to fund root growth later in the growing season. Root diameter growth in open trees, however, appeared to be ahead of the understory trees; in late June, 50% of the roots of open grown spruce showed visible diameter growth compared to only 10% of the understory spruce. Warmer surface soil temperatures in open conditions could account for the difference in timing; however, I did not observe any differences in soil temperature at 10 cm depth (data not shown). The difference in timing of growth may account for the sharp drop in TNC in roots between late June and mid-July in open grown trees and the later drop in TNC in the understory trees between mid-July - September. Delay in root growth compared to above-ground growth was also observed in *Picea sitchensis,* roots (Deans and Ford 1986). After September, however, the understory spruce in my study had similar concentrations of root TNC compared to open grown spruce.

4.4.1 Conclusions

White spruce, a long-lived and shade tolerant boreal conifer, demonstrated surprisingly few differences in NSC between trees growing in a high and low-

light environment. In both environments, there was an increase in starch in twigs and needles prior to spring flush of foliage but this increase was somewhat larger in the open-grown trees. However, after the growing season, there were relatively few differences in NSC except in the bark tissue, where open grown trees tended to have greater sugar concentrations in fall and winter. In general, observable seasonal changes in TNC appeared to be dependent upon the time of sampling relative to the phenological stage of the plant and the type of tissue collected. Consequently, studies which compared NSC in shade and open grown plants should ensure their design captures appropriate timing as this study suggest that are some periods where some differences exist though, overall, those differences wash out to only 10% change over the whole year.

4.5 References

Bansal S, Germino MJ (2009) Temporal variation of nonstructural carbohydrates in montane conifers: similarities and differences among developmental stages, species and environmental conditions. Tree Physiol 29: 559-568

Beckingham JD and Archibald JH (1996) Field Guide to Ecosites of Northern Alberta. University of British Columbia Press. Vancouver, British Columbia.

Chow PS, Landhäusser SM (2004) A method for routine measurements of total sugar and starch content in woody plant tissues. Tree Physiol. 24: 1129-1136

Constabel AJ, Lieffers VJ (1996) Seasonal patterns of light transmission through boreal mixedwood canopies. Can J For Res. 26: 1008-1014

Deans JD, Ford ED (1986) Seasonal patterns of radial root growth and starch dynamics in plantation-grown Sitka spruce trees of different ages. Tree Physiol 1: 241-251

Environment Canada (2010) National climate data and information archive. [WWW document]. URL http://www.climate.weatheroffice.ec.gc.ca/Welcome_e.html [accessed on 1 July 2010]

Galvez D, Landhäusser SM, Tyree MT (2011) Root carbon reserve dynamics in aspen seedlings: does simulated drought induce reserve limitation? Tree Physiol 31: 250-257

Gelman A, Hill J (2007) Data analysis using regression and multilevel/hierarchical models. Cambridge University Press, New York, NY

Gelman A, Su Y, Yajima M, Hill J, Grazia Pittau M, Kerman J, Zheng T (2010) arm: Data Analysis Using Regression and Multilevel/Hierarchical Models. R package version 1.3-08. http://CRAN.R-project.org/package=arm

Gholz HL, Cropper WP (1991) Carbohydrate dynamics in mature *Pinus elliottii* var. *elliottii* trees. Can J For Res. 21: 1742-1747

Gleason SM, Ares A (2004) Photosynthesis, carbohydrate storage and survival of a native and an introduced tree species in relation to light and defoliation. Tree Physiol 24: 1087-1097

Goodsman DW, Lieffers VJ, Landhäusser SM, Erbilgin N (2010) Fertilization lodgepole pine trees increased diameter growth but reduced root carbohydrate concentrations. For Ecol Manage 260: 1914-1920

Hoch G, Popp M, Körner C (2002) Altitudinal increase of mobile carbon pools in *Pinus cembra* suggests sink limitation of growth at the Swiss treeline. OIKOS 98: 361-374

Hoch G, Körner C (2009) Growth and carbon relations of tree line forming conifers at constant vs. variable low temperatures. J Ecol 97: 57-66

Imagi A, Seiwa K (2010) Carbon allocation to defense, storage, and growth in seedlings of two temperate broad-leaved tree species. Oecologia 162: 273-281

Landhäusser SM, Lieffers VJ (2001) Photosynthesis and carbon allocation of six boreal tree species grown in understory and open conditions. Tree Physiol 21: 243-250

Ludovici KH, Allen HL, Albaugh TJ, Dougherty PM (2002) The influence of nutrient and water availability on carbohyrate storage in loblolly pine. For Ecol Manage 159: 261-270

Machado JL, Reich PR (2006) Dark respiration rate increases with plant size in saplings of three temperate tree species despite decreasing tissue nitrogen and nonstructural carbohydrates. Tree Physiol 26: 915-923

Man R, Lieffers VJ (1997) Seasonal variations of photosynthetic capacities of white spruce (*Picea glauca*) and Jack pine (*Pinus banksiana*) saplings. Can J Bot 75: 1766-1771

Messier C, Doucet R, Ruel JC, Claveau Y, Kelly C, Lechowicz MJ (1999) Functional ecology of advance regeneration in relation to light in boreal forests. Can J For Res 29: 812-823

Naidu SL, DeLucia EH (1997) Growth, allocation and water relations of shade-grown *Quercus rubra* L. saplings exposed to a late-season canopy gap. Ann Bot 80: 335-344

R Development Core Team (2010) R: A language and environment for statistical computing. R Foundation for Statistical Computing, Vienna, Austria. ISBN 3-900051-07-0, URL http://www.R-project.org/

Schoonmaker AL, Hacke UG, Landhäusser SM, Lieffers VJ, Tyree MT (2010) Hydraulic acclimation to shading in boreal conifers of varying shade tolerance. Plant Cell Environ 33: 382-393

Streeter JG (2001) Simple partial purfication of d-pinitol from soybean leaves. Crop Sci 41: 1985-1987

Webb WL, Kilpatrick KJ (1993) Starch content in Douglas-fir: Diurnal and seasonal dynamics. For Sci 39: 359-367

Zuur AF, Ieno EN, Walker NJ, Saveliev AA, Smith GM (2009) Mixed effects models and extensions in ecology with R. Springer, New York

Chapter 5: Uniform versus asymmetric shading mediates crown recession in conifers

5.1 Introduction

Light availability is an important driver of plant growth and crown development, particularly in multilayered forests (e.g. Valladares and Niinemets 2007; Pearcy 2007; Niinemets 2010). Under shaded conditions, shade-intolerant species generally allocate carbon to height growth in order to evade shaded areas, potentially at the expense of allocation to other important tissues such as roots and leaves (Naidu et al. 1998; Messier et al. 1999; Souza and Valio 1999). Shade-tolerant species distribute carbon more proportionally within the whole plant, but with a preference towards photosynthetic tissues to increase light capture under shaded conditions (Messier et al. 1999; Souza and Valio 1999).

Light limitation is thought to be a significant driver of lower branch mortality and crown recession for trees growing in closed-canopy forests (e.g. Makela 1997; Witowski 1997). As it relates to carbon (C), it is also thought that branches in a crown behave as autonomous units (Sprugel 1991), as there is little evidence for long-distance C movement between branches within a crown (Kozlowski and Winget 1964; Ericsson 1978; Hansen and Beck 1994; von Felten et al. 2007; Lippu 1998; Schier 1970; Sneider and Schmitz 1989; Kagawa et al. 2006). There is growing evidence, however, that C limitation due to reduced light is not the only driver of branch mortality, especially in large trees. Other factors such as nutrient limitation (Pate and Arthur 2000; Amponsah et al. 2004); hydrological constraints (Protz et al. 2000; Burgess et al. 2006), and heterogeneity in light within crowns (Henriksson 2001; Sprugel 2002; Yoshimura 2010) have also been linked to the mortality of lower branches, which makes branch recession a more complex issue than previously thought.

Sprugel (2002) showed that a suppressed (fully shaded) individual of the shade-tolerant amabilis fir (*Abies amabilis* (Dougl.) Forbes) carried live branches in a light environment that would normally result in the mortality of lower branches for trees in a dominant canopy position where the lower portion of the

crown is shaded. Similarly, when one branch of a two-branched *Betula pubescens* ssp. *czerepanovii* (N.I. Orlova) seedling was shaded, greater growth reduction and increased mortality occurred in the shaded branches compared to shaded branches of a fully-shaded seedling (Henriksson 2001).

In this study I systematically explore the impact of asymmetrical vs. uniform crown shading on the mortality and growth of upper and lower branches within tree crowns, for two conifer species of differing shade tolerance. I hypothesize that the shading of only the lower crown, as compared to the entire crown, will have a larger negative impact on the lower branches in the shade intolerant lodgepole pine (*Pinus contorta* Douglas ex. Louden) than in shade tolerant white spruce (*Picea glauca* (Moench) Voss). I also explore xylem hydraulics, foliar nutrition and carbohydrate status as drivers for growth and expansion of the lower and upper branches in various types of shading.

5.2 Methods

5.2.1 Study sites

Ten study sites were selected in the lower foothills natural subregion (Beckingham and Archibald 1996) approximately 40-70 km north of Whitecourt, Alberta, Canada (54.14N -115.68W). Site elevations ranged from 840-960 m. Average annual precipitation in this region is 578 mm and annual precipitation during the study period was 439 mm in 2008 and 438 mm in 2009. Daily average temperature is 2.6 ºC with a mean monthly temperature of -12.1 ºC in January and 15.7 ºC in July (Environment Canada 2011). The selected sites were areas that had been harvested in 1991-1992 and were planted with or naturally regenerated to lodgepole pine, white and black spruce (*Picea mariana* (Mill.) Britton, Sterns & Poggenb.). Sites were located over a 100 km^2 area. Early silvicultural treatments included herbicide applications to reduce competition from hardwoods and some density management through pre-commercial thinning. Densities of conifers in 2008 ranged from 500-2250 stems ha^{-1}. Within each site, 3-4 white spruce and lodgepole pine each were randomly selected from a pool of twenty

trees identified as being 'well-spaced' in that neighboring trees were more than 2 m from the target trees. Shade treatments were applied in spring of 2008 (described below). The average height of selected pine in spring 2008 was 3.4 m (0.4 SD) and spruce was 3.3 m (0.4 SD). At the termination of the experiment (October 2009), the average height of the pine was 4.5 m (0.4 SD) and spruce was 4.4 m (0.4 SD).

5.2.2 Experimental design

Trees were assigned to one of four shading treatments: (1), complete uniform shading of the entire tree (US) with a single layer of shade cloth, (2) light asymmetric shading (AS-L) where the lower 1/4-1/3 of the tree crown was shaded with a single layer of shade cloth, (3) heavy asymmetric shading (AS-H) as in (2) except the lower crown was shaded with a second layer of shade cloth and (4) control (NS) in which no artificial shading occurred and most of the entire crown was exposed to full light . Treatment 3 was applied to trees at only 6 sites and the other treatments were applied at all 10 sites. Asymmetric shading (treatments 2 and 3) involved the construction of a self-supporting wooden structure around the lower branches of each tree, covered with shade cloth (Figure 1a). Shading the entire tree was accomplished by building a cone-shaped wooden structure (teepee) that was covered with shade cloth (Figure 1b). All structures were large enough to minimize the abrasion of branches and accommodate any future growth during the two years of study. The shade cloth was permeable to rain but reduced incoming light by ~75%, however, due to self-shading and surrounding neighbor trees the actual light reduction was greater than 85% (Table 1). As a reference point, an estimate of mean percentage of light saturated photosynthesis was also determined:

$$\text{Estimated available PAR} = \frac{\%\ \text{reduction of full light} \times 1000\ \text{PAR}}{100}$$

$$\text{Mean percentage of light saturated photosynthesis} = \frac{\text{A}}{\text{A}_{\text{sat}}} \times 100$$

where 1000 PAR was used an estimate of full light. Apparent photosynthetic rate (A) was determined from light response curves (Landhausser and Lieffers 2001) and the estimated available PAR. Light saturated photosynthesis (A_{sat}) was determined in the same study (Landhausser and Lieffers 2001).

Each year shade cloth was installed at the onset of shoot and needle expansion and removed in late-September to avoid damage due to snow-loading. The shade treatments were applied in late May in 2008 and early May in 2009. To allow for acclimation of the trees to the different shade treatments, measurements of growth and physiology were taken during the 2009 growing season.

Table 5.1: Summary of average light level (expressed as a percentage of full light) in upper and lower crown positions. Measurements were conducted between 11:30 - 16:00 hours in mid-summer. Mean percentage of light saturated photosynthesis was estimated from light response curves (Landhausser and Lieffers 2001) and PAR estimates determined from light reduction imposed by shading treatments. Treatment codes are as follows: NS = non-shaded, AS-L = asymmetric-light shaded, AS-H = asymmetric-heavy shaded and US = uniform-shaded. Values in brackets represent the range of measurements observed. Light was measured with multiple readings around the position with an Acupar Ceptometer.

	NS	US	AS-L	AS-H
Percentage of full light				
upper crown	82.7 (68.1-100.0)	14.3 (13.5-15.2)	-	-
lower crown	57.9 (42.8-71.9)	10.8 (7.6-12.8)	7.1 (2.3-9.5)	2.9 (0.8-5.6)
Mean percentage of light saturated photosynthesis				
Pinus contorta				
upper crown	100.0	41.2	-	-
lower crown	94.1	20.6	29.4	1.2
Picea glauca				
upper crown	100.0	45.0	-	-
lower crown	95.0	22.0	30.0	5.0

5.2.3 Sample collection and growth measurements

In 2009, lateral branches from both upper and lower positions were collected from the trees in June, late-August and October. These collections were

made from the two most recent age classes of a branch: current-year (expanded in 2009) and one-year-old (expanded in 2008). In June, I collected a one-year-old internode from each tree for needle carbohydrate and nitrogen reserves; this time was chosen because it is a time of peak shoot growth and thus a period of high C and nitrogen (N) demand. In late August, the one-year-old section of a terminal shoot of the upper and lower branches of each species was collected in 6-8 replicate trees on the south aspect to determine hydraulic conductivity (k_h) (see below). In October the two most recent age classes of four branches were collected (one from each cardinal direction) in both the upper and lower crown positions. The length of terminal shoots (current-year and previous year) were measured. To determine the frequency of bud expansion, I also counted the number of terminal buds for each branch that did or did not flush in the various treatments. In October during dormancy and just prior to the onset of ground frost, I also collected root samples (1 cm diameter) for root carbohydrate reserve analyses; this late collection was done to minimize disturbance to the tree during time of shade treatment.

Figure 5.1: Photographs of the (a) asymmetric shading treatment structure (before the shade cloth was applied) in *Picea glauca* and (b) uniform shading treatment on *Pinus contorta*.

5.2.4 Carbohydrate and Nitrogen analyses

To analyze tissue samples (needles and roots) for total non-structural carbohydrates (water soluble sugars and starch), samples were immediately frozen on dry ice in the field, transported to the laboratory and stored at -20 °C until further processing. Shoots were oven dried at 100 °C for 1 hour and then 70 °C until weight constancy. Needles were ground to pass 40-mesh (0.4 mm) in a Wiley-Mill (Thomas Scientific, Swedesboro New Jersey, USA). Non-structural

carbohydrates in tissues were quantified by boiling 50 mg of dried and ground tissue with 80% ethanol (3 times) to extract the water soluble sugars followed by treatment with phenolsulfuric acid which breaks down sugars into monosaccharides, which are subsequently quantified colorimetrically. The remaining residue from the initial extraction was separately digested with enzymes (α-amylase and amyloglucosidase) in order to break down starch into glucose, which is then quantified colorimetrically (Chow and Landhäusser 2004). Total nitrogen was determined using the Dumas combustion method (Sparks 1996) with a 4010 CHNS analyzer (Costech Analytical Technologies, Inc., Valencia, California). Soluble sugars, starch and nitrogen were presented as a percentage of total dry weight.

5.2.5 Hydraulic conductivity

For the hydraulic conductivity (k_h) of one-year-old terminal shoots, I followed the methodology described in Schoonmaker et al. (2010), except that in the current study, the segments were 5 to 10 cm in length. Samples were refrigerated and measurements were conducted within four days of collection. Briefly, sealed hoses were connected to both ends of the shoot segments and a small pressure head of filtered (0.2 um) 20 mM KCl + 1 mM $CaCl_2$ solution was applied; the outflow hose emptied into a sealed container on a balance (CP225D, Sartorius, Göttingen, Germany). After the rate of outflow stabilized, within 2-3 minutes, the average outflow over the next 40 s were used to calculate k_h:

$$k_h = \frac{\text{water flow } (\text{mm}^3\ \text{s}^{-1}) \text{ x segment length(mm)}}{\text{pressure head (kPa)}}$$

Hydraulic conductivity was scaled to sapwood cross-sectional area to give sapwood-area specific conductivity (k_s):

$$k_s = \frac{k_h}{\text{sapwood cross} - \text{sectional area } (\text{mm}^2)}$$

Sapwood area was determined with a stereomicroscope (MSF, Leica, Wetzlar, Germany) and image analysis software (ImagePro Plus 6.1, Media Cybernetics, Silver Spring, MD, USA).

5.2.6 Data analysis

All statistical analyses were carried out using R statistical software (R Development Core Team 2011). Linear mixed-effects models using shading treatment as the fixed effect and site as a random effect were used as a starting point for parameter estimates of treatment means and variances. Individual models were run for measurements conducted in upper and lower crown positions as I was not interested in direct comparisons between crown positions but in relative changes within crown position due to shading treatments. However, 95% confidence intervals (CI) around treatment means are presented and can be used to estimate differences between treatments for interested readers as it has been suggested that a CI bars can overlap by as much as one half the length of one boundary and still correspond with a p-value < 0.05 (Cumming 2009). Bootstrap simulations from these models were generated to obtain confidence intervals around treatment means. Bootstrap simulations were also generated on the difference in means of NS from treated trees (AS-L, AS-H, US) and 95% confidence intervals around the mean differences. Where subsamples within tree-crown position were collected (in growth October); individual branches were first averaged for each individual tree. Model assumptions were checked with diagnostic plots and where strong evidence of non-normality or unequal variance were observed, data were log-transformed (data presentation however, is based on back-transformed values).

Visual comparisons of the differences of means and their 95% confidence intervals were my main method of interpretation (Cohen 1994; Di Stefano 2004; Crawley 2007). As a guide, I have included a comparison graph indicating the zero-line on the difference of means from the control. When confidence intervals of the mean difference intersect this line, it approximately corresponds to a p-value of > 0.05 (Cumming and Finch 2005). However, I have not limited my

discussion of results to this somewhat arbitrary cut-off. As 95% confidence intervals of treatment means and associated differences between means provides a measure of the effect size of treatments (Kellow 1998), I believe this information will allow the reader to make their own judgment as to the statistical or biological relevance of the data.

5.3 Results

5.3.1 Expansion and Growth

In pine, the lower branches had a low frequency of bud expansion (~ 40 %) in both the AS-L and AS-H treatments after two growing seasons of shading, while in US trees, expansion was much higher (~ 80%) and 100% in the NS trees (Figure 2). In contrast, frequency of bud expansion of the lower branches in spruce and upper branches of both species was 100 % across all treatments (data not shown).

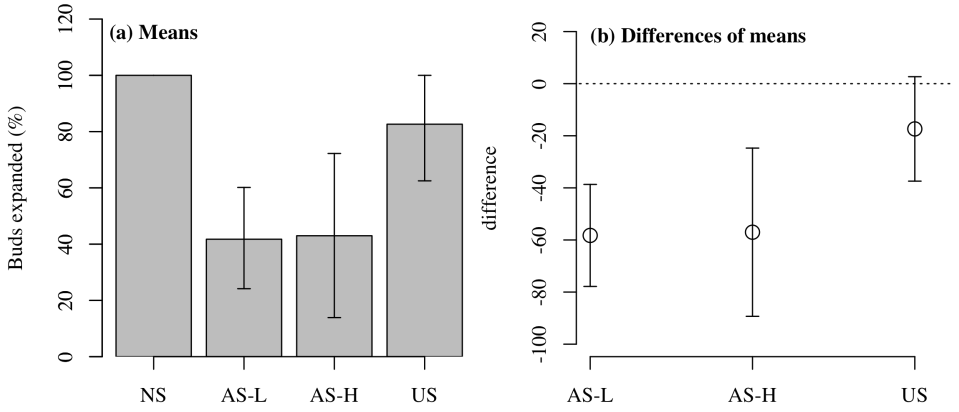

Figure 5.2: (a) Frequency of bud expantion of current-year growth in the lower crown of pine (*Pinus contorta*) collected after the second year of treatment (October 2009). Where NS = non-shaded, AS-L = asymmetric-light shaded, AS-H = asymmetric-heavy shaded and US = uniform-shaded. (b) Mean difference of shading treatments relative to un-shaded control (NS). Error bars represent 95% CI (n=6-10).

Terminal shoot growth of the upper branches of US pine trees was reduced by 6 cm compared with NS trees while asymmetrical shading (AS-H and AS-L) had little effect on the terminal shoot growth of the upper branches (Figure 3a,b). The growth of terminal shoots of the lower branches was 2.5 cm less in the US treatment compared to the control (NS) trees (Figure 3e,f); however, the terminal shoots of lower branches in both the AS-L and AS-H was 5 cm less compared to the NS control (> 50% reduction in shoot growth) (Figure 3e,f). In spruce, terminal shoots of the upper branches of US trees grew 4 cm longer compared to shoots in the NS trees (Figure 3c,d). Lower branches in spruce showed no difference in shoot growth between the US and NS trees while asymmetric shading (AS-H and AS-L) of lower branches led to a 2.0 cm reduction in shoot length relative to lower branches of NS trees (Figure 3g,h).

In the upper branches of shaded pine, sapwood area tended to be smaller than those in the NS trees in all shading treatments, particularly in US trees (Figure 3i, j), while in spruce, sapwood area was only smaller in the AS-L trees and was not affected in US trees (Figure 3k,l). In the lower branches of pine, sapwood cross-sectional area of new shoots also declined with the shading treatments (Figure 3m,n), while in spruce the sapwood area was reduced only in the AS-H and slightly in the AS-L trees, but not in US trees (Figure 3o,p).

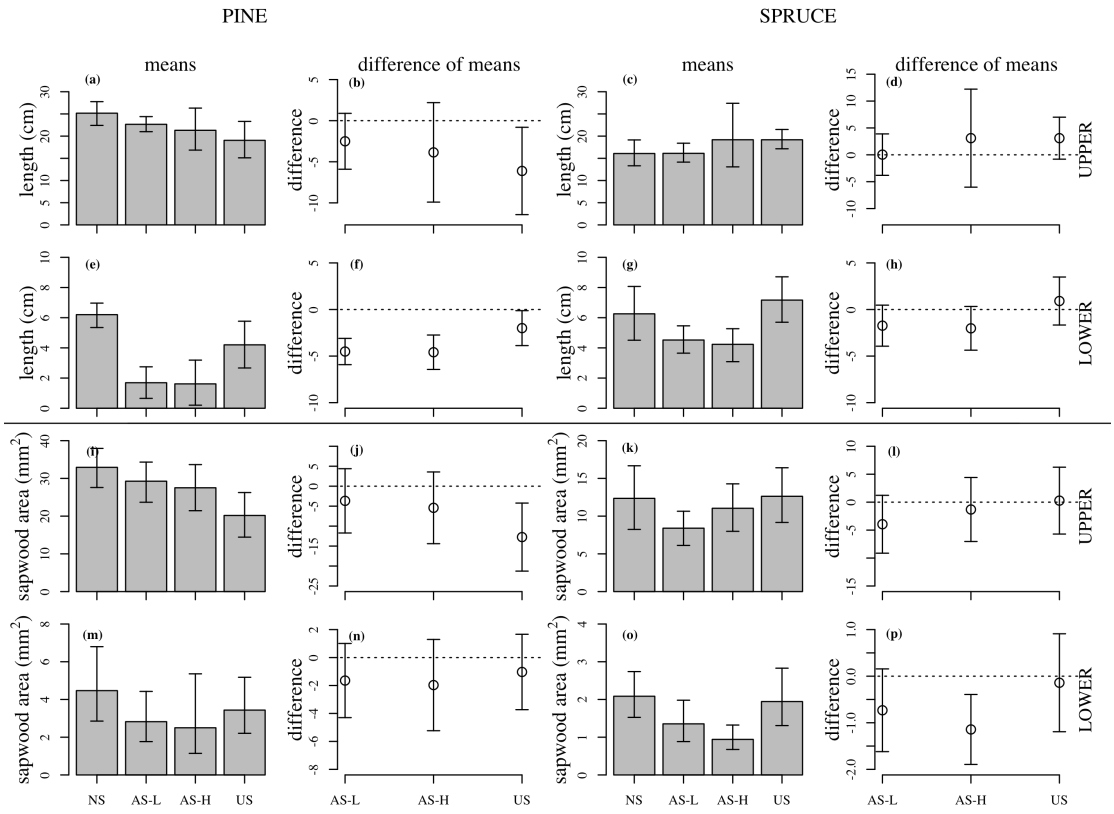

Figure 5.3: Growth in length of current-year shoots and xylem cross-sectional area of shoots of pine (*Pinus contorta*) and spruce (*Picea glauca*) from branches located in the upper (upper rows) and lower crown (lower rows) in October 2009. Note that length measurements were based on shoots collected on upper and lower branches in October (up to 4 shoots per treatment) and sapwood area measurements were based on shoots collected on upper and lower branches in August for measurement of specific conductivity. The difference of means indicates the control minus the shade treatment. Treatment codes are represented as: NS = non-shaded, AS-L = asymmetric-light shaded, AS-H = asymmetric-heavy shaded and US = uniform-shaded. Error bars represent 95% CI (n=6-10).

5.3.2 Carbohydrate concentrations

Total concentrations of nonstructural carbohydrates (TNC) in one-year-old needles (grown in 2008) of the upper branches of both species was only lower (relative to the control) in the US trees (Figure 4a-d). TNC concentrations in needles of the lower branches of pine were reduced by all shading treatments, especially in the AS-H treatment, where needle concentration were only 9% compared to 17% in the NS treatment (Figure 4e,f). In the spruce, needle TNC

concentrations were uniformly reduced regardless of the shading treatment (Figure 4g,h). Starch concentrations in the one-year-old needles mirrored the changes in TNC concentrations in both upper and lower branches of both species (Figure 4).

To allow for comparison in the allocation of TNC relative to the NS trees, the differences in needle TNC concentrations between lower and upper branches (lower-upper) for one-year-old needles are presented in Figure 5. In pine, the needles from the lower branches had lower TNC concentrations compared with the upper needles in both asymmetric shading treatments (Figure 5a). In the US treatment needles on lower branches tended to have higher TNC concentrations relative to needles on upper branches (Figure 5a). In spruce, TNC concentrations of the needles on lower branches were higher than in the needles of upper branches in the NS and US treatment, but tended to be similar to the AS treatment (Figure 5b).

In pine, root TNC concentration was about 10% in the NS and AS treatments, but was only 8% in the US treatment (Figure6a,b). For spruce, shading did not reduce root TNC concentrations (Figure 6c,d). The decline in TNC in the US pine trees was mostly driven by a decline in root starch concentration (Figure 6e,f), while in spruce root starch concentrations tended to increase across all shading treatments (Figure 6g,h).

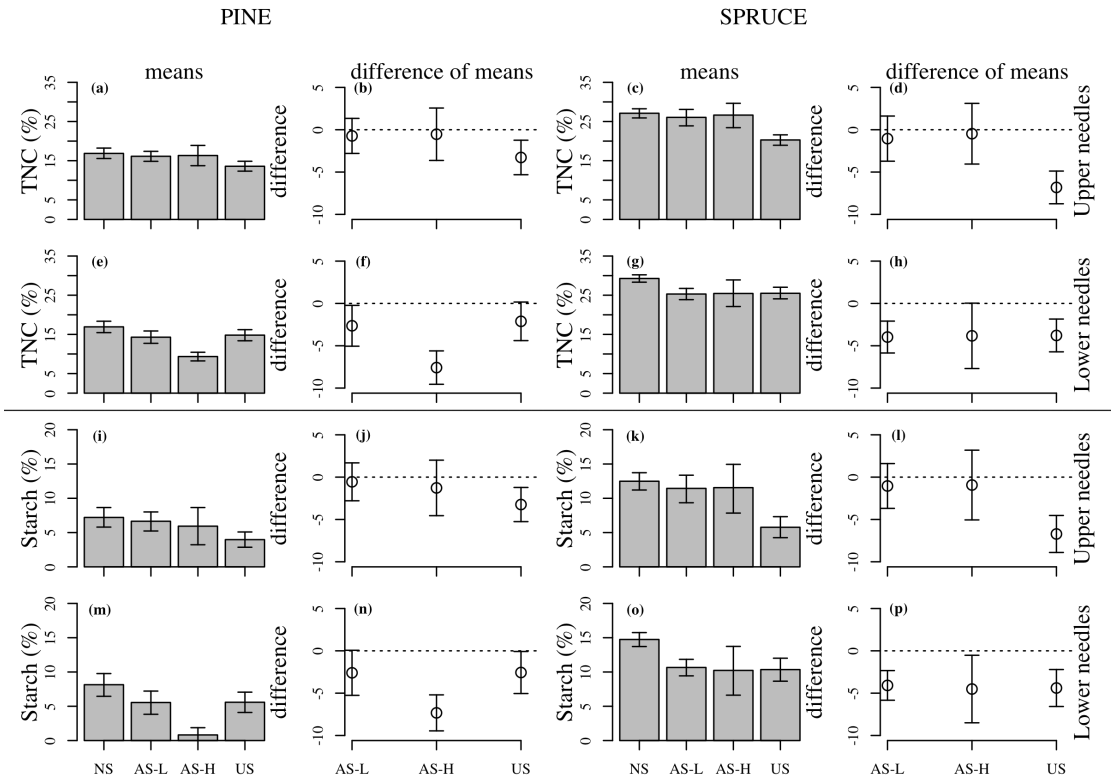

Figure 5.4: Total non-structural carbohydrates (TNC) and starch in previous year needles (one-year-old) of pine (*Pinus contorta*) and spruce (*Picea glauca*) from branches located in the upper and lower crown in late June 2009. The difference in means indicates the control minus the shade treatment. Treatment codes are: NS = non-shaded, AS-L = asymmetric-light shaded, AS-H = asymmetric-heavy shaded and US = uniform-shaded. Error bars represent 95% CI (n=6-10).

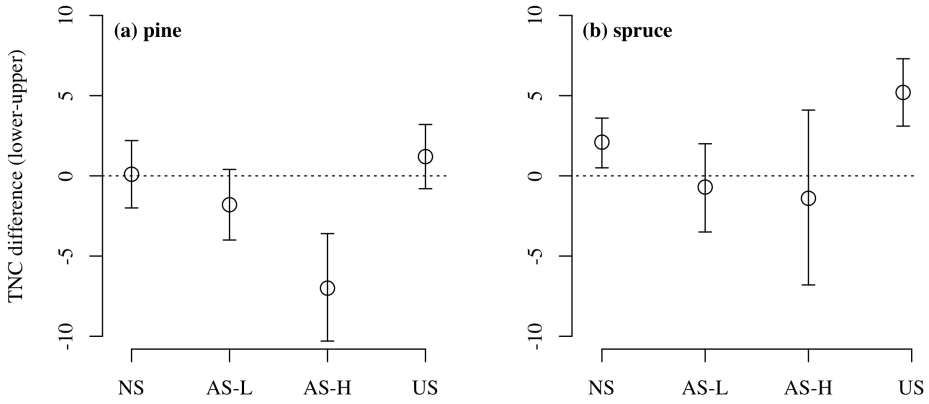

Figure 5.5: Difference in total non-structural carbohydrate (TNC) of one-year-old needles between the lower and upper crown (lower- upper) of pine (*Pinus contorta*) and spruce (*Picea glauca*). Values below 0 indicate less TNC in lower than upper foliage. Treatment codes are: NS = non-shaded, AS-L = asymmetric-light shaded, AS-H = asymmetric-heavy shaded and US = uniform-shaded. Error bars represent 95% CI (n=6-10).

5.3.3 N concentration

Needles of the upper branches of pine tended to have higher total N concentrations in the AS-H trees (Figure 7g,h) and in spruce both the AS-H and US trees had higher needle N than the control (Figure 7c,d). Nitrogen concentrations in the needles of lower branches of pine and spruce were similar across shading treatments (Figure 7a,b,e,f).

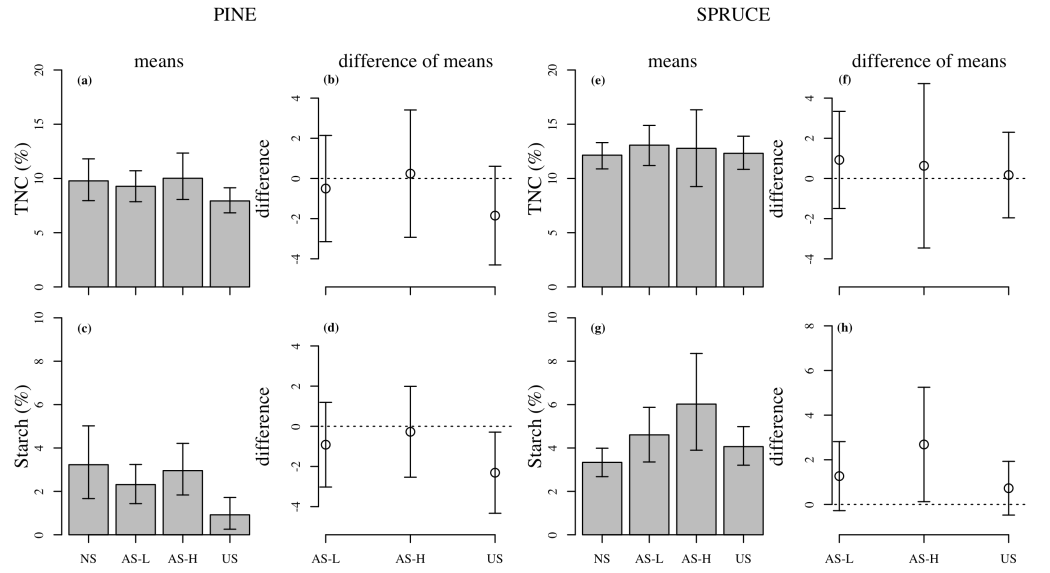

Figure 5.6: Total non-structural carbohydrate concentration (TNC, upper row) and starch (lower row) in roots of pine (*Pinus contorta*) and spruce (*Picea glauca*) in October 2009. The difference of means indicates the control minus the shaded treatment. Treatment codes are represented as: NS = non-shaded, AS-L = asymmetric-light shaded, AS-H = asymmetric-heavy shaded and US = uniform-shaded. Error bars represent 95% CI (n=6-10).

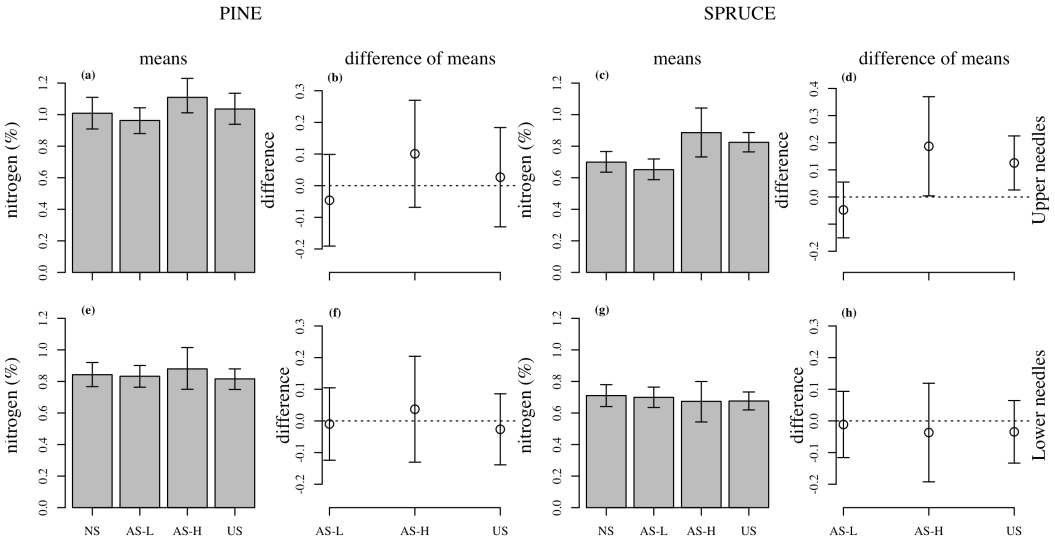

Figure 5.7: Nitrogen concentration in one-year-old needles and shoots of pine (*Pinus contorta*) and spruce (*Picea glauca*) collected from branches in the upper (upper row) and lower (lower row) crown in late June 2009. The difference of means indicate the control – the shaded treatment. Treatment codes are represented as: NS = non-shaded, AS-L = asymmetric-light shaded, AS-H = asymmetric-heavy shaded and US = uniform-shaded. Error bars represent 95% CI (n=6-10).

5.3.4 Hydraulic conductivity

Shoots of the upper branches in pine had lower sapwood area specific conductivity (k_s) in the US treatment compared to the other treatments (Figure 8a,b). Shading had little impact on k_s in the upper or lower branches of spruce (Figure 8c,d,g,h). In the lower branches of pine, k_s declined by up to 40% in all shading treatments (Figure 8e,f).

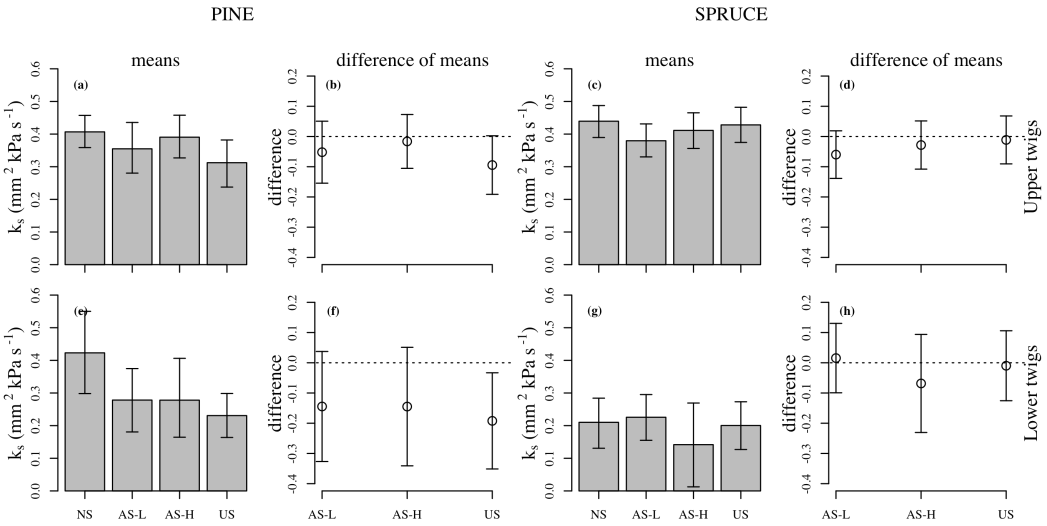

Figure 5.8: Sapwood area specific conductivity in one-year-old shoots of pine (*Pinus contorta*) and spruce (*Picea glauca*) collected from upper (upper row) and lower branches (lower row) of the crown in October 2009. The difference of means indicate the control – the shaded treatment. Treatment codes are represented as: NS = non-shaded, AS-L = asymmetric-light shaded, AS-H = asymmetric-heavy shaded and US = uniform-shaded. Error bars represent 95% CI (n=6-10)

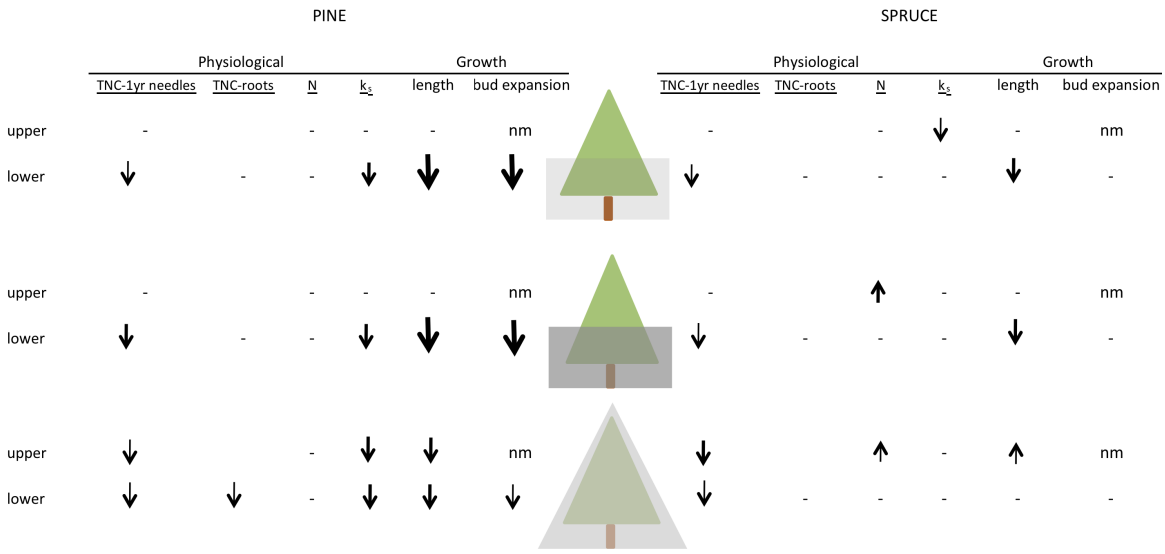

Fig 5.9: Summary of effects of shading treatments on growth, expansion and physiological parameters, in pine (*Pinus contorta*) and spruce (*Picea glauca*). The top row (tree) corresponds with asymmetrical-light shading, the middle row (tree) with asymmetrical-heavy shading and the lower row (tree) with uniform shading. 'nm' indicates that no measurement was not taken, a dash (-) indicates no difference between non-shaded control tree and shaded tree, a downward arrow (🡻) indicates a reduction and an upward arrow (🡹) an increase as a result of shading. Small non-bolded arrows indicate < 20% changes, small bolded arrows indicate 20-50% change and large bolded arrows >50% change relative to non-shaded trees.

5.4 Discussion

Overall, my study suggests that crown recession is not only driven by the quantity of light, but also by the relative difference in light between the lower and upper branches (see also Figure 9). Asymmetrical shading of the lower crown (AS) had a larger negative impact on bud expansion and growth than did uniform shading of the whole crown (US). This effect was strongest in the shade intolerant lodgepole pine. These strong reductions in growth and bud expansion observed in the lower AS branches of pine are consistent with more severe self-pruning behavior observed in closed-canopy pine stands, compared to spruce. The impact of AS vs. US on the lower branches of the shade-intolerant pine (and to a lesser extent in spruce) is also consistent with observations made in *Betula pubescens,* a shade-intolerant deciduous species (Henriksson 2001). Similar ideas have been generated in more indirect studies on *Cedrela sinensis* A. Juss, a

deciduous pioneer species (Yoshimura 2010), *Litsea acuminata* (Bl.) Kurata, an evergreen broad-leaved understory tree (Takenaka 2000) and other conifers (Sprugel 2002). The strong reaction to asymmetric shade in lower branches of the intolerant pine may be indicative of the fundamental differences in shade tolerance among species. my contribution to this topic relates to the understanding of the mechanisms on why disparity in light among branches within a crown is detrimental to the health and longevity of the shaded branches.

The average percentage of full light available in the lower branches of US and AS-L were intended to be the equivalent although mean values for US were 10.8% and 7.1% for AS-L. There was however, overlap in the range of values (Table 1) and the photosynthetic responses at these levels suggests a much larger effect between AS-H and AS-L where the percentage of light saturated photosynthesis in AS-H pine is 1.2% and 5.0% in spruce (Table 1). Moreover, if the difference in light at the already low values experienced in across all shading treatments, were responsible for difference in responses between the lower branches of AS-L and US than I would also have expected differences in TNC between these treatments, which I did not (Figure 4).

In both species, the relative difference in TNC reserves between the branches of the upper and lower crown may provide an explanatory mechanism for the observed distinction between the growth response of the lower branches of AS and US (and reduced occurrence of bud expansion in pine). In pine, difference in TNC between the needles of lower branches and upper branches was greatest in the AS-H, followed by the AS-L (Figure 5); which suggests a greater allocation differential between the shaded zone and the well-lighted upper zone. In the NS and US trees there was no difference in TNC concentration between needles of the upper and lower shoots. Spruce tended to have higher needle TNC in the lower branches in the NS and US treatments, while in the AS treatments TNC concentrations in the upper and lower branches were not different. Particularly for pine, this suggests that under AS, carbon was (1) being moved out of the newer needles of lower shaded branches to other growth or maintenance sinks and/or (2) there was simply less C being accumulated in lower branches due

to reduced photosynthesis (as suggested by Sprugel (2002)). In spruce, it appears that C was actually accumulating in the needles of lower branches under the NS and US treatments – potentially a very conservative system for the maintenance of lower branches in a shade tolerant species.

Spruce maintained intrinsically much higher needle carbohydrate levels (>30% more) than pine, providing this species with a larger reserve storage buffer that likely allowed it to extend growth in the shade. In pine, even the lower branches of NS trees maintained average TNC values of only 9% (compared with nearly 17% in spruce) during the growing season, and in AS pine trees, TNC concentrations in needles of the lower branches were between 7-8%. The reliance of shaded trees on stored TNC reserves was also shown in seedlings of tropical species, where seedlings with the highest TNC concentrations had the greatest shoot expansion when exposed to deep shade (Myers and Kitajima 2007).

The reduced levels of bud flush and shoot development in the lower branches of pine (particularly in the AS treatments) might also be related to the lower needle carbohydrates, as shoot flush and shoot expansion has been linked to C supply from nearby needles (Kozlowski and Winget 1964). Poor development of shoots was particularly evident in the lower branches, where one-year-old shoots of AS-H pine showed an almost a 50% decline in TNC. Even though TNC in lower one-year-old shoots of AS-L and US trees were similar in concentration (though both lower than NS trees), they were vastly different in terms of expansion and growth (US shoots on lower branches performing better). Therefore, C available in the AS-L branches at this time of year is not completely indicative of bud expansion and the eventual fate of the distal shoot.

Carbohydrate reserves in the pine roots were reduced in the US treatment, but in spruce, root TNC reserves were not affected by the shade treatments over the two growing seasons. In fact, there was more starch stored in roots with AS treatments – although retention of the root starch late into the fall may have been related to warmer soils under the shade cloth. The long-term consequence of reducing reserves to roots in the US pine could result in a negative feedback loop on root growth and expansion including reduced uptake of water and nutrient

(Landhäusser and Lieffers 2012). Souza and Válio (1999) similarly observed a decline in the translocation of radioactively labeled carbon to roots in forest-shaded (versus fully-illuminated) early-successional seedlings of the tropical species *Cecropia pachystachya* Ambay and *Schizolobium parahyba* (Vell.) S.F.Blake. This suggests that reduced C allocation to roots in light-deprived trees may be an important component of shade intolerance. In the more shade tolerant spruce, root TNC concentrations were maintained despite the overall lower C status of the trees in the US treatment.

Sapwood area specific conductivity (k_s) declined in the shaded lower branches and upper branches (US) of pine, while shading treatments caused little change the k_s of lower branches in the spruce. It is likely that the reduction in conductivity under low light would correspondingly reduce photosynthesis (e.g. Renninger et al. 2007) and increase the susceptibility of trees to drought (Cochard et al. 1999; Schoonmaker et al. 2010; Plavcova et al. 2011). Low light has been attributed to reduced conductivity in previous studies of *Pinus contorta* (Protz et al. 2000), *Pseudotsuga menziesii* (Mayr) Franco and *Tsuga heterophylla* (Raf.) Sarg. (Renninger et al. 2007). Kupper et al. (2006) also observed declines in branch conductance and transpiration of fully-illuminated lower branches compared with upper branches of *Larix decidua* Mill. Both the current study, as well as those described above, suggests an additive effect of branch position and light on water relations. However, in the current study, this mechanism appears to only be apparent for the shade intolerant pine.

Surprisingly, I observed no change in N concentration in the lower branches of both species even though needle N concentrations indicated N was deficient on these sites (Brockley 1996). This suggests that with these conifers, there was little extraction of N out of lower branches under shaded conditions. Yoshimura (2010) similarly did not observe reduced N in leaves of partially or fully shaded *Cedrela sinensis* saplings. Nonetheless, periods of N limitation have been associated with N translocation from the lower to upper crown in *Eucalyptus* (Pate and Arthur 2000). Livingston et al. (1998) also observed increased N concentration with height in *Pinus radiata* D.Don that was not attributable to

changes in light. Strangely, I did observe an increase in N content in upper branches in AS-H and US treatments of spruce (but not in AS-L); perhaps related to having a fixed pool of N dispersed to smaller growth sinks in the heavily shaded trees.

In summary, my study showed two strong physiological differences between pine and spruce which may indirectly affect lower branch survival in shade. The first difference being lower inherent levels of shoot and root carbohydrate reserves in pine relative to spruce which may make pine potentially less resilient to stress. Secondly, a decline in xylem-area specific conductivity of lower branches in pine where any type of shading would make lower branches less likely to maintain stomatal conductance and C fixation. I saw no difference in foliar N in response to shading in lower branches in either species. The only clear evidence across both species that asymmetric shade is more stressful to lower branches than uniform shade relates to carbohydrate storage. In both species, the needles of lower branches tended to store less C than upper branches under asymmetric shade and this effect was strongest in pine. Thus resources were more limiting in lower branches under asymmetric than under uniform shade, thereby make them more vulnerable to mortality.

5.5 References

Amponsah IG, Lieffers VJ, Comeau PG, Brockley RP (2004) Growth response and sapwood hydraulic properties of young lodgepole pine following repeated fertilization. Tree Physiol 24: 1099-1108

Beckingham JD, Archibald JH (1996) Field guide to ecosites of northern Alberta. Natural Resources Canada, Canadian Forest Service, Northwest Re- gion, Northern Forest Centre, Special Report 5. Edmonton, Alberta.

Brockley RP (1996) Lodgepole pine nutrition and fertilization: a summary of B.C. Ministry of Forests research results. Canadian Forest Service and B.C. Ministry of Forests, Victoria, B.C. FRDA Rep. 266

Burgess SSO, Pittermann J, Dawson TE (2006) Hydraulic efficiency and safety of branch xylem increases with height in *Sequoia sempervirens* (D. Don) crowns. Plant Cell Environ 29: 229-239

Chow PS, Landhausser SM (2004) A method for routine measurements of total sugar and starch content in woody plant tissues. Tree Physiol 24: 1129-1136

Cochard H, Lemoine D, Dreyer E (1999) The effects of acclimation to sunlight on the xylem vulnerability to embolism in Fagus sylvatica L. Plant Cell Environ 22: 101-108

Cohen J (1994) The earth is round ($p < 0.05$). Am Psych Assoc 49: 997-1003

Crawley MJ (2007) The R book. John Wiley and Sons, West Sussex, United Kingdom.

Cumming G (2009) Inference by eye: Reading the overlap of independent confidence intervals. Stat Med 28: 205-220

Cumming G, Finch S (2005) Inference by eye: confidence intervals and how to read pictures of data. Am Psych 60: 170-180

Di Stefano J (2004) A confidence interval approach to data analysis. Forest Ecol Manage 187: 173-183

Environment Canada (2011) National climate data and information archive. [WWW document]. URL http://www.climate.weatheroffice.ec.gc.ca/Welcome_e.html [accessed on 8 June 2011]

Ericsson A (1978) Seasonal changes in translocation of ^{14}C from different age-classes of needles on 20-year-old Scots pine trees (*Pinus silvestris*). Physiol Plant 43: 351-358

Hansen J, Beck E (1994) Seasonal changes in the utilization and turnover of assimilation products in 8-year-old Scots pine (*Pinus sylvestris* L.) trees. Trees 8: 172-182

Henricksson J (2001) Differential shading of branches of whole trees: expansion, growth, and reproduction. Oecol 126: 482-486

Kagawa A, Sugimoto A, Maximov TC (2006) Seasonal course of translocation, storage and remobilization of 13C pulse-labeled photoassimilate in naturally growing *Larix gmelini* saplings. New Phytol 171: 793-804

Kellow JT (1998) Beyond statistical significant tests: the importance of using other estimates of treatment effects to interpret results evaluation. Am J Eval 19: 123-134

Kozlowski TT, Winget CH (1964) The role of reserves in leaves, branches, stems and roots on shoot growth of red pine. Am J Bot 51: 522-529

Landhäusser SM, Lieffers VJ (2012) Defoliation increases risk of carbon starvation in root systems of mature aspen. Trees 26: 653-661.

Lippu J (1998) Redistribution of ^{14}C-labelled reserve carbon in *Pinus sylvestris* seedlings during shoot elongation. Silva Fenn 32: 3-10

Livingston NJ, Whitehead D, Kelliher FM, Wang Y-P, Grace JC, Walcroft AS, Byers JN, Mcseveny TM, Millard P (1998) Nitrogen allocation and carbon isotope fractionation in relation to intercepted radiation and position in a young *Pinus radiata* D. Don tree. Plant Cell Environ 21: 795-803

Mäkelä A (1997) A carbon balance model of growth and self-pruning in trees based on structural relationships. For Sci 43: 7-24

Messier C, Doucet R, Ruel JC, Claveau Y, Kelly C, Lechowicz MJ (1999) Functional ecology of advance regeneration in relation to light in boreal forests. Can J For Res 29: 812-823

Myers JA, Kitajima K (2007) Carbohydrate storage enhances seedlings shade and stress tolerance in a neotropical forest. J Ecol 95: 383-395

Naidu SL, DeLucia EH, Thomas RB (1998) Contrasting patterns of biomass allocation in dominant and suppressed loblolly pine. Can J For Res 28: 1116-1124

Niinemets U (2010) A review of light interception in plant stands from leaf to canopy in different plant functional types and in species with varying shade tolerance. Ecol Res 25: 693-714

Pate JS, Arthur DJ (2000) Uptake, partitioning and utilization of carbon and nitrogen in the bark bleeding tree, Tasmanian blue gum (*Eucalyptus globulus*). Aust J Plant Physiol 27: 869-884

Pearcy RW (2007) Responses of plants to heterogeneous light environments. In: Functional Plant Ecology, eds: Pugnaire FI, Valladares F. CRC Press, Boca Raton, Florida USA.

Plavcova L, Hacke UG, Sperry JS (2011) Linking irradiance-induced changes in pit membrane ultrastructure with xylem vulnerability to cavitation. Plant Cell Environ 34: 501-513

Protz CG, Silins U, Lieffers VJ (2000) Reduction in branch sapwood hydraulic permeability as a factor limiting expansion of lower branches of lodgepole pine. Can J For Res 30: 1088-1095

R Development Core Team (2011) R: A language and environment for statistical computing. R Foundation for Statistical Computing, Vienna, Austria. ISBN 3-900051-07-0, URL http://www.R-project.org/.

Renninger HJ, Meinzer FC, Gartner BL (2007) Hydraulic architecture and photosynthetic capacity as constraints on release from suppression in Douglas-fir and western hemlock. Tree Physiol 27: 33-42

Schier GA (1970) Seasonal pathways of ^{14}C-Photosynthate in Red Pine labeled in May, July, and October. For Sci 16: 1-13

Schoonmaker AL, Hacke UG, Landhäusser SM, Lieffers VJ, Tyree MT (2010) Hydraulic acclimation to shading in boreal conifers of varying shade tolerance. Plant Cell Environ 33: 382-393

Schneider A, Schmitz K (1989) Seasonal course of translocation and distribution of ^{14}C-labelled photoassimilate in young trees of Larix decidua Mill. Trees 4: 185-191

Souza RP, Válio IFM (1999) Carbon translocation as affected by shade in saplings of shade tolerant and intolerant species. Biol Plant 42: 631-636

Sparks DL (1996) Micro-chemical determination of carbon, hydrogen and nitrogen, automated method. *In* Methods of Soil Analysis, Part 3 Chemical methods. Soil Science Society of America, Inc., Madison Wisconsin.

Sprugel DG (2002) When branch autonomy fails: Milton's Law of resource availability and allocation. Tree Physiol 22: 1119-1124

Sprugel DG, Hinckley TM, Schaap W (1991) The theory and practice of branch autonomy. Ann Rev Ecol Sys 22: 309-334

Takenaka (2000) Shoot growth responses to light microenvironment and correlative inhibition in tree seedlings under a forest canopy. Tree Physiol 20: 987-991

Valladares F, Niinemets U (2007) The architecture of plant crowns: from design rules to light capture and performance. In: Functional Plant Ecology, eds: Pugnaire FI, Valladares F. CRC Press, Boca Raton, Florida USA.

von Felten S, Hättenschwiler S, Saurer M, Siegwolf (2007) Carbon allocation in shoots of alpine treeline conifers in a CO_2 enriched environment. Trees 21: 283-294

Witowski J (1997) Gas exchange of the lowest branches of young Scots pine: a cost-benefit analysis of seasonal branch carbon budget. Tree Physiol 17: 757-765

Yoshimura K (2010) Irradiance heterogeneity within crown affects photosynthetic capacity and nitrogen distribution of leaves in *Cedrela sinensis*. Plant Cell Environ 33: 750-758

Chapter 6: Decline in productivity in old *Pinus contorta* stands is not linked to decline in stand leaf area

6.1 Introduction

It is has been well documented that stand-level productivity peaks early on in forest stand development and subsequently declines slowly thereafter (Ryan et al. 1997, Smith and Resh 1999). Leaf-area index will often follow a similar temporal pattern (Pearson et al. 1984, Smith and Resh 1999) and has been cited as a contributing factor to productivity decline (Ryan et al. 1997). Increased respiration was put forward early on as a cause of productivity decline (Whittaker and Woodwell 1967) though subsequent investigations have largely refuted this mechanism (Ryan et al. 1997, see also Drake et al. 2011). Ryan et al. (1997) provided the most comprehensive review of stand decline to date and have suggested a number of mechanisms including: increased carbon allocation to roots, increasing hydraulic resistance with tree height, constraints in hydraulic functioning, nutritional limitations in the soil, increasing crown abrasions reducing leaf area, increased mortality of older trees, and increased reproduction and genetic changes related to meristematic age. More recently, changes in the patterns of tree dominance have also been suggested (Binkley et al. 2004; Sillett et al. 2010).

Evidence for the hypothesis of increasing hydraulic constraints finds support in Drake et al. (2010, 2011), while others appear to refute it (see Ryan et al. 2006 for examples). Crown abrasions or crown shyness has been demonstrated in lodepole pine stands (Rudnicki et al. 2003; Fish et al. 2006). Xu et al. (2012) have found evidence of increasing mortality of dominant trees in *Quercus* dominated stands. With every study that supports a hypothesis of stand decline, there appears to be another that refutes it. It seems probable that though the pattern of decline is a consistent phenomenon spanning different ecosystem types and forest biomes; the mechanisms for decline may not be consistent across all stand types and forest ecosystems.

In a lodgepole pine chronosequence, carbon (C) allocation to leaves and branches remained relatively constant while it was found that stemwood production and root C allocation declined over time (Smith and Resh 1999). However, in a recent review of carbon allocation patterns in trees, Litton et al. (2007) stated that the "changes in flux and partitioning with forest development, particularly to belowground, remain poorly understood". Roots of trees are inherently difficult to study due to the physical obstruction of soil. Most estimates of belowground allocation typically lump all parameters related to roots together in a parameter known as total belowground carbon allocation (TBCA) (Ryan et al. 2004; Litton et al. 2007). The main drawback of this approach is that it does not separate roots by their function, i.e. the roots used in the acquisition of nutrients and water (analogous to aboveground leaf area) and the roots used for transport and structural support (analogous to the stem and branches). To incorporate the functionality of root into TBCA, an estimation of root surface area may provide another angle from which to explore mechanistic explanations for stand decline, as fine roots are mostly responsible for resource uptake.

Another reason for examining how tree size and age influence fine root surface area and dry mass is related to the fact that the supply of root reserves might be related to tree and crown size. Source-sink dynamics in plants are thought to be a function of proximity, growth activity and hormones (Sprugel et al. 1991). Proximity to the source may become a significant constraint as trees in forest stands gain height, the live crown ratio decreases and the physical distance between the site of carbon fixation and roots increases (Landhäusser and Lieffers 2012).

Other factors that change with stand development and could influence stand productivity through root activity are: reduced soil temperature (Minchin et al. 1994) and site level nutrition (Burton et al. 2000). In sugar maple forests root longevity was positively correlated with better site nutrition (Burton et al 2000). The explanation for this pattern was that demand for carbon (sink strength) was being driven by increasing physiological activity. Once this physiological activity

declined (low nutrient uptake) the supply of carbohydrates correspondingly declined.

Roots are the farthest organ from the site of carbon fixation, as such, they are likely to be a weaker sink for carbon relative to actively growing aboveground meristems (Landhausser and Lieffers 2012). This situation is likely to become exacerbated as the tree gains height and the physical distance between the site of carbon fixation and roots increases. In a lodgepole pine chronosequence, C allocation to leaves and branches remained relatively constant while it was found that stemwood production and root C allocation declined over time (Smith and Resh 1999). In addition, the light environment will change dramatically over the life of the stand and it is known from seedling work on *Pinus contorta* that shaded seedlings will have lower root allocation relative to shoots (Landhausser and Lieffers 2001).

In this paper I explore the influence of root and leaf allocation patterns in a fire-origin lodgepole pine (*Pinus contorta* Loudon) chronosequence. I assess stand-level changes in pine root mass and fine root surface area and leaf area with stand age. I hypothesize that fine root surface area and leaf area will 'track' each other over the life of a stand, as one decreases, so must the other. However, I hypothesize that roots will tend to decrease first, while leaf area will lag behind.

6.2 Methods

6.2.1 Site selection and characterization

The study sites were located along a 33 km north-south band, south of Hinton, Alberta, Canada (53° 14.384' -117° 28.596' to 53° 3.43' -117° 4 .145'). Elevation ranged from 1420 – 1577m and all stands had south facing aspects (Table 1) with slopes ranging from 3-33% (Table 1). Soils were Dystric Brunisoils and soil texture was primarily silty and sandy loams and similar among sites. This elevation range is transitional between the upper foothills and the sub-alpine natural subregions (Beckingham et al. 1996) of Alberta. The understory plant community in these stands included: *Vaccinium vitis-idaea*, *Linnaea*

borealis, *Vaccinium caespitosum, Rosa acicularis*, *Ledum groenlandicum*, *Rubus pedatus*, *Rubus idaeaus*, *Cornus canadensis, Pyrola asarifolia, Orthilia secunda, Arnica cordifolia, Elymus innovatus,* and the feather mosses *Hylocomium splendens* and *Pleurozium schreberi*. Five stands each were identified within four age classes from natural fires originating in: 1997, 1988, 1956 and ~1910 (1900-1910). Hereafter, age classes are presented as the number of years post-disturbance: 12, 21, 53 and 100+ years of age. Regional weather from a nearby station (1010 m elevation, coordinates: 53.4° -117.54°) indicated that during the year of field measurements (2009), total precipitation was 429 mm (approximately half as snow) and mean temperature in January was -6.7°C and in July +16.5°C (Environment Canada).

Table 6.1: Geographic location, elevation, aspect and slope of study sites. The known or estimated year of fire is also included as well as tree ring counts based on stem samples collected at stump height (0.3m) for age classes 12 and 21 and breast height (1.3m) for age classes 53 and 100+. Site index (at 50 yrs) was determined by the average number of tree rings at breast height and maximum tree height (Table 2) from site index curves of interior lodgepole pine (Farnden 1996).

										Number of tree rings			
Age class (years)	Site number	Location				Elevation (m)	Aspect	Slope (%)	Year of fire	mean	st dev	n	Site index
12	1	53°	10.676'	117°	28.810'	1564	SW	15	1997	8	1	16	12.5
12	2	53°	14.384'	117°	28.596'	1464	S	9	1997	8	2	16	12.5
12	3	53°	14.210'	117°	28.236'	1420	S	14	1997	9	2	15	13.5
12	4	53°	14.343'	117°	28.029'	1459	S-SE	23	1997	10	1	16	15.5
12	5	53°	14.344'	117°	27.740'	1502	S-SW	16	1997	9	1	15	14.0
21	1	53°	7.578'	117°	21.799'	1583	SW	12	1988	16	1	15	15.0
21	2	53°	7.237'	117°	21.379'	1499	S	18	1988	15	5	16	15.0
21	3	53°	7.195'	117°	22.849'	1521	S	3	1988	15	1	16	16.0
21	6	53°	7.379'	117°	21.432'	1577	S-SE	25	1988	16	1	16	16.0
53	1	53°	12.881'	117°	23.924'	1491	SE	9	1956	39	4	16	15.3
53	2	53°	12.708'	117°	24.007'	1449	S-SE	17	1956	37	5	16	15.3
53	3	53°	10.581'	117°	27.344'	1528	S	21	1956	37	5	15	15.3
53	4	53°	10.719'	117°	27.011'	1588	S	23	1956	38	6	16	16.0
53	5	53°	12.799'	117°	24.319'	1462	S	18	1956	45	12	15	14.5
100+	1	53°	7.436'	117°	21.855'	1529	SW	33	1900-1910	93	15	16	13.5
100+	2	53°	7.321'	117°	21.633'	1519	S-SE	24	1900-1910	88	11	15	15.3
100+	3	53°	7.165'	117°	22.144'	1523	S	2	1900-1910	95	18	16	12.5
100+	4	53°	4.891'	117°	9.154'	1472	SW	17	1900-1910	82	25	16	15.3
100+	5	53°	3.430'	117°	4.145'	1455	W-SW	18	1900-1910	86	15	15	15.3

We selected stands of similar productivity and growth potential based upon matching the site index of these stands. The largest 15% of trees within each plot were used to determine top height. In the 100+ stands, tree cores at 1.3

m height from all trees in each plot were used to confirm stand age, as the original year of fire was not known. Site index curves from lodgepole pine (Farnden 1996) were used to estimate site index (SI) of all stands at age 50. During site selection, I were targeting sites with a site index of 15. In practice, SI ranged from 12.5-16.0m across age classes and individual stands (Table 1). One stand from the 1988 fire was removed as it exceeded the site index criteria; therefore 19 stands were included in all subsequent analyses.

Our intent was to sample within each stand, an area representing approximately the same number of individual trees in each age class (targeting 50-70 trees $stand^{-1}$). Therefore, in the 12 year-old age class I measured 3m radius plots, 4m radius plots in the 21 year-old age class, 7m radius plots in the 53 year-old age class and 10m radius plots in 100+ year old age class. In practice, however, this tended to oversample the youngest age class (77-172 trees $plot^{-1}$).

Within each stand, the total height, height at the base of the crown, diameter at breast height (dbh) and stump diameter (30 cm from ground) were measured on all of the trees within the sampling area described above. In the case of the 12 and 21 year old age classes, DBH was not measured as many trees were shorter than 1.3m. Two trees from each stand were destructively harvested for leaf mass and area determination (detailed below) and tree cookies (for the two destructively harvested trees) or increment cores obtained from 16 trees for tree ring analyses (detailed below).

To estimate soil nutrient availability in each site, five anion and five cation resin exchange probes (PRS™ Probes, Western Ag Innovations) were installed in each stand in late May- early June and removed at 7.5 weeks (52 days) for analysis of soil macro- and micronutrients. All probes within each stand were pooled for laboratory extraction; therefore the stand-level values are a single number representing soil averaged from five locations.

Relevant stand characteristics (height, diameter, live crown ratio, tree density, basal area and relative density) for each site and averaged over age classes are summarized in Table 2. Relative density was calculated as described in Curtis (1982):

$$\text{Relative density} = \frac{\text{basal area}}{\text{quadratic mean diameter}^{0.4}} \quad (1)$$

A similar quantity, stand density index was also quantified (Long 1985):

$$\text{SDI=stems per hectare} \times \left(\frac{\text{DBHq}}{25}\right)^{1.6} \quad (2)$$

Where DBHq is the diameter of the average basal area of the stand.

Table 6.2: Tree and stand characteristics (height, diameter, live crown ratio and tree density, basal area, relative density and stand density index (SDI)) in 2009. Mean and maximum height (max 15%) are shown with standard deviations of the mean (st dev). Values were based on measurement of all trees within a circular plot. Note that plot size varied by age class: (12 year old) - 3.0 m radius, (21 year old) - 4.0 m radius, (53 year old) - 7.0 m radius, (100+) - 10.0 m radius.

		2009 Height (m)				2009 Diameter (cm)		Live crown length (m)		Live crown ratio			Tree density	Basal area	Relative	SDI
Age class	Site	mean	st dev	max 15%	st dev	mean	st dev	mean	st dev	mean	st dev	n	(stems ha^{-1})	(m^2 ha^{-1})	density	
12	1	1.0	0.5	1.9	0.2	1.7	0.8	1.01	0.49	1.00	0.00	90	31831	8.9	6.9	511
12	2	1.4	0.6	2.2	0.3	2.2	1.2	1.37	0.60	1.00	0.00	77	27233	13.8	9.5	701
12	3	1.5	0.7	2.5	0.3	1.9	1.1	1.46	0.72	1.00	0.00	118	41734	16.2	11.8	868
12	4	1.5	0.7	2.6	0.3	1.7	0.9	1.46	0.71	1.00	0.00	147	51991	15.7	12.0	884
12	5	1.2	0.6	2.3	0.4	1.5	0.8	1.23	0.58	1.00	0.00	172	60833	14.1	11.4	839
	age class 12	1.3	0.2	2.3	0.3	1.8	0.3	1.32	0.65	1.00	0.00		42724	13.7	10.3	761
21	1	2.1	0.9	3.5	0.4	3.6	1.6	1.82	0.87	0.81	0.13	97	19298	23.6	13.6	1006
21	2	2.3	1.1	4.0	0.2	4.2	2.6	1.98	1.14	0.82	0.09	56	11141	21.5	11.4	838
21	3	2.3	1.1	4.2	0.5	4.0	1.9	2.04	1.08	0.84	0.09	61	12136	18.4	10.2	751
21	6	3.7	1.0	4.8	0.1	5.5	2.2	2.88	1.09	0.77	0.17	62	12335	34.1	16.7	1234
	age class 21	2.6	0.7	4.1	0.5	4.3	0.8	2.33	1.15	0.78	0.14		13727	24.4	13.0	957
53	1	12.6	1.3	14.3	0.4	12.2	3.1	4.61	1.47	0.36	0.09	54	3508	43.4	15.8	1164
53	2	13.3	1.4	15.2	0.3	12.4	3.2	4.15	1.38	0.31	0.08	52	3378	43.2	15.6	1151
53	3	11.0	1.2	12.7	0.5	10.4	2.8	3.73	1.25	0.33	0.08	74	4807	43.6	16.9	1246
53	4	10.9	1.7	13.5	0.8	11.3	3.0	3.86	1.40	0.35	0.09	74	4807	51.2	19.2	1415
53	5	12.6	1.4	14.6	0.8	10.0	2.4	3.68	1.33	0.29	0.08	65	4222	35.2	13.8	1021
	age class 53	12.1	1.1	14.1	1.0	11.2	1.0	3.97	1.39	0.33	0.09		4145	43.3	16.2	1199
100+	1	15.8	2.7	18.9	0.7	17.1	4.3	6.18	2.22	0.39	0.12	67	2133	52.2	16.5	1222
100+	2	16.2	4.1	20.7	0.7	18.1	5.9	5.11	3.09	0.30	0.18	47	1496	42.4	13.1	964
100+	3	14.6	2.4	18.0	0.8	16.3	4.1	5.30	1.94	0.36	0.12	70	2228	49.3	16.0	1178
100+	4	16.0	2.9	20.1	0.7	17.8	5.0	6.05	1.99	0.37	0.08	54	1719	46.1	14.4	1061
100+	5	17.3	2.8	20.6	0.5	17.4	4.1	6.37	1.85	0.37	0.08	62	1974	49.5	15.6	1153
	age class 100+	16.0	0.9	19.7	1.2	17.3	0.7	5.82	2.25	0.36	0.12		1910	47.9	15.1	1116

6.2.2 Fine root collection

In August, 110 soil core samples from the upper 30 cm of the soil profile were excavated. Soil cores were separated into two layers: 0-15 cm and 15-30 cm. Previous studies have found that over 90% of fine roots were located in the upper 20 cm (*Picea abies*, Ostonen et al. 2003) or 30 cm (*Pinus sylvestris*, Xiao et al.

2003) of the soil profile. In the current study, I also found that 80% of all the fine roots collected were in the upper 15 cm of the soil profile (data not shown).

The volume of soil from which roots were extracted ranged from 0.009 m^3 to 0.05 m^3 depending on stand age (square sample being 17 x 17 cm for 12 and 21 year old stands, 34 x 34 cm for 53 year old stands and 41 x 41cm for 100+ year old stands). Five soil samples were collected in the 12 and 53 year-old stands and six samples in the 21 and 100+ year-old stands. This amounted to sampling a total volume of 0.145 m^2 in each 12 year-old stand, 0.173 m^2 in a 21 year-old stand, 0.578 m^2 in a 53 year-old stand and 1.01 m^2 in a 100+ year-old stand. Sampling effort on an area basis ranged from 0.3-0.5 % of total stand area, in which aboveground measurements were quantified. Sampling was more intensive relative to other studies, e.g., Xiao et al. 2003 sampled 0.003% of a 73 year-old *Pinus sylvestris* stand, Ruess et al. (1996) sampled 0.036 m^2 per stand and Litton et al. (2003) 0.048 m^2 for each stand (13 years old). Samples were collected in heavy-duty plastic bags and roots enclosed in soil and stored in a 3°C cooler until processing (Ruess et al. 1996).

The upper portion of the sample was most often a large 'mat' of understory shrub, grass and pine roots and organic material in which case it could not be sifted and was placed directly into plastic bags. The mineral soil portions were initially sieved (4 mm mesh) in the field in order to reduce the soil volume to be carried out. Care was taken to minimize disturbance of intact root mats (combination of coarse and fine roots). In order to account for loss of roots from coarse sieving, a sub-sample of the soil that passed the sieve was additionally collected and brought back to the lab. Fine roots were manually separated (see also methodology below) and the estimate of the fine roots lost by coarse sieving (hereafter called the field fine root fraction, FFRF) was scaled up to the sample-level:

$$\text{FFRF} = \frac{\text{amount fine roots collected}}{\frac{\text{mass soil collected}}{\text{soil bulk density}}} \times \text{volume of soil sieved} \qquad (3)$$

Soil bulk density samples were collected concurrently with root samples at 15 cm depth using a stainless steel circular core (5 cm diameter x 5 cm depth). Samples were collected in plastic bags and stored until lab processing. Soil bulk density samples were oven-dried at 105°C until weight constancy. Bulk density was determined as:

$$\text{bulk density (g cm}^{-3}) = \frac{\text{dry soil mass}}{\text{core volume}} \quad (4)$$

6.2.3 Lab-processing of soil samples

Our root washing and separation procedure follows Teste et al. (2012). Soil samples were dry-sieved (4mm and 1.4 mm) and then were sieved wet (1.0mm, 0.8mm and 250 μm) to separate roots from soil. Even with washing, in the upper 15 cm there would remain a dense mat of moss fragments, shrub roots and in some stands grass roots. These samples would then be immersed in water and lodgepole pine roots were manually removed with tweezers (hereafter called the lab fine root fraction, LFRF). Lodgepole pine roots were easily differentiated by distinct coloration and structure relative to roots of other species (grasses and shrubs). Live roots were separated from dead roots based on color and texture (smooth and plump were indicative of live roots while granular and withered were indicative of dead or dying roots) of the cortex (Ruess et al. 1996) and the flexibility of the roots (e.g: did not crumble or further fragment when handled with tweezers) (Comeau and Kimmins 1989). Coarse roots (>2mm in diameter) were separated from fine roots (hereafter lab coarse root fraction, LCRF). Separated pine roots were placed in plastic bags and frozen at -18°C until determination of surface area and diameter.

Small root fragments that had broken off the main root systems during washing were collected in a 250 μm sieve. This would include root fragments, organic matter and woody debris. This material was hand shaken in enough water to create a thick slurry and approximately 5 mL subsampled. In practice, the subsample represented 0.06-2.4% of the total dry mass of the organic fraction collected in the 250 sieve and the actual quantity of fine roots constituted on

average 10-25% of the organic fraction. The subsample was placed in a separate tray of water and pine root fragments were manually separated from remaining organic matter (hereafter called the fine root particulate fraction, FRPF). Both the larger particulate slurry and separated, sub-sampled particulate fraction were also frozen until subsequent analysis.

After initial root extraction was complete, root samples were removed from the freezer. Within each sample, the fine roots were immersed in water and homogenized by cutting them into 4-6 cm fragments. A subsample (or complete sample when there were few roots) of fine roots was then removed and scanned on a flatbed scanner and surface area determined with image analysis software (WinRHIZO Regent Instruments). All roots were oven-dried at 70°C overnight or until weight constancy and then weighed. Fine root density totals were calculated as a composite of:

$$\text{fine root density (Kg m}^{-2}\text{ or m}^2\text{ m}^{-2}) = \frac{\text{FFRF+LFRF+FRPF}}{\text{total soil sample area in each sample}} \qquad (5)$$

6.2.4 Determination of leaf-area index (LAI)

Given the wide range of crown structure across the chronosequence, I produced allometric relationships between tree age, diameter and height to estimate stand-level LAI. This is because indirect measures such as the LAI-2000, AccuPAR or SunScan all underestimate LAI compared with methods that utilize allometric scaling (Bréda 2003). This is due to the clumpy nature of tree foliage; clumpiness of pine foliage tends to increase with age, therefore the error associated with those measures is not constant through stand development and would not be a fair assessment for the current study.

To estimate stand leaf area, two trees were felled in each stand. Trees were selected in order to represent the span of possible tree sizes/classes (eg. dominant, co-dominant or suppressed). On each tree, the crown was separated into 1 m sections (100+ and 53 year old stands) or 0.5m sections (12 and 21 year old stands). Within each section, the branches were removed and the length and base diameter measured. Three branches (spanning a range of sizes) from each

section (12-21 branches per tree) were subsequently collected and brought to the lab for scaling branch leaf mass and area. Along the length of the entire crown, sub-samples of needles of all ages were collected from each tree in order to determine a relationship between leaf-area and leaf-mass. These needles were collected in a plastic bag and frozen (within 8 hours of harvest) until further processing.

Sampled branches were stored for 1-3 weeks in paper bags at room temperature and then dried in a walk-in oven at 70°C for one week. Needles were separated from stems and weighed. Linear regression was used to predict branch leaf mass within each of the four lodgepole pine age classes. All regression models were analyzed using R software (R Development Core Team 2011) and fitted using the LMER function (R package Lme4). Eleven candidate models with parameters for branch length, diameter, crown section and/or a random effect for the individual tree were generated and compared (Appendix, Table 1). The models with greater than 1% probability (Appendix, Table 2) were used in model averaged estimates (model parameter estimates shown in Appendix, Table 3). Model-averaging was a weighted average based on model probabilities (Anderson 2008) which are given as:

$$\text{Delta}_{(i)} = \text{AIC}_{(i)} - \text{AIC}_{(\text{model smallest AIC})} \quad (6)$$

$$\text{Probability}_{(i)} = \frac{\text{likelihood}_{(i)}}{\sum_1^{11} \text{likelihood}} \quad \text{Likelihood}_{(i)} = e^{-0.5 \times \text{Delta}_{(i)}} \quad (7)$$

This allowed for estimation of the leaf mass of each branch measured on the 38 felled trees above. From these estimates, whole tree leaf mass calculated.

Using the tree leaf mass estimates for the 38 trees above, a similar approach to the branch leaf mass estimates was used to generate predictive models of whole tree leaf mass from parameters including: height, diameter, crown length and stand. Again, 11 candidate models (Appendix, A6.4) within each age class were generated and compared. The best models were (Appendix, A6.5) then used to generate model-averaged (weighted) predictive estimates of

tree leaf mass of all individual trees within each plot (Appendix, A6.6). The leaf mass of each tree was then converted to leaf area with the ratio estimates described below.

Sub-sampled needles, which were stored frozen, were scanned with a flatbed scanner and one-sided leaf area measured with WinFolia software (Regent Instruments Inc.). Needles were then oven-dried at 70°C for two days and weighed. For each age class, the specific leaf mass was calculated for each tree and averaged for each age class (Table 3). This ratio was used to estimate tree leaf area from tree leaf mass. Leaf area index (LAI) for each stand is given as:

$$\mathrm{LAI}_{(\text{stand i})} = \frac{\sum_1^n \text{tree leaf area } (m^2)}{\text{plot area } (m^2)} \qquad (8)$$

6.2.5 Estimation of annual wood volume

Tree cores or cross sectional cookies were obtained from 16 trees (from a range of sizes) within each of the 19 stands. Cores and cookies were taken at stump height (30 cm) for the 12 and 21 year old stands and at breast height (1.3 m) for the 53 and 100+ year old stands. Cores and cookies were oven-dried and sanded (400 grit) in order to identify annual rings.Tree cookies and cores were scanned with a flatbed scanner and the number of rings and width determined with image analysis software (WinDENDRO, Regent Instruments Inc.). When rings were difficult to see with the scanner, ring width was verified manually on a velmex microscope system. Ring width was measured in two positions at a 90° angle and values averaged for each tree. From the tree ring data, the diameter of measured trees in 2004 was calculated. These trees formed the basic data set from which linear models were developed within age classes to predict 2004 diameter.

All regression models were analyzed using R software (R Development Core Team 2011) and fitted using the LM and/or LMER function (R package Lme4). Three candidate models (Appendix, A6.7) were compared for the prediction of diameter in 2004 within each age class. The model selection of the lowest AIC model (Appendix, A6.8) was used to generate estimates of 2004 diameter of trees within measurement plots (Appendix, A6.9). Similarly, models

for prediction of height, which were required to correspond with estimates of 2004 diameter, were also generated from plot data (with height and diameter) obtained in 2009. These candidate models had the same structure as described above (Appendix, A6.7) and the model with the lowest AIC (Appendix, A6.10) was used for prediction 2004 heights (Appendix, A6.11).

Tree volume was then determined from estimated diameter and tree heights, for each tree in the stand for the following years: 2004 and 2009. For the younger age classes (12 and 21 years old), the volume of a cone was used as a proxy for tree volume. For the older stands (53 and 100+ years old), I utilized taper equations specific to lodgepole pine from the upper foothills of Alberta (Huang 1994). Detailed description of taper equations are in Appendix 5. Mean annual volume increment was calculated as:

$$\text{Mean annual volume increment } \left(m^3 \text{ year}^{-1}\right) = \frac{\text{2009 volume-2004 volume}}{5} \qquad (8)$$

6.2.6 Data analysis

All analyses, including those described above, were carried out using R (R Development Core Team 2011). Leaf area, wood volume increment and soil nutrients as a function of age were analyzed as linear models of the form:

y=(m x age class)+b

Diagnostic plots of fitted vs. residuals were used to check for equal variances and histograms of residuals used for assessment of normality. The function LM (Linear Models) was used when assumptions of normality and equality of variance were met. However, when there was indication of unequal variance, the GLS (Generalized Least-Squares) function was used with a parameter to allow for unequal variances by age class. This was further supported by AIC comparisons of the LM model with the GLS model (lower was better). Root area and root mass were analyzed as linear mixed effects models with a random effect for the site included (as I had multiple soil cores collected per site).

The function LME (Linear Mixed-Effects Models; R package NLME) was used when assumptions of normality and equality of variance were met. However, when there was indication of unequal variance, an additional parameter was added to allow for unequal variances by age class.

Graphical presentation of estimated means, confidence intervals and least-significant difference intervals are shown in all subsequent figures. Graphical methods allow the reader to use their own judgment when meriting the statistical or more importantly the biological meaning of the data presented (Cohen 1994; Cumming and Finch 2005; Di Stefano 2003; Johnson 1999). All analyses are presented as means by age class with 95% confidence intervals and least-significant difference intervals (LSD):

$$LSD = \frac{\text{Model Residual Error}}{\sqrt{n}} \times \sqrt{2} \times \text{tvalue}$$

Least-significant difference intervals were used as a visual method of multiple comparisons between age classes (Crawley 2007). Confidence intervals are presented in order to graphically depict the precision of the mean estimates (Cumming and Finch 2005).

6.3 Results

6.3.1 Edaphic factors

There was no difference in total soil available N across all stand ages (Figure 1a) though levels of NO_3^- were elevated in the 12 and 53 year old stands (Figure 1b) and levels of NH_4^+ were higher in the 21 year old and 100+ year old stands (Figure 1c). P and K were 2-3 times higher in the 53 year-old sites compared with 100 year old stands while P and K in the mineral soil was similar across all age classes (Figure 1d-e). Calcium tended to increase with age and peaked at age 53, but was substantially lower in 100+ year old stands (Figure 1f). In terms of micronutrients, Fe, Zn and Al appeared to follow the same pattern as

seen for NH_4^+ (Figure 2a, c and f) while Mn was elevated only in the 100+ year old stand (Figure 2b).

Soil temperature at 10 cm depth the 100+ year age class showed the lowest soil temperatures during the growing season and the 12 year age class was warmest. The trend was reversed in winter (Figure 3).

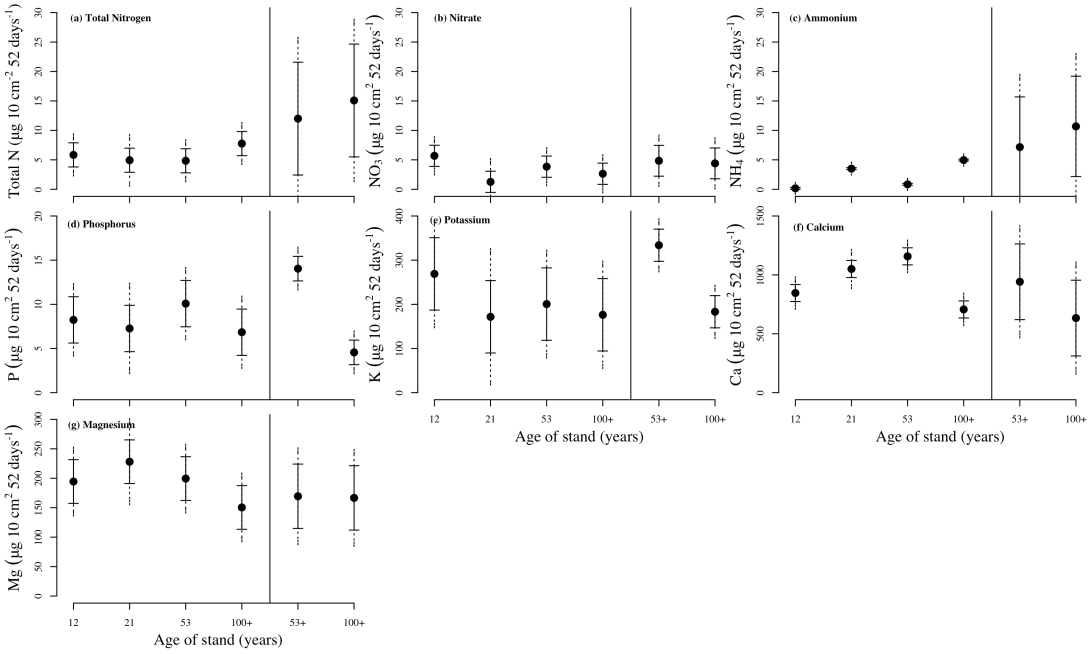

Figure 6.1: Soil available macronutrients recovered from PRS resin probes (5 probes pooled in each stand into a single sample) averaged by age class (year of fire). (a) total N (nitrate and ammonium), (b) nitrate, (c) ammonium, (d) phosphorus, (e) potassium, (f) calcium and (g) magnesium. Means to the left of the vertical line were resin probes inserted at a 45° angle into the mineral soil. Means to the right of the vertical line were resin probes inserted horizontally at the forest floor-mineral soil interface. This could only be accomplished in the older age classes as the younger age classes lacked forest floor development. Solid error bars represent least-significant difference intervals and dotted error bars represent 95% CI (n=4-5).

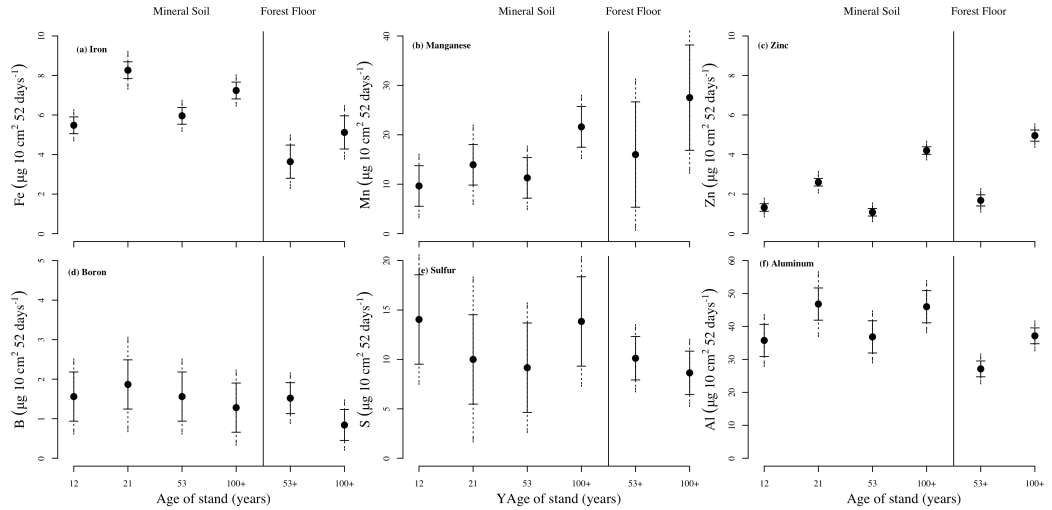

Figure 6.2: Soil micronutrients recovered from PRS resin probes (5 probes pooled in each stand into a single sample) averaged by age class (year of fire). (a) iron, (b) manganese, (c) zinc, (d) boron, (e) sulfur, (f) aluminum. Means to the left of the vertical line represent resin probes inserted at a 45° angle into the mineral soil. Means to the right of the vertical line represent resin probes inserted horizontally at the forest floor-mineral soil interface. This could only be accomplished in the older age classes as the younger age classes lacked forest floor development. Solid error bars represent least-significant difference intervals and dotted error bars represent 95% CI (n=4-5).

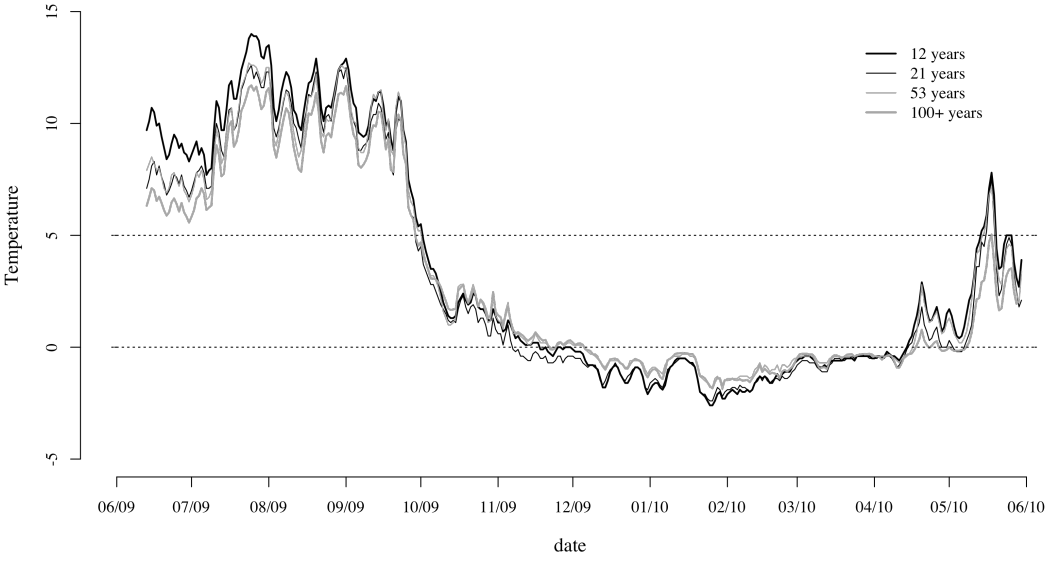

Figure 6.3: Daily mean soil temperature (at 10 cm depth) for each of four stand age classes. Two temperature sensors were logged hourly at each stand; lines are means of all sensors within each stand age. Dotted lines indicate temperatures at 5° and 0° C.

6.3.2 Root dynamics

Fine root surface area (< 2mm root diameter classes) in the 12 year old pine stands was about half of that of the 53 and 100+ year old stands (Figure 4). Root area in the 21 year-old stands was intermediate between these two groups and consequently was not clearly different from either age class (Figure 4).

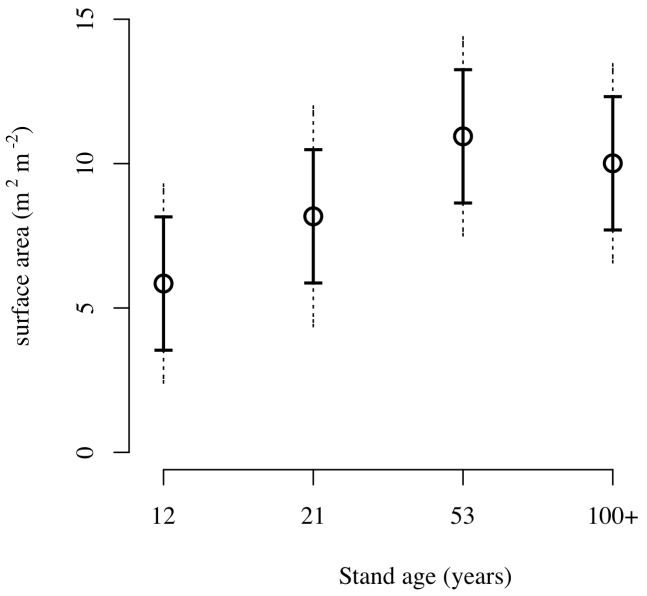

Figure 6.4: Stand-level root surface area of fine root diameter classes (<2 mm). Five to six soil cores were averaged for each stand and age class means represent 4-5 stands. Solid error bars represent least-significant difference intervals and dotted error bars represent 95% CI.

In terms of mass of fine and coarse roots, however, the pattern was more distinct. For the root diameter class < 2 mm, there was a gradual and distinct increase in root mass from the 12 to 21 and 21 to 53 year old stands with no difference in 53 and 100 year old stands (Figure 5a). For all other diameter classes (2-5mm, 5-10mm and > 10mm) root mass consistently increased with age (Figure 5b-d). Total root mass of all diameter classes increased steadily between age classes but more slowly between age 53 and 100 (Figure 5e). Total mass of dead roots (coarse and fine) nearly tripled from the 12 year-old stands to 100 year-old stands (Figure 5f).

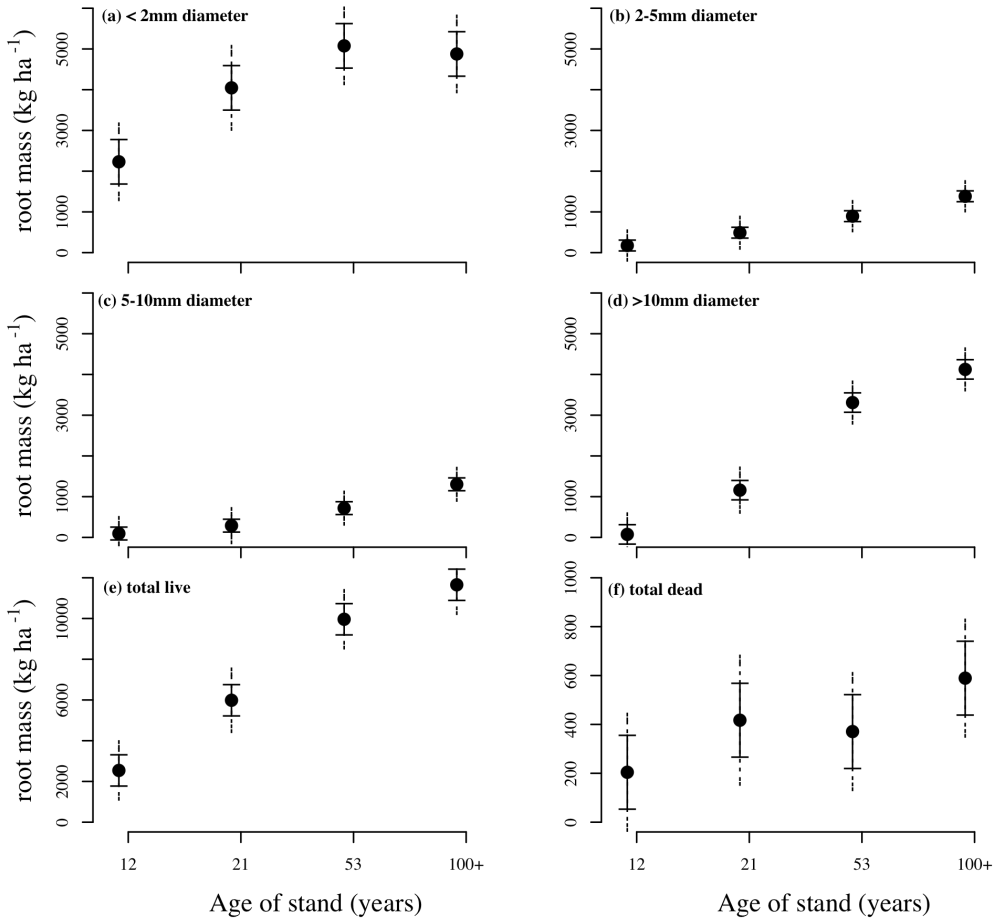

Figure 6.5: Stand-level root mass for root diameter classes: (a) <2mm, (b) 2-5 mm, (c) 5-10mm, (d) >10mm, (e) total live mass and (f) total dead root mass. Five to six soil cores were averaged for each stand and age class means represent 4-5 stands. Solid error bars represent least-significant difference intervals and dotted error bars represent 95% CI. Note that axis scale is the same for (a)-(d) but different for (e) and (f).

The ratio of LAI: fine root surface area was consistent in age classes 12-53 but increased in the 100+ year old stands (Figure 6a). When expressed on a mass basis, the ratio tended to increase between 12 -53 year old stands and then plateaued from 53 to 100+ year old stands (Figure 6b).

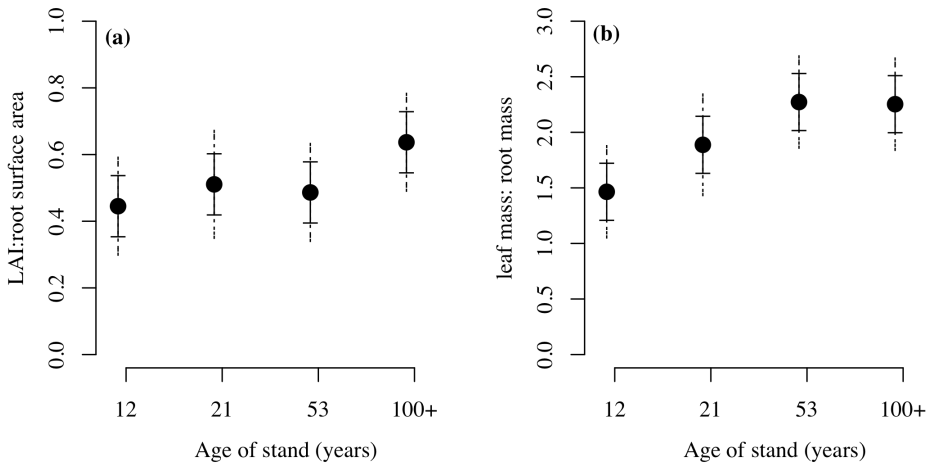

Figure 6.6: (a) Root surface area: LAI ratio averaged by age class (year of fire). (b) Root mass: leaf mass ratio averaged by age class (year of fire). Solid error bars represent least-significant difference intervals and dotted error bars represent 95% CI (n=4-5).

Specific root length (SRL) and specific root area (SRA) were highest in the youngest age classes (12 and 21) and lowest in the older age classes (53 and 100+) (Table 3). The youngest stand, in particular, had nearly twice the root length per unit mass compared with the oldest age class (Table 3).

Table 6.3. Specific leaf area (SLA), specific root length (SRL) and specific root area (SRA) of four lodgepole pine age classes with least-significant difference intervals (LSD) and 95% confidence intervals (CI). Values are averages from 8-10 trees within each age class for SLA. Root parameters are based on scanned, sub-sampled fine root measurements from each of 5-6 cores per stand (n= 4-5 stands per age class).

	SLA ($cm^2\ g^{-1}$)			SRL ($m\ g^{-1}$)			SRA (x 10 $cm^2\ g^{-1}$)		
Age class	**Mean**	**LSD**	**95% CI**	**Mean**	**LSD**	**95% CI**	**Mean**	**LSD**	**95% CI**
12	64.8	56.5-73.1	53.3-76.3	12.5	10.8-14.2	10.1-14.9	18.7	17.1-20.3	16.5-21.0
21	54.4	46.0-62.7	41.5-67.2	11.5	9.8-13.2	8.9-14.2	17	15.3-18.6	14.5-19.5
53	42.1	33.7-50.3	30.5-53.5	8.4	6.7-10.1	6.0-10.8	13.6	11.9-15.2	11.3-15.8
100+	50.7	42.2-59.0	39.1-62.1	6.3	4.6-8.0	4.0-8.7	11.6	10.0-13.2	9.4-13.8

6.3.3 Leaf area index

Leaf area index (LAI) nearly doubled from two to four between age 12 to age 21 (Figure 7). LAI continued to increase steadily across the older age classes, peaking at ~ 5.5 at age 100+ (Figure 7a). However, when expressed as leaf mass (Mg ha^{-1}), the two oldest age classes showed similar values at ~11 Mg ha^{-1} (Figure 7b). Specific leaf area declined with age and was at its lowest (42.1 cm^2 g^{-1}) in the 53 year-old stand but then appeared to increase again at 100+ at 50.7 cm^2 g^{-1} (Table 3).

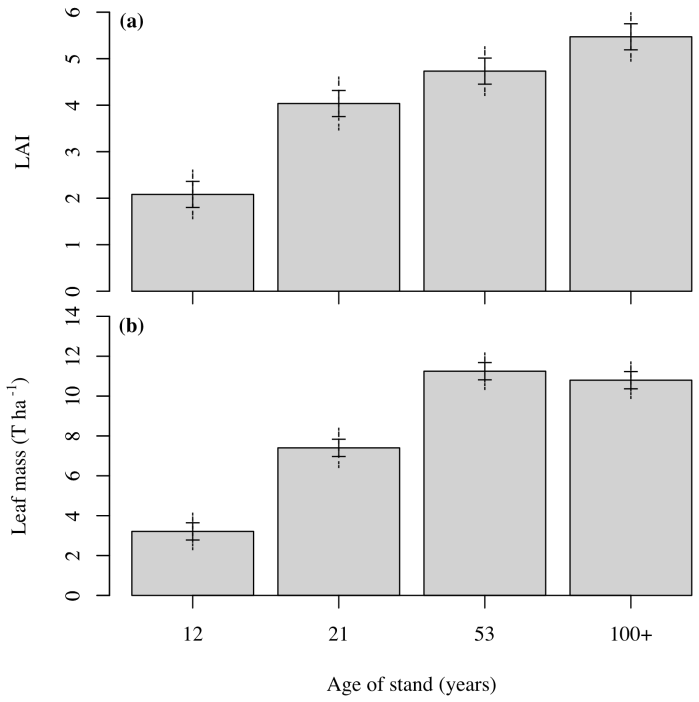

Figure 6.7: (a) Leaf area index (LAI) averaged by age class (year of fire) and (b) leaf mass (T ha^{-1}) by age class. Solid error bars represent least-significant difference intervals and dotted error bars represent 95% CI (n=4-5).

6.3.4 Wood volume increment

Mean annual wood volume increment averaged over the 5-year period (2004-2009) doubled from 1.2 m^3 ha^{-1} in the 12 year-old to 3.2 m^3 ha^{-1} in the 21 year-old stands and then doubled again from the 21 to the 53 year-old stands (Figure 8). At age 53, wood volume increment was over 6.5 m^3 ha^{-1} and then declined to 4.8 m^3 ha^{-1} at age 100+ (Figure 8).

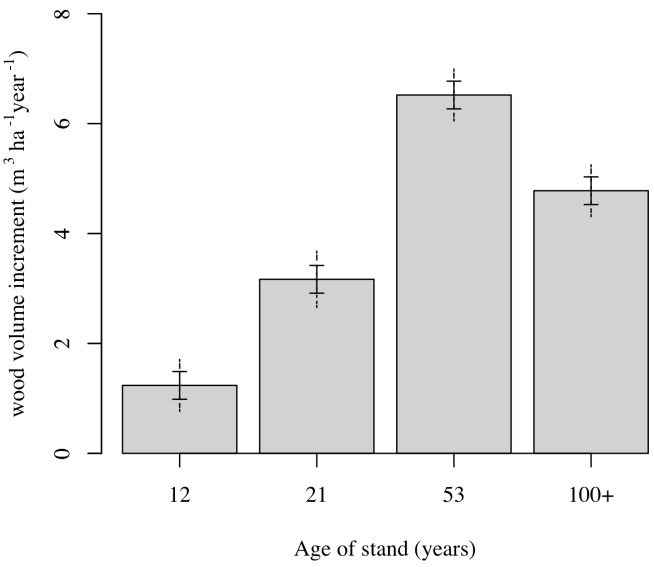

Figure 6.8: Annual wood volume increment averaged by age class (year of fire), expressed as a yearly average over the previous 5 years (2005-2009). Solid error bars represent least-significant difference intervals and dotted error bars represent 95% CI (n=4-5).

6.4 Discussion

Root surface area increased steadily from age 12 to 53 years old and remained stable from 53 to 100+. This pattern was more clearly observed on a fine root mass basis (roots less than 2 mm diameter). Furthermore, the ratios of leaf area to root area and leaf mass to root mass both tended to increase with age class (Figure 6). This suggests that needles in younger stands may have greater access to soil resources than older stands. Vogt et al. (1987) observed in a high productivity mixed deciduous-coniferous forest that the fine root mass of *Pseudotsuga menziesii* appeared to plateau by age 33-46 and that leaf mass to root mass ratio generally increased with age, but not necessarily so in a low productivity forest. This suggests that this relationship is likely to vary across stand types and resource gradients.

Unexpectedly, leaf mass and area showed no evidence for decline in the oldest age class; indeed, the 100 year-old stands had the highest leaf area of the entire age sequence and in terms of leaf mass was comparable to the 53 year old stands. This is in contrast to most other literature describing leaf area

development with time in forest stands (Ryan et al. 1997 for review). Foliage in these taller and older conifer stands are highly clumped (Kucharik et al. 1999) and in narrow crowns that are shaped through crown friction (Fish et al. 2006). The more direct measurement of leaf area that I used avoids the underestimate of leaf area using light extinction techniques as a result of clumping of foliage which would not have been uniform across the chronosequence. However, my absolute measurements of leaf biomass are still well within the range of variation observed in *Pinus contorta* stands (Table 5).

Similar to most other studies, however, wood productivity peaked and then showed a clear decline in the 100 year age class, therefore, the high level of leaf area was not translating into sustained productivity. The decline in stand productivity in the oldest age class is likely related to several interacting features that might make older and taller trees less efficient including: reduced soil temperatures, crown structural changes and fine roots supporting increased leaf area.

The build-up of forest floor in the 100+ years following fire is the most probable cause of reduced soil warming in the summer resulting in soil temperatures in the 100+ stands being 2-4 °C lower than in the younger stands. Colder soils reduce the physiological activity of the roots (Tyron and Chapin 1983; Minchin et al. 1994) and therefore reduce the movement of water and nutrients to the stem and leaves. Though not universal (refer to Ryan et al. 2006 for review), reductions in stomatal conductance have been observed with stand age (Drake et al. 2010). Reduced physiological activity may have reduced the sink strength of the roots thereby reducing movement of C to roots. Further, cold soils may reduce mineralization rate, explaining the decline in available P and K in the forest floor-mineral soil interface in the 100+ year old stands compared with the 53 year-old stands. Surprisingly, however, available inorganic N was similar across age classes and appeared to be on the increase at the oldest age class. A lodgepole pine chronosequence in Wyoming, which also utilized resins to quantify relative shifts in available soil inorganic N, found that total N peaked at 30 years of age (this was also the minimum age which was measured) and then

followed a slow decline to age 100 (Olsson et al. 1998). In that study, resin beads (in bags) were installed for a one-year period while resins in the current study were in place during the late spring and early summer period (June-July). Differences in the type (beads versus membrane) (Skogley and Doberman 1996), placement, soil temperature and precipitation will likely have substantial influences on the nutrient dynamics on resin membranes; therefore comparison of results between studies should be intepreted with caution.

Second, there was likely more crown shyness in the older pine stands as it has been previously demonstrated that taller pine stands in this region have increasing canopy openness (Fish et al. 2006). However, counter to Fish et al. (2006) I observed increasing crown length with stand age (height). This may be a unique feature to the stand types chosen as they were all located on southerly-facing slopes. This aspect could have stimulated branch growth along the south face of the stem, or perhaps the aspect interacted with prevailing winds in region. Certainly, increasing foliage clumping (Kucharik et al. 1999; Meng et al. 2006) and self-shading of foliage is adding another factor decreasing foliage efficiency.

Third, my study indicates that the older stands had proportionately less fine roots to support their leaves (either by weight or area). It has been demonstrated with some species that relative rates of production of foliage scales with roots/total belowground across stand ages (Smith and Resh 1999; Hendricks et al. 2006). If this holds true for my chronosequence, then belowground C allocation is possibly supporting coarse root development, higher specific fine root density (Rosenvald et al. 2013), or possibly a higher mycorrhizal component. In my study coarse root biomass continued to increase with age, likely as a consequence of greater structural requirements of larger trees. Increasing coarse root biomass quantified through excavation methods has also been observed in *Pinus resinosa* (King et al. 2007). I did observe a decrease in two related root morphological parameters: specific root length (SRL) and specific root area (SRA). In young, vigorously growing stands, root development is prolific resulting in fine roots with low wood density (Rosenvald et al. 2013). Consequently, this also means that older trees are paying higher C costs for the

fine roots they are producing compared with younger stands. Lastly, shifts in mycorrhizal community composition are known to occur throughout stand development (eg. Twieg et al. 2007; LeDuc et al. 2013; Rosenvald et al. 2013) and it is possible that these shifts could also be associated with increased C demand to symbionts.

6.4.1 Soundness of methodology

We are confident in my estimates of fine root surface area based on the following reasoning. Firstly, my method in quantifying fine roots far exceeded the sampling intensity utilized in many previous studies (Xiao et al. 2003; Ruess et al. 1996; Litton et al. 2003). Secondly, estimates of fine root biomass are well within the ranges reported in previous studies of *Pinus contorta* and when other Pinaceae are included, fine root estimates in the present study are often higher (Table 4). Thirdly, I accounted for loss of roots during the sampling process. During field sampling, I initially sieved soil samples and picked out root fragments and pieces. This process was not usually feasible in the 0-15 cm soil layer as the root mass was not easy to separate therefore this portion applied mostly to field sieving of the 15-30 cm layer. Sieved soil was sub-sampled and additional root fragments sorted in laboratory conditions. I found that the 'missed' fraction sieved out in the field contributed, on average, 3% to total fine root mass. The second type of sub-sampling occurred during the soil core washing stage where small root tips and fragments (1-3 mm length) tended to wash into the pool of organic materials. I sub-sampled from this organic pool and hand-sorted any visible root fragments. On average, the quantity of roots from the organic residue pool contributed 50% to total fine root mass.

Coarse root estimates in the younger age classes are similar to that reported in 13-year old *Pinus contorta* stands of comparable density (Litton et al. (2003), Table 4). There are no comparable data available in which to compare the 21 year-old age class. In the older age classes (53 and 100+), it is likely that my sampling tended to underestimate the coarse root contribution and therefore these estimates should be taken with caution (Table 4). This is likely due in part to the

fact that my estimates do not include the stumps which have been found to contribute as much as 50% of total root biomass in mature *Picea abies* stands (Ostonen et al. 2005) and 64-80% of coarse root biomass in a *Pinus resinosa* chronosequence (King et al. 2007). Therefore, coarse root estimates are probably representative of lateral root structure.

Table 6.4: Summary of previous studies reported fine and coarse root biomass. Values in brackets represent either the: standard error of the mean (SE), 95% confidence interval (CI).

	Species	age (years)	Density (stems ha^{-1})	Fine root biomass ($Mg\ ha^{-1}$) by age class (years)	Total root biomass ($Mg\ ha^{-1}$) by age class (years)	Fine root biomass method of determination	Coarse root biomass method of determination
Present study	*Pinus contorta*	10-20	31,831-60,833	2.2 (0.8 CI)	2.2 (0.3 CI)	soil cores (square cores: 17 cm)	soil cores (square cores: 17 cm)
		20-30	11,141-19,298	4.0 (0.8 CI)	6 (0.4 CI)	soil cores (square cores: 17 cm)	soil cores (square cores: 17 cm)
		50-60	3,378-4,807	5.1 (0.8 CI)	10 (0.3 CI)	soil cores (square cores: 34 cm)	soil cores (square cores: 34 cm)
		100-150	1,496-2,228	4.9 (0.8 CI)	12 (0.3 CI)	soil cores (square cores: 43 cm)	soil cores (square cores: 43 cm)
Comeau and Kimmins (1989)*	*Pinus contorta*	70-80	1,770-3,580	4.3-6.4	30-73	soil cores (5 cm (forest floor) and 10 cm diameter (mineral soil)	Allometric equations developed on site
Litton et al (2003)	*Pinus contorta*	10-20	425-598,462	0.2-1.8	0.3-3.6	soil cores (6.35 cm diameter)	Allometric equations developed on site
Pearson et al (1984)	*Pinus contorta*	70-80	1280	nr	26	-	Plane-intersect method for root determination, scaled by basal area
		100-150	1,850-14,640	nr	38-56	-	Plane-intersect method for root determination, scaled by basal area
		150+	420	nr	38	-	Plane-intersect method for root determination, scaled by basal area
Litton et al (2004)	*Pinus contorta*	100-150	1,320-3,360	1.4 (0.1 SE)	21 (3.6 SE)	Allometric equations from Comeau and Kimmins (1989)	
Ruess et al (1996)	*Picea glauca*	10-20		0.3-3.7	6.9 (0.8 SE)	soil cores (5.5 cm diameter)	Soil cores (5.5 cm diameter)
		100-150		3.1 (0.2 SE)			
Xiao et al (2003)	*Pinus sylvestris*	70-80		2.2	19.2	soil cores (15 cm (forest floor) and 8 cm diameter (mineral soil))	Allometric equations developed on site
King et al (2007)**	*Pinus resinosa*	0-10	1750-2400	nr	0.06-2.1	-	10 x 15m, 10 x 10 m plot; complete excavation
		10-20	1750	nr	5.6-8.5	-	15 x 15 m plot; complete excavation
		20-30	1750-2400	nr	3.6-23.6	-	15 x 15 m plot; complete excavation
		50-60	622	nr	23.3	-	15 x 15 m plot; complete excavation

* fine root biomass was <5mm diameter

**total root biomass does not include stump

A surprising and unexpected result was that LAI did not peak in the middle age class (53 years old) but instead continued to increase at the 100+ year old age class. The stands in the current study were all fully stocked as they all exceeded the minimum SDI value of 600 (Long 1985). Peak LAI in a previous study of *Pinus contorta* found that peak LAI occurred at 30-50 years (4.1 at age 50) (Smith and Resh 1999) and then declined to ~3.5 at age 100 and 2.3 at age 260 though the 30-50 year old sites were not fully-stocked (Table 5), this study also used allometry of individual trees to develop stand LAI. A similar result was found across a 75-240 year age sequence in an earlier *Pinus contorta* study, however this chronosequence was only replicated at the 100-150 year old age range and the stocking was not consistent (Pearson 1984); further 75 years is likely past the time of peak productivity.

Table 6.5: Summary of previous studies reported leaf biomass in lodgepole pine (*Pinus contorta*). Where available, tree density, basal area and SDI (estimated based on available data) are also presented as a reference point for comparison. Values in brackets represent either the: standard error of the mean (SE) or 95% confidence interval (CI).

	Species	Age (years)	Leaf mass biomass (Mg ha^{-1})	LAI	Tree density (stems ha^{-1})	Basal area (m^2 ha^{-1})	SDI	Foliage biomass method of determination
Present study	*Pinus contorta*	10-20	3.2 (0.6 CI)	2.1 (0.4 CI)	31,831-60,833	8.9-16.2	511-884	Allometric equations developed on site
		20-30	7.4 (0.7 CI)	4 (0.4 CI)	11,141-19,298	18.4-34.1	751-1,234	Allometric equations developed on site
		50-60	11.2 (0.6 CI)	4.7 (0.4 CI)	3,378-4,807	35.2-51.2	1,021-1,415	Allometric equations developed on site
		100-150	10.8 (0.6 CI)	5.5 (0.4 CI)	1,496-2,228	42.4-52.2	964-1,222	Allometric equations developed on site
Comeau and Kimmins (1989)	*Pinus contorta*	70-80	3.9-10.8		1,770-3,580	-	-	Allometric equations developed on site
Pearson et al (1984)	*Pinus contorta*	70-80	12.3		1280	26	632	Allometric equations developed on site
		100-150	8.4-11.4		1,850-14,640	42-64	1,035-1,736	Allometric equations developed on site
		150+	6.9		420	37	671	Allometric equations developed on site
Litton et al (2004)	*Pinus contorta*	10-20	0.2-3.6		425-598,462	0.1-2.2	14-3,165	Allometric equations developed on site
	Pinus contorta	100-150	6.0 (0.7 SE)		1,320-3,360	38-52	1,043-1,115	Allometric equations from Comeau and Kimmins (1989)
Smith and Resh (1999)	*Pinus contorta*	15		1.0	12,500	18.5	759	Allometric equations from Long and Smith (1988, 1990, 1992), Smith and Long (1989), Pearson et al 1984. These studies all took place in the same study area
		30		3.8	1,075	17.8	451	
		50		4.1	1,316	23	576	
		100		3.3	1,766	39.5	942	
		260		2.3	1,133	42.2	908	

When I observe the actual standing leaf mass, however, there is very little difference between the 53 and 100+ year old stands; in fact, the younger age class is slightly higher. This is a result of lower specific leaf area (42.1 cm^2 g^{-1}) in the 53 year-old age class compared with the 100+ age class (50.7 cm^2 g^{-1}). Low specific leaf area in the 53 year-old stand could be the result of onset of crown abrasions or shyness at that age class in *Pinus contorta* stands (eg. Fish et al. 2006). Given the wide space between crowns in the taller stands (Fish et al. 2006), it is possible that there may be less chronic abrasion at the older age class. Given that I observed an increase in crown length at age 100+ coupled with increased specific leaf-area suggests that crown abrasions were possibly reduced in the older age class or there was increased self-shading of highly clumped foliage.

6.4.2 Conclusions

We did observe a clear decline in annual wood volume increment from age 53 to 100+. This did not correspond with a decline in leaf area, however the leveling-off of root surface area preceded this decline. This suggests that in the oldest stands the leaves were less well-served by fine roots than in the younger

stands. Further, the clumped nature of this leaf area in the oldest stands would make needles less uniformly illuminated than in the younger stands. Soil temperature is also a likely driver, as growing season soil temperature in the oldest stands were the coldest during the growing season (June-August). Reduced availability of P and K in the oldest stand may also have been a contributing factor. Lastly, substantial changes in the structure of needles (specific leaf area), perhaps driven by crown abrasions or self-shading, further contributed to a change in the leaf area to fine root area and the leaf mass to root mass ratio.

6.5 References

Anderson DR (2008) Model based inference in the life sciences: a primer on evidence. Springer, New York, USA.

Beckingham JD, Corns IGW, Archibald JH (1996) Field guide to ecosites of west-central Alberta. Northern Forestry Centre, Canadian Forest Service. 380 pp.

Binkley D (2004) A hypothesis about the interaction of tree dominance and stand production through stand development. For Ecol Manage 190: 265-271

Bréda NJJ (2003) Ground-based measurements of leaf area index: a review of methods, instruments and current controversies. J Exp Bot 54: 2403-2417

Burton AJ, Pregitzer KS, Hendrick RL (2000) Relationships between fine root dynamics and nitrogen availability in Michigan northern hardwood forests. Oecol 125: 389-399

Cohen J (1994) The earth is round ($p<0.05$). Am Psy 49: 997-1003

Comeau PG, Kimmins JP (1989) Above- and below-ground biomass and production of lodgepole pine on sites with differing soil moisture regimes. Can J For Res 19: 447-454

Crawley MJ (2007) The R book. John Wiley and Sons, West Sussex, United Kingdom.

Cumming G, Finch S (2005) Inference by eye: confidence intervals and how to read pictures of data. Am Psych Assoc 60: 170-180

Curtis RO (1982) A simple index of stand density for Douglas-fir. For Sci 28: 92-94

Di Stefano J (2004) A confidence interval approach to data analysis. For Ecol Manage 187: 173-183

Drake JE, Davis SC, Raetz LM, DeLucia EH (2011) Mechanisms of age-related changes in forest production: the influence of physiological and successional changes. Global Change Biol 17: 1522-1535

Drake JE, Raetz LM, Davis SC, DeLucia EH (2010) Hydraulic limitation not declining nitrogen availability causes the age-related photosynthetic decline in loblolly pine (*Pinus taeda* L.). Plant Cell Environ 33: 1756-1766

Farnden C (1996) Stand density management diagrams for lodgepole pine, white spruce and interior Douglas-fir. Natural Resources Canada, Pacific Forestry Canada. Victoria, BC. Report BC-X-360

Fish H, Lieffers VJ, Silins U, Hall RJ (2006) Crown shyness in lodgepole pine stands of varying stand height, density, and site index in the upper foothills of Alberta. Can J For Res 36: 2104-2111

Hendricks JJ, Hendrick RL, Wilson CA, Mitchell RJ, Pecot SD, Guo D (2006) Assessing the patterns and controls of fine root dynamics: an empirical test and methodological review. J Ecol 94: 40-57

Huang S (1994) Ecologically based individual tree volume estimation for major Alberta tree species. Alberta Sustainable Resource Development. Pub No. T/288. ISBN: 0-7732-1267-1

Johnson DH (1999) The insignificance of statistical significance testing. J Wild Manage 63: 763-772

King JS, Giardina CP, Pregitzer KS, Friend AL (2007) Biomass partitioning in red pine (*Pinus resinosa*) along a chronosequence in the Upper Peninsula of Michigan. Can J For Res 37: 93-102

Kucharik CJ, Norman JM, and Gower ST (1999) Characterization of radiation regimes in non-random forest canopies; theory, measurements and simplified modeling approach. Tree Physiol 19: 695–706

Landhausser SM, Lieffers VJ (2001) Photosynthesis and carbon allocation of six boreal tree species grown in understory and open conditions. Tree Physiol 21: 243-250

Landhausser SM, Lieffers VJ (2012) Defoliation increases risk of carbon starvation in root systems of mature aspen. Trees 26: 653-661

LeDuc SD, Likkeskov EA, Horton TR, Rothstein DE (2013) Ectomycorrhizal fungal succession coincides with shifts in organic nitrogen availability and canopy closure in post-wildfire jack pine forests. Oecol 172: 257-269

Litton CM, Raich JW, Ryan MG (2007) Carbon allocation in forest ecosystems. Global Change Biol 13: 2089-2109

Litton CM, Ryan MG, Knight DH (2004) Effects of tree density and stand age on carbon allocation patterns in postfire lodgepole pine. Ecol App 14: 460-475

Litton CM, Ryan MG, Tinker DB, Knight DH (2003) Belowground and aboveground biomass in young postfire lodgepole pine forests of contrasting tree density. Can J For Res 33: 351-363

Long JN (1985) A practical approach to density management. For Chron 61: 23-27

Magnani F, Mencuccini M, Grace J (2000) Age-related decline in stand productivity: the role of structural acclimation under hydraulic constraints. Plant Cell Environ 23: 251-263

Minchin PEH, Farrar JF, Thorpe MR (1994) Partitioning of carbon in split root systems of barley: effect of temperature of the root. J Exp Bot 45: 1103-1109

Ostonen I, Lohmus K, Pajuste K (2005) Fine root biomass, production and its proportion of NPP in a fertile middle-aged Norway spruce forest: Comparison of soil core and ingrowth core methods. For Ecol Manage 212: 264-277

Olsson U, Binkley D, Smith FW (1998) Nitrogen supply, nitrogen use, and production in an age sequence of lodgepole pine. For Sci 44: 454-457

Pearson JA, Fahey TJ, Knight DH (1984) Biomass and leaf area in contrasting lodgepole pine forests. Can J For Res 14: 259-265

Rosenvald K, Ostonen I, Uri V, Varik M, Tdersoo L, Lohmus K (2013) Tree age effect on fine-root and leaf morphology in a silver birch forest chronosequence. Eur J For Res 132: 219-230

Ruess RW, Van Cleve K, Yarie J, Viereck LA (1996) Contributions of fine root production and turnover to the carbon and nitrogen cycling in taiga forests of the Alaskan interior. Can J For Res 26: 1326-1336

Ryan MG, Binkley D, Fownes JH, Giardina CP, Senock RS (2004) An experimental test of the causes of forest growth decline with stand age. Ecol Mono 74: 393-414

Ryan MG, Binkley D, Fownes JH (1997) Age-related decline in forest productivity: pattern and process *in* Advances in Ecological Research Vol 27. ISBN 0-12-013927-8

R Development Core Team (2011) R: A language and environment for statistical computing. R Foundation for Statistical Computing, Vienna, Austria. ISBN 3-900051-07-0, URL http://www.R-project.org/.

Sillett SC, Van Pelt R, Koch GW, Ambrose AR, Carroll AL, Antoine ME, Mifsud BM (2010) Increasing wood production through old age in tall trees. For Ecol Manage 259: 976-994

Skogley EO, Doberman A (1996) Synthetic ion-exchange resins: soil and environmental studies. J Environ Qual 25: 13-24

Smith FW, Resh SC (1999) Age-related changes in production and below-ground carbon allocation in *Pinus contorta* forests. For Sci 45: 333-341

Teste FP, Lieffers VJ, Strelkov SE (2012) Ectomycorrhizal community responses to intensive forest management: thinning alters impacts of fertilization. Plant Soil. DOI 10.1007/s11104-012-1231-6

Twieg BD, Durall DM, Simard SW (2007) Ectomycorrhizal fungal succession in mixed temperate forests. New Phytologist 176: 437-447

Tyron PR, Chapin III FS (1983) Temperature control over root growth and root biomass in taiga forest trees. Canadian Journal of Forest Research 13: 827-833.

Vogt KA, Vogt DJ, Moore EE, Fatuga BA, Redlin MR, Edmonds RL (1987) Conifer and angiosperm fine-root biomass in relation to stand age and site productivity in Douglas-Fir forests. J Ecol 75: 857-870

Xiao CW, Yuste JC, Janssens IA, Roskams P, Nachtergale L, Carrara A, Sanchez BY, Ceulemans R (2003) Above- and belowground biomass and net primary production in a 73-year-old Scots pine forest. Tree Physiol 23: 505-516

Xu CY, Turnbull MH, Tissue DT, Lewis JD, Carson R, Schuster WSF, Whitehead D, Walcroft AS, Li J, Griffin KL (2012) Age-related decline of stand biomass accumulation is primarily due to mortality and not to reduction in NPP associated with individual tree physiology, tree growth or stand structure in a *Quercus*-dominated forest. J Ecol 100: 428-440

Chapter 7: Thesis Discussion

The overall objective of my thesis was to understand how hydraulic architecture, crown form and resource allocation are affected by shading trees of opposing shade tolerance. Five studies were developed to further this objective and five questions were posed in the introduction. These questions are discussed in the following paragraphs. A conceptual framework and suggestions for future work are outlined in the final sections.

7.1 How do trees of opposing shade tolerance adjust hydraulically to the understory environment

Light is one of the three key components (water and nutrients) driving whole plant as well as individual branch survival and growth. Reduced carbon fixation and alterations to leaf morphology are readily known to alter in a reduced light environment. Demand for water correspondingly declines. In Chapter 2, I observed that the decline in k_l and $K_{s\text{-}p}$ in the understory environment supports the notion of reduced need for water. Similarly, increased LA:SA in the leading shoots are indicative of a shift in allocation from stem growth (hydraulics) to leaf area (light capture).

What was perhaps the most interesting finding in Chapter 2 was that the changes in wood anatomical features in shaded leading shoots of two very different species (*Pinus contorta* and *Picea mariana*). Understory trees tended to produce narrower tracheids that were still capable of comparable flow to that of open grown trees with larger diameter tracheids. This was probably driven by changes in pit structure, which is supported from my observations of larger maximum pore sizes in the margo of shaded *Pinus contorta* and *Picea mariana*. Having relatively efficient sapwood water transport means that understory conifers could invest less carbon into wood production by producing bordered pits with a more porous but fragile structure, corresponding with increased xylem vulnerability.

Alterations in water transport properties will critically impact to crown structure throughout stand development. Branches begin their lives at the top of crown in full light, as time progresses these branches come into increasingly lower light levels and are eventually self-pruned. However, in older stands (50+ years) these branches may actually persist for many years in shade, producing xylem that is less drought resistant (as demonstrated in Study 2). During this period the stand may begin to open again, re-illuminating these branches. This reintroduces branches into a higher degree of light for which the branch may not be developmentally prepared for (from a water relations perspective). At the minimum, photosynthetic rates may decline as stomata close earlier in the day due to lower tolerance for water stress. Reduced ability to photosynthesize and water stress may contribute to increased lower branch mortality and lower tree-level rates of NPP with stand age.

7.2 Are seasonal carbohydrate changes in tissues of Picea glauca and Pinus contorta trees similar?

In general the slower growing and long-lived *Picea glauca* maintained higher TNC concentrations than fast-growing *Pinus contorta* and the differences between these species were most striking in the needles and bark. *Picea glauca* also had wider absolute seasonal changes in TNC (and in sugar alcohols in some tissues) than *Pinus contorta*, suggesting that storage plays a more important role in *Picea glauca* than in *Pinus contorta*. This capacity for larger carbon storage/reserves provides *Picea glauca* with greater buffering capacity during periods of stress (eg. immediate onset of shading).

However, both species demonstrated remarkably similar C reserve strategies in their roots. Given what was observed in aboveground tissues, this would indicate that there are overriding environmental factors driving this pattern. The study sites in this region experience short summers and long periods where soil temperatures are below freezing. Therefore, there is only a limited period in

which roots are physiologically active and able to aquire or store C. As these stands age, soil temperature is likely to become even more limiting and may further contribute to belowground limitations in root activity and therefore soil resource acquisition.

7.3 Does cohort position (co-dominant versus suppressed) influence seasonal carbohydrate dynamics and fluxes in shade tolerant Picea glauca?

Overall, both fully shaded (suppressed) and illuminated (co-dominant) *Picea glauca* trees showed remarkably similar seasonal fluxes of non-structural carbohydrates. This was somewhat surprising as these trees originated from different stands (though within the same overall area). The co-dominant trees were in a *Pinus*-*Picea* mixture while the suppressed trees were growing under the shade of a mature *Populus tremuloides* stand. This further supports the findings in Chapter 3 that *Picea glauca* has a very conservative carbohydrate reserve strategy.

7.4 What is the impact of asymmetrical vs. uniform crown shading on the mortality and growth of upper and lower branches within tree crowns? Are these impacts similar for species with opposing levels of shade tolerance?

In Chapter 5 I observed across two species (*Pinus contorta* and *Picea glauca*) that the needles of lower branches tended to store less C than upper branches under asymmetric shade.. I had hypothesized that asymmetric shading would larger, negative consequences for *Pinus contorta* compared with *Picea glauca* and this is certainly what I observed throughout this study.

Reduced C storage in the lower branches suggests that resources were either: (1) being extracted more heavily from asymmetrically shaded lower branches or (2) that they showed greater reductions in net photosynthesis compared with fully shaded branches. The increased asymmetry in C storage between upper and lower branches may also indirectly indicate a tipping point in

crown structural dynamics. In *Pinus contorta*, when the TNC difference favored the upper branches, the asymmetrically shaded branches suffered the greatest reduction in bud flushing. For *Picea glauca*, the study may have been too short to observe the point were the balances tipped enough to drive lower shoot mortality. As described in Chapters 3 and 4, *Picea glauca* is a highly C conservative species and therefore may require longer periods of stress to elucidate a similar response or the light level was not significantly inhibitory in *Picea*.

Differences between these species in terms of response to asymmetrical shading were also apparent. Sapwood-area specific conductivity declined in shaded (uniform and asymmetric) lower branches in *Pinus contorta*; making these branches less likely to maintain stomatal conductance and C fixation. This decline was not observed in *Picea glauca,* suggesting that compromised water transport in pine makes it more sensitive to any light reductions. This is consistent with *Pinus contorta* being a light requiring, shade intolerant species and is also evidenced in Chapter 5 as uniformly shaded branches of *Pinus contorta* also showed a decline in shoot growth (though not to the same extent as in asymmetrical shade) while *Picea glauca* did not.

Secondly, the lower inherent levels of shoot carbohydrate reserves in *Pinus contorta* relative to *Picea glauca* are also likely to make *Pinus contorta* less resilient to shading. Consequently as reserves dwindled in shaded lower branches, there was very little buffer with which to work with. Similar differences in shoot carbohydrates were also observed between these species in Chapter 3. For the shade tolerant spruce, however, fully shaded trees showed remarkably similar seasonal fluxes in carbohydrates compared with fully illuminated trees in Chapter 4.

The net result for *Pinus contorta* is that crown recession will likely operate sooner and at higher light levels compared with *Picea glauca*. At the stand-level, I know that light dichotomy changes substantially through time. Increasing numbers of branches are placed into subordinate positions with light levels that may be high enough to maintain a positive carbon balance in principal (if I only considered light-saturated photosynthetic curves), but due to the light dichotomy

between branches, crown recession ensues and overall crown lengths decline. This will ultimately influence standing LAI and perhaps long-term stand productivity in comparable ecosystems.

7.5 How does the interplay between the fundamental resource acquisition organs of forest stands change through stand development?

In Chapter 6, I had hypothesized that root area and leaf area would track each other throughout stand development and that fine root area would decline preceeding the well-known pattern of leaf area decline. Surprisingly, I did not observe this characteristic LAI decline observed so many times in previous studies. Instead, LAI continually increased to age 100+. Root surface area also did not experience a decline but instead leveled off prior to peak annual wood volume increment at age 21. The net result of these patterns is that leaf area in the oldest stands was supported by fewer fine roots than in the younger stands. Presumably this would make the leaf area unable to aquire soil resources as readily and lead to reduced photosynthetic efficiency of this leaf area. Though the LAI was high in the oldest stands, it is likely that the leaf area was highly clumped and therefore the needles less uniformly illuminated than in the younger stands which would further contribute to reduced photosynthetic efficiency.

In addition, the study sites were located in mid-elevation forests near the Rocky mountains where growing season soil temperature is limiting in all of these stands. The oldest stands were coldest during the growing season (June-August), which would further contribute to decreased resource acquisition efficiency of fine roots. Reduced availability of P and K in the oldest stand may also be a contributing factor.

All of these factors are likely to contribute to reductions in NPP throughout stand development and consequently the decline in wood volume increment shown in this study as well as others.

7.6 A conceptual framework of crown recession and stand decline

Sunlight is critical to plant survival. Variation in the quantity of light has driven plants to employ a host of morphological and physiological strategies in order to persist in high and low light. The light environment changes substantially for a tree during forest stand development. Certainly crown recession is at least partly driven by light-driven qualities creating a negative carbon balance for plants as they go into less illuminated conditions. However, I have demonstrated in chapters 2 and 5 that there are additional constraints to consider including impacts of shade on hydraulic architecture as well as asymmetry in light within the crown:

- A reduced light environment alters the xylem vulnerability of shoots. Shaded shoots are not as drought resistant as those in high light.
- Hydraulic conductivity declined in all shaded shoots of *Pinus contorta* (but not *Picea glauca*) in Chapter 5. This was not observed, however, in Chapter 2. Light quantity are likely be contributing factors to this discrepancy as the aspen-dominated understory in Chapter 2 exhibited light levels of approximately 30% of full sunlight while in Chapter 5 light was reduced, on average to 3-11% of full light.
- Asymmetric shading placed less-illuminated shoots at a greater disadvantage in terms of bud expansion and growth compared with uniform shading of the entire crown. This suggests that the light reduction in itself is not necessarily driving shoot mortality under low light.
- Relative reductions in TNC appear to follow similar patterns to bud expansion and growth observations, suggesting that carbon dynamics or fluxes are playing a role in dictating physiological activity of branches.
- In all cases, responses to asymmetric shade were always more extreme in *Pinus contorta* compared with *Picea glauca*. This is likely due, in part, to different C storage patterns as observed in Chapter 3 *Pinus contorta* exhibited

lower overall TNC concentrations and smaller (or non-existent) seasonal fluxes in TNC.

Reduced leaf area has been cited as a potential mechanism driving stand decline through reductions in NPP. Crown recession is likely an important driver contributing to leaf-area decline in many forest stands. As described above, crown recession is operating throughout stand development as asymmetry in light is present to increasing degrees from stand initiation and until full crown closure (Figure 7.1) and probably at its most severe point during the stem exclusion phase as light levels down the tree stem are at a low point. In addition, shade itself is also likely contributing as reduced light appears to compromise the hydraulic architecture of the wood and consequently may further interact with asymmetry related factors.

Fine root surface area is the first stand parameter to level-off. This corresponds with declining soil temperatures but still during a period of rapid wood volume increment increases and continued leaf area development. However, during the period of peak wood volume increment, a number of pressures are also converging including: light asymmetry (driving crown recession), crown friction and reduced ability to aquire soil resources (due to a combination of low soil temperatures and reduced fine root area supplying an increasing pool of leaves). Based on this conceptual diagram, I suggest that it is these factors, operating together, that contribute to the eventual stand decline (expressed through declining wood volume increment).

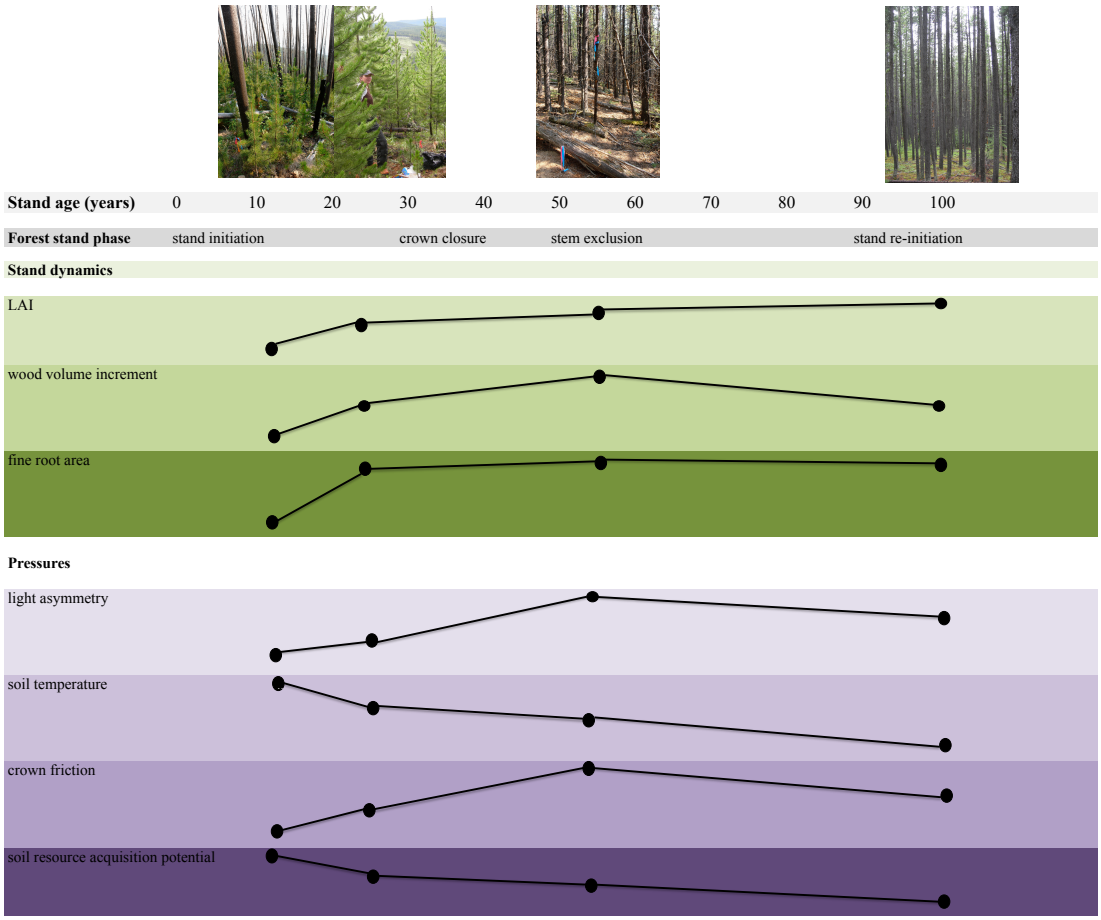

Figure 7.1: Conceptual diagram of stand dynamics for *Pinus contorta* in relation to environmental and stand related pressures throughout stand development.

7.7 Management implications

This work suggests that forest managers should employ caution during stand management exercises. Exposing suppressed individuals to full light can compromise the ability of those trees to respond positively to the increased light environment as their ability to withstand water stress is reduced. This is particularly evident for both the spruce species studied (*Picea glauca* and *P. mariana*). Stand thinning is likely to have a greater benefit to *Pinus contorta* than *Picea glauca* (at least based on the two years of study in Chapter 5). Asymmetry

in light had significantly negative consequences (growth and survival) for lower branches of *P.contorta* and very little effect on growth (no effect on survival) of lower branches of *P.glauca*. In Chapter 6, I observed that fine root densities leveled off early on in stand development. It is plausible that this lack of root production is contributing to a cycle of reduced water and nutrient uptake later on in the stand life and therefore lowering productivity. Efforts to stimulate root production could aid in prolonging the high productivity observed in the 50 year age range in these *Pinus contorta* stand types.

7.8 Suggestions for future studies

The following points are suggestions for future avenues of research to extend the findings described above as well as to further elucidate areas that remain unclear:

- Chapter 2 was conducted at a single location, therefore it would be informative to conduct a broader analysis of wood anatomical properties (bordered pit structure in particular) for conifers exposed to full light and shade growing in a variety of sites.
- The results from Chapter 3 suggest that substantial differences exist in the baseline carbohydrate storage capability of *Pinus contorta* and *Picea glauca*. At the same time, Chapter 4 suggests very little change in seasonal carbohydrate dynamics for *Picea glauca* as a co-dominant tree or as an understory species. Assessment of biomass partioning in both species and open-grown versus shaded *Picea glauca* will elucidate whether the pool size fractions are convergent or divergent.
- Chapter 4 examined seasonal C dynamics in a shade tolerant species, Picea glauca where very little difference existed between open-grown and shaded individuals in terms of the magnitudes or fluxes of carbohydrates. Study of shade intolerant species (such as *Pinus contorta*) may elucidate different results as I observed in Chapter 3 that this species

- Study 5 was conducted over a two-year period, which may not have been long enough for a carbon conservative species such as *Picea glauca* (as found in Chapter 3). Longer-term monitoring of fully and partially shaded tree crowns of shade tolerant species, such as *Picea glauca*, would provide additional evidence as to whether the responses experienced in the shade intolerant species (*Pinus contorta*) are eventually observed for this species.
- We found a significant divergence in LAI for this chronosequence. This divergence altered the relations between leaf area and root area. At this point, it is unclear if my results are a unique feature of the stand types chosen. Leaf-area dynamics in the foothills region needs further work in stratified regions (elevation, aspect) utilizing similar destructive methods employed in Chapter 5.
- Though daunting, Chapter 6 should be repeated in a shade tolerant species such as *Picea glauca*. I observed substantial differences in physiological responses of this species and *Pinus contorta* to shading though both species tend to converge in terms of belowground seasonal C dynamics. At this point, it is unclear if the same patterns will emerge.

Appendix 1 (Chapter 2)

Predawn (3:00-6:00) and midday (11:30-15:00) water potential (WP) measurements of *Pinus banksiana*, *P.contorta*, *Picea mariana* and *P. glauca* grown in an open field (open) or aspen dominated understory (understory).

Treatment	Predawn WP (MPa)	Midday WP (MPa)
Pinus banksiana		
open	0.40 (0.01)	1.24 (0.03)
understory	0.42 (0.01)	1.04 (0.06)
Pinus contorta		
open	0.44 (0.02)	1.39 (0.05)
understory	0.45 (0.03)	1.05 (0.05)
Picea mariana		
open	0.40 (0.01)	1.49 (0.04)
understory	0.35 (0.02)	1.33 (0.09)
Picea glauca		
open	0.42 (0.02)	1.59 (0.05)
understory	0.39 (0.01)	1.26 (0.09)

Appendix 2 (Chapter 2)

Frequency histograms of tracheids diameters for *Pinus banksiana* (a,b), *Pinus contorta* (c,d), *Picea mariana* (e,f) and *Picea glauca* (g,h) grown in an open field (open) or in an aspen dominated understory (understory).

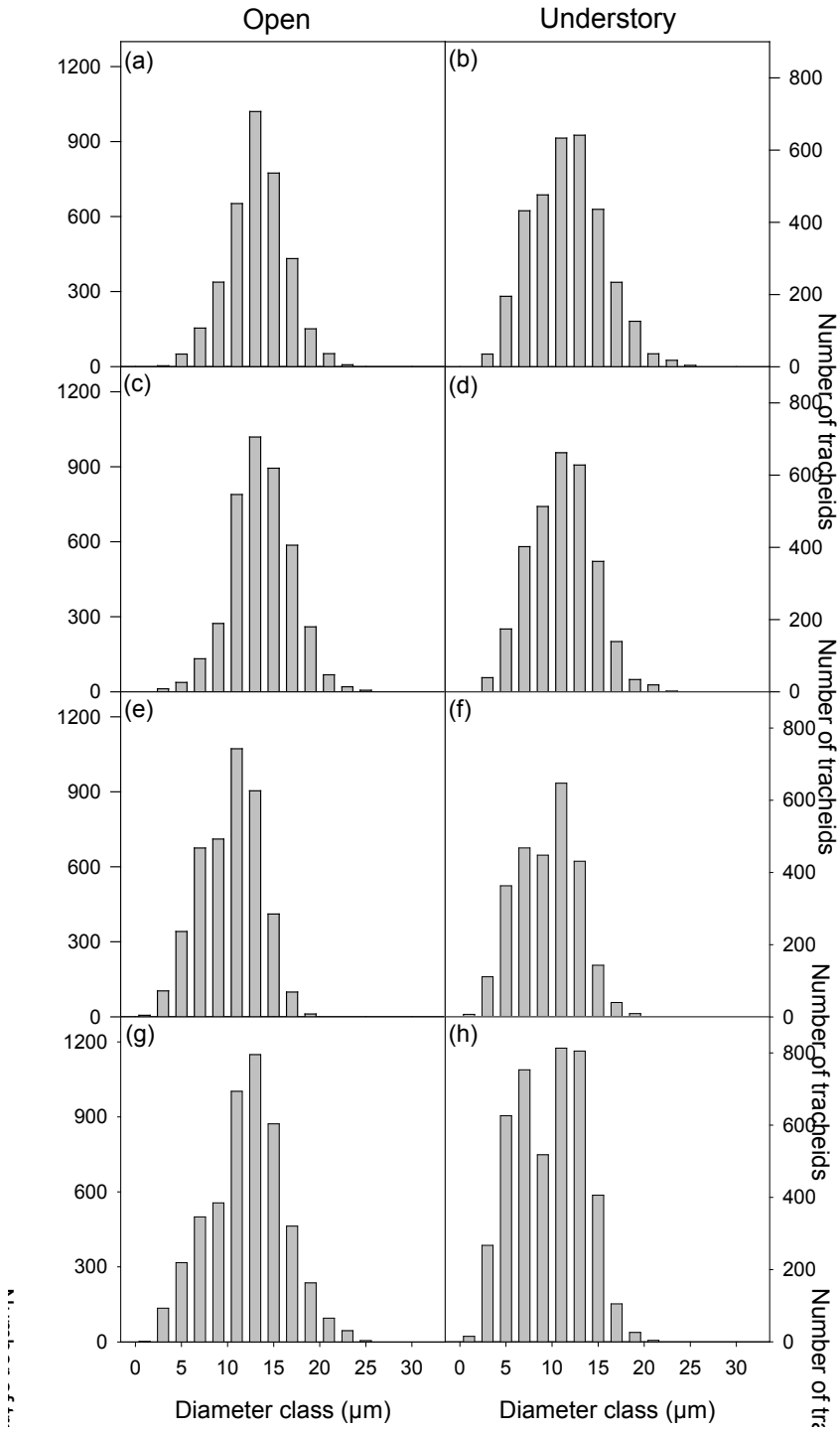

Appendix 3 (Chapter 2)

P-values (degrees of freedom) from within species t-test comparisons (open-grown versus understory) for *Pinus banksiana*, *P.contorta*, *Picea mariana* and *P. glauca* grown in an open field or in an aspen dominated understory. Bolded values indicate that within species comparison between open and understory conditions was statistically significant at $\alpha \leq 0.05$.

Parameter	Units	*Pinus banksiana*	*Pinus contorta*	*Picea mariana*	*Picea glauca*
Physiological measurements					
P_{50}	MPa	**0.0460 (10)**	**0.0446 (10)**	**0.0042 (10)**	**0.0333 (10)**
sapwood-area specific conductivity (k_s)	$mm^2\ s^{-1}\ kPa^{-1}$	0.6090 (10)	0.1134 (10)	0.0669 (10)	0.3171 (10)
leaf area specific conductivity (k_l)	$mm^2\ s^{-1}\ kPa^{-1}$	**0.0105 (5.8)**	**0.0100 (6.2)**	**0.0360 (10)**	**0.0197 (9)**
soil-to-plant hydraulic conductance (K_{s-p})	$mmol\ m^{-2}\ MPa^{-1}s^{-1}$	0.5870 (22)	**0.0038 (21)**	0.7961 (22)	**0.0298 (21)**
Light microscopy measurements					
wood density (ρ)	$g\ cm^{-3}$	**0.0244 (5.4)**	**0.0025 (10)**	**0.0276 (5.6)**	**0.0112 (10)**
tracheid length (L)	µm	0.1273 (10)	0.7418 (10)	0.1260 (10)	0.0672 (10)
lumen diameter (D)	µm	0.1299 (10)	**0.0055 (10)**	0.1586 (10)	**0.0077 (6.2)**
tracheid density	$\#\ mm^{-2}$	0.1173 (5.8)	**0.0307 (6.0)**	**0.0102 (10)**	**0.0035 (10)**
tracheid resistivity (R_C)	$MPa\ s\ mm^{-4}$	0.2375 (5.5)	0.9528 (10)	0.5889 (10)	0.5674 (10)
lumen resistivity (R_L)	$MPa\ s\ mm^{-4}$	0.0895 (10)	**0.0109 (10)**	0.2094 (7.2)	**0.0016 (10)**
wall fraction	-	0.3320 (10)	**0.0005 (10)**	0.0908 (10)	**0.0141 (10)**
pit resistance (r_p)	$MPa\ s\ mm^{-1}$	0.8127 (10)	**0.0341 (10)**	0.2064 (10)	0.2561 (10)
number pits per tracheid	-	0.8453 (10)	0.5434 (10)	**0.0364 (6.3)**	0.3625 (10)
fraction of area occupied by pits (F_p)	-	0.5090 (10)	0.2499 (10)	0.1546 (10)	0.1353 (10)
SEM measurements					
strand width	µm	-	**0.0119 (10)**	**0.0294 (10)**	-
strand length	µm	-	0.8076 (10)	0.2888 (10)	-
mean pore area	μm^2	-	0.2729 (10)	**0.04816 (6.3)**	-
max pore area	μm^2	-	**0.0231 (10)**	**0.0040 (6.1)**	-
pore fraction	-	-	0.0800 (10)	**0.0121 (10)**	-
extended torus area	μm^2	-	0.1903 (10)	**0.0151 (10)**	-
Torus/pit area	-	-	**0.0088 (10)**	0.6627 (10)	-
Aperture/pit area	-	-	0.1117 (10)	0.1558 (10)	-
Torus/aperture area	-		0.8636 (10)	**0.0177 (10)**	
Torus diameter	µm	-	**0.0322 (10)**	**0.0026 (10)**	-
Pit diameter	µm	-	0.3118 (10)	**0.0015 (10)**	-
Aperture diameter	µm	-	**0.0239 (10)**	0.5802 (10)	-
Whole plant measurements					
total height	m	**0.0000 (10)**	**0.0000 (10)**	**0.0008 (6.2)**	**0.0013 (6.3)**
root collar diameter	mm	**0.0003 (5.2)**	**0.0004 (5.2)**	**0.0003 (5.3)**	**0.0002 (5.3)**
total leaf area (Al)	m^2	**0.0000 (10)**	**0.0024 (5.0)**	**0.0000 (6.2)**	**0.0000 (10)**
leader LA:SA	-	**0.0001 (10)**	**0.0009 (5.5)**	**0.0002 (12)**	**0.0013 (10)**

Appendix 4 (Chapter 5)

A4.1

Total non-structural carbohydrates in current-year needles of pine and spruce from branches located in the upper (a-d) and lower (e-h) crown in late June 2009. The difference of means indicates the control minus the shade treatment. Treatment codes are: NS = non-shaded, AS-L = asymmetric-light shaded, AS-H = asymmetric-heavy shaded and US = uniform-shaded. Error bars represent 95% CI (n=6-10).

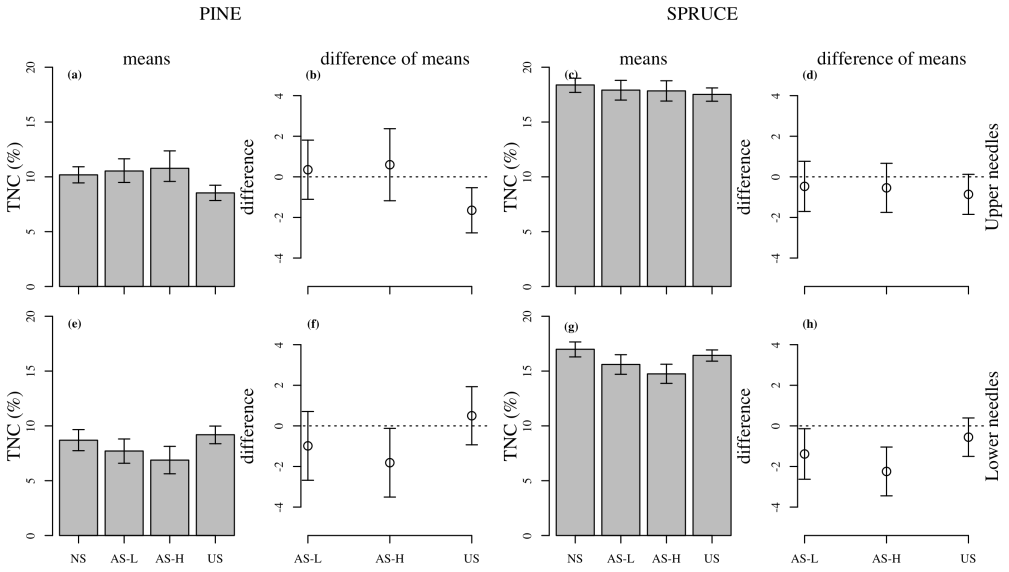

A4.2

Stem and root diameter increment and shoot extension of lodgepole pine (pine) and white spruce (spruce). Root and stem measurements are means of trees sampled from Sept 9 2007-May 7 2008 (n=32). Branch measurements are means of the July 19 2007 collection (n=8). Confidence interval is at the 95% level.

		Pine		Spruce	
Tissue	**year**	**mean**	**confidence interval**	**mean**	**confidence interval**
root (mm)	2007	**0.61**	0.45-0.77	**0.58**	0.45-0.69
	2006	**0.62**	0.46-0.78	**0.52**	0.39-0.63
stem (mm)	2007	**3.26**	2.71-3.81	**3.50**	3.17-3.84
	2006	**3.51**	2.95-4.09	**3.64**	3.34-3.95
	2005	**3.41**	2.77-4.05	**3.80**	3.48-4.12
upper branch (cm)	2007	**17.67**	14.28-20.92	**15.34**	12.89-17.80
	2006	**11.64**	8.35-14.86	**16.60**	14.16-19.03
lower branch (cm)	2007	**7.96**	4.59-11.36	**8.29**	5.76-10.77
	2006	**7.14**	3.83-10.42	**9.54**	7.06-12.01

Appendix 5 (Chapter 6)

Determination of tree volume follows Huang et al. (1994) and is described as:

$$d = a_0 D^{a1} a_2^D X^{y*}$$

where:

$$y^* = b_1 Z^2 + b_2 \ln(Z + 0.001) + b_3 \sqrt{Z} + b_4 e^Z + b_5 (\frac{D}{H})$$

$$X = (1 - \sqrt{h/H}\,/(1 - \sqrt{p})$$

and:

d = diameter inside bark at h (cm)
h = height above the ground (m)
H = total tree height (m)
D = diameter at breast height outside bark (cm)
Z = h/H
p = location of the inflection point, assumed to be at 22.5% of total height above the ground.
e = base of the natural logarithm

The following coefficients are from Huang (1994) and are specific to lodgepole pine in the upper foothills and subarctic ecological areas of Alberta:

a_0 = 0.828665
a_1 = 1.024196
a_2 = 0.997492
b_1 = 0.596193
b_2 = -0.118777
b_3 = 0.465591
b_4 = -0.196176
b_5 = 0.083094

Then the diameter of the inside of the bark is required based on known diameter of the outside bark:

$$DOB = a + bDIB$$

DOB = diameter outside bark (cm)
DIB = corresponding diameter inside the bark (cm)

As above, coefficients specific to lodgepole pine in upper foothills and sub-arctic ecological areas:

a = 0.308258
b = 1.024549

Then, the diameter of the stump is estimated, based on known diameter at breast height:

$$DOB_{stp} = a + bD + cD^2$$

DOB_{stp} = stump diameter outside bark (cm)

Coefficents specific to lodgepole pine in upper foothills and sub-arctic ecological areas:

a = -0.487166
b = 1.112282
c = 0.000347

Appendix 6 (Chapter 6)

Tables summarizing equations used for estimation of leaf mass and wood volume production

A6.1 Candidate regression models used to predict branch leaf mass. Individual trees had 12-21 branches sampled. Regression models were generated for each of the four lodgepole pine age classes (12, 21, 53 and 100+ years).

Model	Equation
1	$\ln(y) = B_o + B_1 \times \ln(L)$
2	$\ln(y) = B_o + B_2 \times \ln(D)$
3	$\ln(y) = B_o + B_1 \times \ln(L) + B_2 \times \ln(D)$
4	$\ln(y) = B_o + B_1 \times \ln(L) + B_2 \times \ln(D) + B_3 \times S$
5	$\ln(y) = B_o + B_1 \times \ln(L) + B_2 \times \ln(D) + B_4 \times$ TREECLASS
6	$\ln(y) = B_o + B_1 \times \ln(L) + B_2 \times \ln(D) + B_3 \times S + B_4 \times$ TREECLASS
7	$\ln(y) = (B_o + a_i) + B_1 \times \ln(L)$
8	$\ln(y) = (B_o + a_i) + B_1 \times \ln(L) + B_2 \times \ln(D)$
9	$\ln(y) = (B_o + a_i) + B_2 \times \ln(D)$
10	$\ln(y) = (B_o + a_i) + (B_1 + b_i) \times \ln(L)$
11	$\ln(y) = (B_o + a_i) + (B_2 + b_i) \times \ln(D)$

symbol	description
L	branch length
D	branch base diameter
S	crown section
TREECLASS	tree class (dominant, codominant or suppressed)
a_i	random intercept specific to tree (i)
b_i	random slope specific to tree (i)

A6.2 AIC results from linear regression of branch leaf mass. Values in bold are models that were used to average biomass estimates. Delta values were calculated as the relative difference between the model with lowest AIC and model AIC.

Age class	model	AIC	delta	likelihood	probability	Age class	model	AIC	delta	likelihood	probability
12	1	99.1	27.2	0.00	0.00	53	1	246.6	86.1	0.000	0.000
	2	138.8	66.9	0.00	0.00		2	216.5	55.9	0.000	0.000
	3	**82.8**	**10.9**	**0.00**	**0.00**		3	207.7	47.1	0.000	0.000
	4	**79.1**	**7.1**	**0.03**	**0.01**		4	181.2	20.6	0.000	0.000
	5	**72.1**	**0.2**	**0.91**	**0.33**		5	208.8	48.2	0.000	0.000
	6	**71.9**	**0.0**	**1.00**	**0.37**		**6**	**160.5**	**0.0**	**1.000**	**1.000**
	7	88.7	16.8	0.00	0.00		7	251.2	90.7	0.000	0.000
	8	**72.4**	**0.5**	**0.80**	**0.29**		8	217.9	57.4	0.000	0.000
	9	131.1	59.2	0.00	0.00		9	224.7	64.2	0.000	0.000
	10	92.5	20.6	0.00	0.00		10	255.0	94.5	0.000	0.000
	11	134.2	62.3	0.00	0.00		11	228.7	68.2	0.000	0.000
21	1	348.1	106.1	0.00	0.00	100+	1	371.7	163.5	0.000	0.000
	2	290.4	48.4	0.00	0.00		**2**	**208.2**	**0.0**	**1.000**	**0.586**
	3	257.6	15.5	0.00	0.00		**3**	**210.1**	**1.9**	**0.378**	**0.221**
	4	**250.9**	**8.9**	**0.01**	**0.01**		**4**	**212.1**	**3.9**	**0.139**	**0.082**
	5	258.0	15.9	0.00	0.00		**5**	**212.6**	**4.4**	**0.110**	**0.065**
	6	**242.1**	**0.0**	**1.00**	**0.99**		**6**	**214.6**	**6.4**	**0.041**	**0.024**
	7	333.3	91.2	0.00	0.00		7	361.9	153.7	0.000	0.000
	8	269.8	27.7	0.00	0.00		8	223.0	14.8	0.001	0.000
	9	299.7	57.6	0.00	0.00		9	218.2	10.0	0.007	0.004
	10	334.4	92.3	0.00	0.00		10	349.2	141.0	0.000	0.000
	11	303.7	61.6	0.00	0.00		**11**	**215.2**	**7.0**	0.030	0.017

A6.3 Branch-level leaf mass prediction equations for all age classes.

Age class	Model	Equation	Residual error	R^2
12	3	ln(y) = -4.0459 + 1.2247 x ln(L) + 0.8469 x ln(D)	0.3730	0.87
	4	ln(y) = -3.88792 + 0.98811 x ln(L) + 1.20575 x ln(D) + 0.03547 x S	0.3740	0.87
	5	ln(y) = -1.38521 + 0.03452 x ln(L) + 1.96974 x ln(D) + 0.08379 x TREECLASS D + -0.02156 x TREECLASS S	0.3477	0.88
	6	ln(y) = -3.52447 + 1.20896 x ln(L) + 0.60637 x ln(D) + -0.40450 x TREECLASS D + -0.40450 x TREECLASS S + -0.0292 x S	0.3544	0.88
	8	ln(y) = (-3.9575 + a_i) + 1.1633 x ln(L) + 0.8949 x ln(D)	0.3049	0.91
21	4	ln(y) = -4.15439 + 0.91636 x ln(L) + 1.72706 x ln(D) + -0.07175 x S	0.4953	0.86
	6	ln(y) = -3.92571 + 1.13576 x ln(L) + 1.21088 x ln(D) + 0.25230 x TREECLASS D + -0.23425 x TREECLASS S + -0.11108 x S	0.4799	0.86
53	6	ln(y) = -3.41672 + 1.30928 x ln(L) + 1.05429 x ln(D) + 0.16442 x TREECLASS D + -0.68097 x TREECLASS S + -0.29787 x S	0.4572	0.80
100+	2	ln(y) = -1.3577 + 2.02519 x ln(L)	0.4509	0.78
	3	ln(y) = -1.39932 + 0.2182 x ln(L) + 2.0054 x ln(D)	0.4523	0.78
	4	ln(y) = -1.39039 + 0.016836 ln(L) + 2.007314 x ln(D) + 0.002071 x S	0.4537	0.78
	5	ln(y) = -1.38521 + 0.03452 x ln(L) + 1.96974 x ln(D) + 0.08379 x TREECLASS D + -0.02156 x TREECLASS S	0.4530	0.78
	6	ln(y) = -1.38731 + 0.035762 x ln(L) + 1.9692088 x ln(D) + 0.0838855 x TREECLASS D + -0.0216844 x TREECLASS S + -0.0005072 x S	0.4544	0.78
	11	ln(y) = (-1.4242 + a_i) + (2.00549 + b_i) x ln(D)	0.4317	0.80

Parameters

age class	tree (i)	a	age class	tree (i)	a	b	symbol	description
21	1	-0.18	100+	1	0.07	-0.17	L	branch length
	2	-0.12		2	-0.04	0.09	D	branch base diameter
	3	-0.19		3	0.28	-0.68	S	crown section
	4	-0.05		4	-0.02	0.04	TREECLASS D	dominant tree class
	5	0.30		5	0.30	-0.74	TREECLASS S	suppressed tree class
	6	0.35		6	-0.07	0.17		
	7	-0.14		7	-0.45	1.12		
	8	0.01		8	0.00	0.00		
				9	0.01	-0.02		
				19	-0.08	0.19		

A6.4 Candidate regression models used to predict tree-level leaf mass. Two trees were sampled from each site (n=10 for each age class). Regression models were generated for each of the four lodgepole pine age classes (12, 21, 53 and 100+ years).

Model	Equation
1	$\ln(y) = B_o + B_1 \times \ln(H)$
2	$\ln(y) = B_o + B_2 \times \ln(D)$
3	$\ln(y) = B_o + B_3 \times HTLC$
4	$\ln(y) = B_o + B_1 \times \ln(H) + B_2 \times \ln(D)$
5	$\ln(y) = Bo + B1 \times \ln(H) + B2 \times \ln(D) + B_3 \times HTLC$
6	$\ln(y) = (B_o + a_i) + B_1 \times \ln(H)$
7	$\ln(y) = (B_o + a_i) + B_2 \times \ln(D)$
8	$\ln(y) = (B_o + a_i) + B_3 \times HTLC$
9	$\ln(y) = (B_o + a_i) + B_1 \times \ln(H) + B_2 \times \ln(D)$
10	$\ln(y) = (B_o + a_i) + (B_1 + b_i) \times \ln(H)$
11	$\ln(y) = (B_o + a_i) + (B_2 + b_i) \times \ln(D)$

symbol	description
L	branch length
D	branch base diameter
HTLC	height to live crown ratio
a_i	random intercept specific to site (i)
b_i	random slope specific to site (i)

A6.5 AIC results from linear regression of tree leaf mass. Values in bold are models that were used to average biomass estimates. Delta values were calculated as the relative difference between the model with lowest AIC and model AIC.

age class	model	AIC	delta	likelihood	probability	age class	model	AIC	delta	likelihood	probability
12	1	25.1	18.4	0.00	0.00	53	**1**	**20.5**	**8.3**	**0.02**	**0.01**
	2	**11.9**	**5.1**	**0.08**	**0.04**		**2**	**12.3**	**0.0**	**1.00**	**0.50**
	3	38.4	31.6	0.00	0.00		3	29.1	16.8	0.00	0.00
	4	**6.7**	**0.0**	**1.00**	**0.53**		**4**	**13.6**	**1.3**	**0.51**	**0.26**
	5	7.3	0.6	0.76	0.40		**5**	**15.5**	**3.2**	**0.20**	**0.10**
	6	27.8	21.0	0.00	0.00		**6**	**22.1**	**9.8**	**0.01**	**0.00**
	7	17.1	10.4	0.01	0.00		**7**	**16.9**	**4.6**	**0.10**	**0.05**
	8	35.9	29.2	0.00	0.00		8	34.3	22.0	0.00	0.00
	9	**13.1**	**6.4**	**0.04**	**0.02**		**9**	**16.2**	**3.9**	**0.14**	**0.07**
	10	31.1	24.3	0.00	0.00		10	26.2	14.0	0.00	0.00
	11	18.9	12.2	0.00	0.00		**11**	**20.9**	**8.6**	**0.01**	**0.01**
21	1	27.5	27.6	0.00	0.00	100+	1	16.6	18.4	0.00	0.00
	2	**5.8**	**5.9**	**0.05**	**0.03**		**2**	**0.6**	**2.5**	**0.29**	**0.17**
	3	41.5	41.6	0.00	0.00		3	24.3	26.1	0.00	0.00
	4	**-0.1**	**0.0**	**1.00**	**0.58**		**4**	**-0.1**	**1.7**	**0.42**	**0.24**
	5	**0.9**	**1.0**	**0.60**	**0.35**		**5**	**-1.8**	**0.0**	**1.00**	**0.57**
	6	30.1	30.2	0.00	0.00		6	18.7	20.6	0.00	0.00
	7	12.7	12.8	0.00	0.00		**7**	**7.6**	**9.4**	**0.01**	**0.01**
	8	41.7	41.8	0.00	0.00		8	30.2	32.0	0.00	0.00
	9	**5.3**	**5.4**	**0.07**	**0.04**		**9**	**5.3**	**7.1**	**0.03**	**0.02**
	10	34.1	34.2	0.00	0.00		10	22.7	24.6	0.00	0.00
	11	14.1	14.1	0.00	0.00		11	11.6	13.4	0.00	0.00

A6.6 Model parameters for tree level model of leaf mass prediction.

Age class	Model	Equation	Residual error	R^2
12	2	ln(y) = 2.3996 + 2.6534 x ln(D)	0.3626	0.95
	4	ln(y) = 2.2232 + -1.7839 x ln(H) + 4.2939 x ln(D)	0.2716	0.97
	5	ln(y) = 2.0437 + -2.2884 x ln(H) + 4.5987 x ln(D) + 1.2390 x HTLC	0.2728	0.97
	9	ln(y) = (2.228 + a_i) + -1.712 x ln(H) + 4.232 x ln(D)	0.2461	0.98
21	2	ln(y) = 2.4405 + 2.3103 x ln(D)	0.2676	0.97
	4	ln(y) = 2.6620 + -1.0851 x ln(H) + 3.0414 x ln(D)	0.1930	0.99
	5	ln(y) = 2.6052 + -0.7833 x ln(H) + 2.8978 x ln(D) + -0.1348 x HTLC	0.1985	0.99
	9	ln(y) = (2.6315 + a_i) + -1.1437 x ln(H) + 3.1111 x ln(D)	0.0803	1.00
53	1	ln(y) = -1.785 + 3.815 x ln(H)	0.5591	0.53
	2	ln(y) = 1.8045 + 2.4961 x ln(D)	0.3700	0.80
	4	ln(y) = 0.5599 + 0.8475 x ln(H) + 2.1351 x ln(D)	0.3824	0.78
	5	ln(y) = 0.30972 + 1.0908 x ln(H) + 2.05812 x ln(D) + -0.02193 x HTLC	0.4103	0.75
	6	ln(y) = (-2.029 + a_i) + 3.915 x ln(H)	0.5001	0.63
	7	ln(y) = (1.8046 + b_i) + 2.496 x ln(D)	0.3699	0.80
	9	ln(y) = (0.5599+ c_i) + 0.8475 x ln(H) + 2.1351 x ln(D)	0.3824	0.78
	11	ln(y) = (1.8045 + d_i) + (2.4961 + e_i) x ln(D)	0.3700	0.80
100+	2	ln(y) = 1.1116 + 2.6014 x ln(D)	0.2069	0.93
	4	ln(y) = 4.1072 + -1.80 x ln(H) + 3.3334 x ln(D)	0.1930	0.94
	5	ln(y) = 3.63438 + -1.64834 x ln(H) + 3.60154 x ln(D) + -0.07524 x HTLC	0.1731	0.95
	7	ln(y) = (1.1116 + a_i) + 2.6014 x ln(D)	0.2069	0.93
	9	ln(y) = (4.1072 + b_i) + -1.80 x ln(H) + 3.3334 x ln(D)	0.1929	0.94

Parameters

age class	site (i)	a	age class	site (i)	a	b	c	d	e	symbol	description
12	1	-0.02	53	1	-0.05	0.0001	0.00	0.00	0.00	L	branch length
	2	0.03		2	-0.05	0.0002	0.00	0.00	0.00	D	branch base diameter
	3	0.04		3	-0.17	-0.0003	0.00	0.00	0.00	S	crown section
	4	-0.09		4	0.23	-0.0001	0.00	0.00	0.00	HTLC	height to live crown ratio
	5	0.06		5	0.03	0.0002	0.00	0.00	0.00		
21	1	-0.22	100+	1	0.00	0.00					
	2	0.13		2	0.00	0.00					
	3	0.18		3	0.00	0.00					
	6	-0.03		4	0.00	0.00					
	7	-0.06		5	0.00	0.00					

A6.7 The observed diameter in 2009 was used to generate predictive models of previous year's diameters (2004) and height. Candidate regression models used to predict tree-level leaf mass. Two trees were sampled from each site (n=10 for each age class). Regression models were generated for each of the four lodgepole pine age classes (12, 21, 53 and 100+ years).

Model	Equation
1	$y = B_o + B_1 \times DBH$
2	$y = (B_o + a_i) + B_1 \times DBH$
3	$y = (B_o + a_i) + (B_1 + b_i) \times DBH$

symbol	description
DBH	diameter
a_i	random intercept specific to site (i)
b_i	random slope specific to site (i)

A6.8 Summary of AIC scores from linear regression models. AIC score in BOLD was used for all predictions of 2004 diameter.

	2004 diameter		
Age class	Model 1	Model 2	Model 3
12	10.5	-14.4	**-19.8**
21	41.4	**36.5**	38.5
53	**18.3**	32.6	36.5
100+	**14.2**	29.7	31.4

A6.9 Results from linear regression of 2004 diameter against observed 2009 diameter. These models were used to predict diameter of trees in 2004.

Age class	Model	Equation	Residual error	R^2
12	3	$y = (-0.01795 + a_i) + (0.34672 + b_i)$ x DBH	0.2707	0.61
21	2	$y = (0.04907 + a_i) + 0.58812$ x DBH	0.4928	0.97
53	1	y = 0.528 + 0.90047 x DBH	1.3330	0.79
100+	1	y = 0.360295 + 0.95493 x DBH	1.7780	0.87

Parameters

age class	site (i)	a	b
12	1	-0.051278	-0.05886
	2	0.0527312	-0.06671
	3	0.0621448	-0.01289
	4	-0.041615	0.142943
	5	-0.021983	-0.00448
21	1	-0.114472	
	2	0.1938317	
	3	-0.238862	
	6	0.1595016	

A6.10 Summary of AIC scores from linear regression models. AIC score in BOLD was used for all predictions of height from diameter.

Age class	Model 1	Model 2	Model 3
12	364	227	**182**
21	477	421	**421**
53	1161	1002	**999**
100+	1121	**1093**	1095

A6.11 Results from linear regression of tree height and DBH. Models shown were used to determine tree height (from diameter) for 2004 and 2009 volume estimation.

Age class	Model	Equation	Residual Error	R^2
12	3	$y = (0.21693 + a_i) + (0.60078 + b_i) \times DBH$	0.270731	0.83
21	3	$y = (0.6977 + a_i) + (0.4434 + b_i) \times DBH$	0.484687	0.83
53	3	$y = (7.2309 + a_i) + (0.4352 + b_i) \times DBH$	0.993757	0.66
100+	2	$y = (6.64841 + a_i) + 0.53534 \times DBH$	1.63282	0.71

Parameters

age class	site (i)	a	b	age class	site (i)	a	b
12	1	-0.14423	-0.06612	53	1	-0.25382	0.058234
	2	0.078466	-0.12774		2	0.78953	-0.01214
	3	0.039685	0.013644		3	-0.07077	-0.06815
	4	0.014859	0.105348		4	-0.94662	-0.02427
	5	-0.01878	0.074872		5	0.481686	0.046329
21	1	-0.20976	0.012309	100+	1	-0.24644	-
	2	-0.10274	-0.04191		2	-0.13722	-
	3	-0.34277	0.057431		3	-0.69334	-
	6	0.655279	-0.02783		4	-0.13237	-
					5	1.209377	-